

University of Warwick institutional repository: <http://go.warwick.ac.uk/wrap>

A Thesis Submitted for the Degree of EngD at the University of Warwick

<http://go.warwick.ac.uk/wrap/36741>

This thesis is made available online and is protected by original copyright.

Please scroll down to view the document itself.

Please refer to the repository record for this item for information to help you to cite it. Our policy information is available from the repository home page.

Biocomposites for Bone Tissue Engineering

Innovation Report

by

James Meredith

Engineering Doctorate portfolio submission
This work is submitted in partial fulfilment for the degree of
Engineering Doctorate (EngD).



Warwick Manufacturing Group
School of Engineering
University of Warwick

February 2009

Abstract

Historically, bone defects resulting from trauma, disease or infection are treated with autograft or allograft. Autograft is bone transplanted from a non-critical area of the skeleton and allograft is bone donated from another member of the same species. The drawbacks with these treatments such as limited availability, donor site morbidity, high cost and disease transmission have driven increasing use of bone graft substitute (BGS) materials. These represent 15% of the £1.6 billion global orthobiologics market. BGS materials available to date are not suitable for use in grafts that are intrinsic to the stability of the skeleton. Thus, the aim for this project was to fabricate an off the shelf and economically viable BGS that will support the skeletal structure whilst healing occurs.

This project employed an empirical approach utilising both rapid prototyping (RP) and conventional manufacturing processes to produce novel BGSs. A range of RP techniques were attempted and discovered to be unsuitable as a result of their long build and post-processing times, poor availability of suitable materials, and undesirable surface finish. Experiments with injection moulding and laser drilling of polylactic acid (PLA) successfully produced 10 mm blocks with a compressive strength of 67 – 80 MPa and compressive modulus of 1.5 – 2.2 GPa. This line of research led to the hypothesis that ceramic extrusion, a process hitherto untested for use in bone tissue engineering (BTE), may be feasible for production of a novel and high strength BGS.

In collaboration with an international expert in the manufacture of ceramic monoliths it was possible, for the first time, to manufacture hydroxyapatite (HA) monoliths by adapting the process used for manufacture of automotive exhaust catalysts. These HA monoliths exhibited a compressive strength of 142 – 265 MPa and compressive modulus of 3.2 – 4.4 GPa. The exceptional strength of these monoliths match the properties of cortical bone whilst retaining the high levels of porosity (> 60 %) found in cancellous bone. This combination of strength and porosity will enable treatment of large structural bone defects where the high strength will withstand typical skeletal forces whilst the high porosity allows blood vessels to infiltrate the monolith and begin the healing process. Furthermore, these HA monoliths support the proliferation and differentiation of human osteoblast-like MG63 cells and compare very favourably with a market leading BGS material in terms of their biological performance.

It is suggested that this work will result in the development of a new family of high strength and high porosity BGSs for use in challenging clinical situations. The International Preliminary Examination Report for the patent issued to the author (WO 2007/125323) decreed that all 45 claims contained novelty and an inventive step. Two successful applications for research funding have raised nearly £50,000 that helped fund this research effort. Warwick ventures are currently involved in negotiating with medical partners to licence this technology for clinical use.

Table of Contents

	Page number
Abstract	i
Table of Contents	ii
List of Figures	iv
List of Tables	vi
List of Tables	vi
Acknowledgements	vii
Declaration	viii
Glossary	ix
Chapter 1 Introduction	12
1.1 Project aim	12
1.2 Engineering Doctorate portfolio structure	12
1.3 Structure of the Innovation Report	14
Chapter 2 Background	16
2.1 Introduction	16
2.2 Bone	16
2.3 Current bone grafting solutions	25
2.4 Tissue Engineering	32
2.5 Specifications for a BGS	35
2.6 The bone graft market	37
Chapter 3 Methodology	39
3.1 Introduction	39
3.2 Experimental work using rapid prototyping methods	39
3.3 Experimental work using conventional methods	45
3.4 Extrusion of ceramic monoliths	48
3.4.1 Physical and mechanical characterisation of HA monoliths	53
3.4.2 Biological characterisation of HA monoliths	54
Chapter 4 Analysis and characterisation of HA monoliths	58
4.1 Results of physical and mechanical characterisation	58

4.2	Results of biological characterisation	65
4.2.1	Results of biological experiment 1	65
4.2.2	Results of biological experiment 2	67
4.2.3	Comparison with an existing BGS material	69
4.2.4	Further sample analysis	72
Chapter 5	Clinical and expert opinion	75
5.1	The key benefits of calcium phosphate monoliths	75
5.2	Clinical input to this research	78
Chapter 6	Design of an implant utilising ceramic extrusion	81
6.1	Introduction	81
6.2	Important design features	86
6.3	Design of a lumbar interbody fusion device	88
6.4	Planning for medical implant approval	91
Chapter 7	Overview	94
Chapter 8	Conclusions	103
References		109

List of Figures

	Page number
Figure 2.1 An anatomical drawing of a human tibia, adapted from [3]	17
Figure 2.2 An illustration demonstrating the anatomical features from a section through a human long bone [9]	18
Figure 2.3 An illustration demonstrating the hierarchical organisation of collagen fibres [8]	18
Figure 2.4 An illustration of a human skeleton highlighting the areas where bone graft materials are commonly required	24
Figure 3.1 Images of (a) lamb femur μ CT data replicated via stereo lithography scale x 4 and (b) selective laser melting scale x 2 [scale bar = 10 mm]	41
Figure 3.2 A 3D CAD model demonstrating a cube with structured porosity	45
Figure 3.3 SEM micrographs of a laser drilled PLA cube (a) a view of the top surface of the cube showing some of the melt debris on the surface of the PLA as well as the regular spacing and circular nature of the holes (b) is a close up of one of these holes demonstrating a hole diameter of 347 μ m (c) is a view on one corner of the cube and shows the holes generated by laser in each of the surfaces (d) is a magnified image of the top hole in image (c)	47
Figure 3.4 An image demonstrating ceramic monoliths with hexagonal and square cells	49
Figure 3.5 A CAD model of the ceramic monolith extrusion apparatus	50
Figure 3.6 An image of the second industrial extrusion attempt with a 50% HAP 100 and 50% HAP 200 paste through a 28/70 die	51
Figure 3.7 SEM images of raw HA powder (a) and (b) are HAP 100, images (c) and (d) are HAP 200	52
Figure 3.8 A schematic view of monolith cells demonstrating cell pitch (CP) and wall thickness (WT)	52
Figure 3.9 Confocal microscopy images (x40) of Actin fibre staining. (a) MG63 cells and (b) SaOS-2 cells stained with DAPI (blue, nucleus) and phalloidin (red, actin fibres) [scale bar = 50 μ m]	55
Figure 3.10 Images extracted from a plate reader demonstrating expression of ALP (a) and OC (b) mRNA in MG63 cells after 6 and 13 days in culture	56
Figure 3.11 Relative AP expression for HA samples and the control at 6 and 13 days in culture	56
Figure 3.12 Relative OC expression for HA samples and the control at 6 and 13 days in culture	57
Figure 4.1 Image comparing the influence of die on the sample. (a) Sample A using a 12/300 die and (b) sample B using the 28/70 die	58
Figure 4.2 Mercury porosimetry plot of wall porosity for HA monolith samples A, B, C, D and E	60
Figure 4.3 A-axis Force <i>versus</i> displacement plot for sample A in compression	60
Figure 4.4 A plot of compressive strength and elastic modulus comparing a range of biomaterials with bone and HA monoliths, adapted from [47]	61

Figure 4.5 XRD plot for HAP 100/200 50:50 sintered at 1150°C (top), HAP 100/200 100:0 sintered at 1150°C (middle) and HAP 100/200 100:0 sintered at 1250°C (bottom) compared with HA standard	62
Figure 4.6 SEM images on the end of a cell wall for scaffold A, (a) illustrates the entire wall thickness with large particles from HAP 100 visible [scale bar = 20µm] (b) illustrates the boundary between one of the large particles and the smaller particles of HAP 200 [scale bar = 10 µm] (c) illustrates the porosity of the monolith [scale bar = 1µm] and (d) illustrates how the particles have been sintered together [scale bar = 1 µm]	63
Figure 4.7 SEM images on the end of a polished cell wall for scaffold A, (a) illustrates a number of monolith cells [scale bar = 200µm] (b) illustrates the entire wall thickness with large particles of HAP 100 visible (c) illustrates the wall microporosity [scale bar = 10 µm]	64
Figure 4.8 Graph of MTT assay results for each sample in biological experiment 1	65
Figure 4.9 Graph of media pH after equilibrating the samples in media for 24 hours	66
Figure 4.10 Graph of MTT assay results for each sample in biological experiment 2	67
Figure 4.11 Graph of MTT assay results for each sample in experiment 2 versus the control	68
Figure 4.12 Graph of summed MTT assay results for cells on samples and cells in wells from experiment 2	69
Figure 4.13 MTT results comparing unwashed HA monoliths with β-TCP Vitoss	70
Figure 4.14 MTT results comparing washed HA monoliths with β-TCP Vitoss	71
Figure 4.15 Image demonstrating the formazan staining on HA monoliths and Vitoss® after 9 days of cell culture and incubation in MTT for 30 minutes	71
Figure 4.16 A GCMS plot for sample C with a methanol solvent	73
Figure 4.17 A magnified comparison of the GCMS hexamethylcyclotrisiloxane peak for A – E and Vitoss	74
Figure 5.1 Illustrations of sections through curved (a) and reduction extruded (b) monoliths that can be utilised to mimic the natural form of bone, adapted from [162]	77
Figure 5.2 An illustration demonstrating four readily achievable extrusion profiles	77
Figure 6.1 Illustration of the anatomy of the human spine [167]	82
Figure 6.2 Conditions that may lead to the requirement for spinal fusion [168]	83
Figure 6.3 The procedure for posterior lumbar interbody fusion, adapted from [169]	84
Figure 6.4 The final layout of spine cages and autograft for a PLIF procedure [169]	84
Figure 6.5 Image demonstrating a range of spinal interbody fusion devices [170-172]	85
Figure 6.6 A 3D rendering of the bones in the pelvis and lumbar spine	89
Figure 6.7 A CAD model of L4 vertebra and its approximate dimensions	90
Figure 6.8 A 3D CAD model of a proposed PLIF device utilising ceramic extrusion	91
Figure 7.1 Diagram describing the A, B and C axis monolith orientations	97

List of Tables

	Page number
Table 2.1 Summary of human long bone mechanical properties [13-18]	20
Table 2.2 BGS materials available in the market in 2009	28
Table 3.1 Summary of Rapid Prototyping processes	44
Table 3.2 HA monolith configuration details	53
Table 4.1 Physical properties for the samples undergoing biological testing	59
Table 5.1 Comparison of strength and porosity for HA monoliths versus bone	75

Acknowledgements

This work could not have been completed without help from the Engineering and Physical Sciences Research Council (EPSRC), everyone at NGK for their expertise in ceramic extrusion, the Warwick Innovative Manufacturing Research Council (WIMRC) and Spinner for funding, Dr. Rosemary Bland and Jeannette Bennett for their enormous knowledge of cell biology and hard work carrying out cell assays, Derrick Tuke-Hastings at Ching communications for his PR expertise, Warwick Ventures and Shum Prakash for their patent expertise, Dr. Kajal Mallick and Dr. Kevin Neailey for their mentorship and last but by no means least, my family for their enduring support.

Declaration

The work presented has been undertaken by me unless otherwise acknowledged. This work has not been previously submitted for any other award.

James Meredith

February 2009

University of Warwick

Glossary

3D	three dimensional
AFM	Atomic Force Microscopy
ALCAP	Aluminium Calcium Phosphate ceramic
Allograft	a tissue graft between two members of the same species
Autograft	a tissue graft taken from one location and transferred to another part of the same individual
AP	alkaline phosphatase
ATP	adenosine triphosphate
BGS	bone graft substitute
BTE	bone tissue engineering
cDNA	complimentary deoxyribonucleic acid
CP	cell pitch
μCT	micro computed tomography
CPC	calcium phosphate cement
CPSI	cells per square inch
DNA	deoxyribonucleic acid
DMSO	dimethyl sulfoxide
ESCA	electron spectroscopy for chemical analysis
EDXA	energy dispersive X-ray analysis
ESEM	environmental scanning electron microscopy
FDA	Food and Drug Administration
FDC	fused deposition of ceramic
IEP	isoelectric point
IP	intellectual property
IRS	infra red spectroscopy
IRAS	infra red reflection absorbtion spectroscopy
<i>In vivo</i>	in the body
<i>In vitro</i>	in the laboratory
GAG	glycosaminoglycan

HA	hydroxyapatite
HCA	hydroxyl carbonate apatite
MHEC	methyl-hydroxy-ethyl-cellulose
Mil	wall thickness in thousandths of an inch
mRNA	messenger ribonucleic acid
MTT	3-(4,5-dimethylthiazol-2-yl)-2,5-diphenyltetrazoliumbromide
OC	osteocalcin
OD	optical density
OFA	open frontal area
PA	polyanhydride
PCR	polymerase chain reaction
PDLGA	poly(DL-lactide-co-glycolide)
PDLLA	poly(DL-lactide)
PE	polyethylene
PEEK	poly(ether ether ketone)
PEG	polyethylene glycol
PGA	polyglycolide
PHA	polyhydroxyalkanoate
PHB	polyhydroxybutyrate
PHV	polyhydroxyvalerate
PLA	polylactide
PLGA	poly(lactide-co-glycolide)
PLLA	poly(L-lactide)
POE	poly(ortho ester)
PPF	poly(propylene fumarate)
PSZ	partially stabilised zirconia
PVA	polyvinyl alcohol
RNA	ribonucleic acid
RP	rapid prototyping
RT-PCR	reverse transcriptase polymerase chain reaction
SEM	scanning electron microscopy
SIMS	secondary ion mass spectrometry

STM	scanning tunnelling microscopy
TCP	tricalcium phosphate
TE	tissue engineering
Vascular	relating to the blood vessels
WT	wall thickness
Xenograft	a tissue graft from one species to another
XPS	X-ray photoelectron spectroscopy
XRD	X-ray diffraction
ZPC	zero point charge

Chapter 1 Introduction

1.1 Project aim

The aim for this Engineering Doctorate is to fabricate an off the shelf and economically viable bone scaffold using suitable biomaterials and manufacturing methods in order to support the skeleton whilst healing occurs.

1.2 Engineering Doctorate portfolio structure

The authors EngD portfolio comprises seven submissions beginning with *Submission 1: A Review of Manufacturing Techniques in Bone Tissue Engineering*. This presents an introduction to bone tissue engineering (BTE) including a summary of the relevant properties of bone, the reasons why bone graft may be required and the surgical approaches for repair of bone defects. It reviews the many different manufacturing techniques that have been attempted in order to create the ideal bone scaffold or bone graft substitute (BGS). These can be split into two groups: Rapid Prototyping (RP) and conventional methods. Both of which have their own specific advantages and disadvantages. After reviewing the manufacturing methods it was important to examine the materials most suitable for use in BGSs. This is covered in *Submission 2: A Review of Degradable Biomaterials for the Repair of Bone Defects*. This reviews the essential requirements of a biomaterial as well as the many different biomaterials available and the properties that make them suitable for use in BTE.

An ideal BGS material has many conflicting requirements e.g. high porosity and high strength. Thus a BGS composed of existing materials is likely to have compromised properties. The challenge is to maximise the benefits from these properties and optimise them for specific skeletal applications. In this way *Submission 3: Specification for a Bone Scaffold* defines a more precise specification for a BGS. This eliminates the inherent uncertainty

when designing a product for a wide range of indications and where the precise biological mechanisms occurring at the implant site are not fully understood. This submission also examines the market for BGS materials and identifies where there is a gap in the market that is open for exploitation. The principal aim for this submission is to tighten the specification in order to provide a focus for the research.

The empirical work begins with *Submission 4: A Study of Cell behaviour on Engineered Surfaces*. This describes an experiment carried out to determine the effect of surface topography on cell behaviour. The original intention was to use RP techniques to create a number of different scaffolds on which to culture cells. This proved difficult and marked a shift in emphasis from RP to conventional processing methods. This study highlighted the effect of both the material and surface topography on cell growth and allowed the author, who is an engineer by training, to gain an understanding of the biological aspects inherent in this field. The next piece of work, *Submission 5: The Development of a Methodology to Manufacture an Innovative Bone Graft Substitute*, further describes the thought processes and empirical approach to this research that shaped the direction of this project. Many different manufacturing techniques were attempted prior to identifying an innovative concept for manufacturing a novel BGS. It culminates in describing the author's attempt to extrude ceramic monoliths on a severely limited budget and the realisation that industrial assistance would be essential.

Submission 6: Extrusion of Ceramic Monoliths for use in Bone Graft Substitutes or Bone Scaffolds describes the work undertaken in conjunction with an industrial partner to manufacture calcium phosphate (CAP) monoliths. HA was chosen as a benchmark material and it rapidly became apparent that HA could be manufactured in this way. Hence, a set of experiments were so designed as to examine their mechanical and biological performance, both of which proved to be excellent when compared with an existing BGS material. The final piece of this work: *Submission 7 – A clinical perspective on the benefit of extruded monoliths for Bone tissue Engineering* delves into the clinical need for bone graft materials in greater detail to identify specific indications where ceramic monoliths may be beneficial. A combination of expert and clinical opinion combined with reviews of relevant literature helped identify an indication where the high strength BGS material created through this research will improve on existing products.

1.3 Structure of the Innovation Report

This report has been structured in such a way as to guide the reader through the topic and highlight the most important aspects when considering the creation of a novel BGS. The report begins with a background section which covers all aspects of this field and then continues to describe the underlying principles of the research methodology and highlights of the research. The main focus for this work has been on manufacturing aspects. This report presents the methodical research undertaken which has led to an innovative approach to manufacture a high strength BGS material. It describes the key innovative aspect in further detail before presenting the design for a medical device utilising this technology. Finally, it summarises the project and discusses areas for future work.

Chapter 2 presents the background of the project including a description of bone and its properties. This is followed by a glimpse at the conditions that effect human bone and the bone grafting techniques available to replace diseased bone. This includes some recent developments in tissue engineering i.e. the use of biological materials to replace or repair tissue. Finally, this chapter reviews the key requirements for a BGS and briefly examines the market opportunities for BGS materials.

Chapter 3 explains the project methodology in a chronological fashion. It starts with the experiments using RP techniques and explains the reasons why later work concentrated on conventional processing techniques as the primary route to produce a novel BGS. This Chapter then elucidates the conventional processes attempted which led to the discovery that extrusion of ceramic monoliths for use as BGSs had not been previously attempted. The remainder of the chapter examines the production of hydroxyapatite monoliths and their physical, mechanical and biological characterisation.

Chapter 4 presents the results from the characterisation of the HA monoliths including their excellent mechanical and biological properties and goes on to compare their performance with an existing commercial BGS. Chapter 5 defines the unique selling points for calcium phosphate monoliths and how they may prove beneficial to patients and clinicians in

challenging orthopaedic cases. This Chapter then summarises the comments made by a number of clinicians and experts on the novel BGS produced as a result of this project.

Chapter 6 considers one of the clinical conditions identified in Chapter 5 and describes the design process of a device for posterior lumbar interbody fusion utilising the innovative BGS material devised during this project. The Chapter then highlights the hurdles that need to be overcome in order to gain approval for such a device.

Chapter 7 is an overview of the project and elucidates the key findings and innovations from the project and the recommendations for future research work. Chapter 8 presents the conclusions derived from this work.

Chapter 2 Background

2.1 Introduction

The human skeleton has a number of functions: it protects internal organs, provides muscle attachment sites to facilitate limb movement, acts as a store for calcium and phosphorus, and provides a site for haematopoiesis [1,2]. The adult skeleton contains 206 bones [3], each one is able to maintain its shape and structure throughout the life of an individual through a continuous process of remodelling. This allows it adapt to the stresses and strains placed upon it according to Wolff's Law [4-6].

2.2 Bone

Bone is a biological composite comprising 90 % extracellular matrix (ECM) and 10 % water [7]. The ECM is composed of 60 – 70 % inorganic mineral usually referred to as hydroxyapatite (HA) which has a similar, but not identical structure to natural bone mineral. HA has a chemical formula of $\text{Ca}_{10}(\text{PO}_4)_6(\text{OH})_2$ and a Calcium Phosphorus (Ca:P) ratio of 5:3 (1.66). Bone apatite is believed to be a carbonate apatite called *dahlite* that is thought to resemble an octacalcium crystal which naturally forms in plates. It is characterised by calcium, phosphate, and hydroxyl deficiency with typical Ca:P ratios between 1.37 and 1.87 [8]. The remaining 30 – 40 % of bone ECM contains organic components composed of type I collagen (90 %) with non-collagenous proteins e.g glycosaminoglycans constituting the remainder. The collagen confers flexibility and fracture toughness to the matrix and the inorganic phase confers stiffness.

Macroscopically two types of bone exist. Cortical bone (also known as compact or dense bone) forms the outer shell of all bones and has a dense structure representing approximately 80 % of skeletal mass. Cancellous bone (also known as spongy or trabecular

bone) has a porous structure and is found in the centre of all bones. Figure 2.1 shown below is a detailed view of the tibia. It demonstrates the layout of cortical and trabecular bone within the tibia as well as the important anatomical features. At the bottom right a detailed section through the bone demonstrates the porous sponge-like structure of trabecular bone surrounded by dense cortical bone.

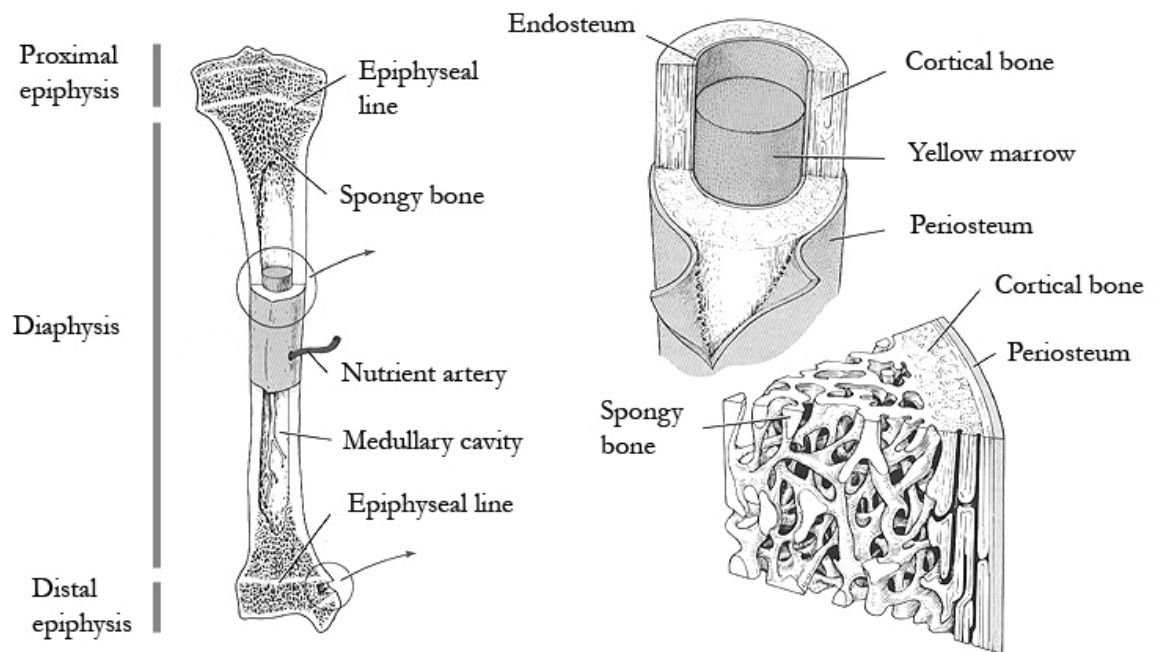


Figure 2.1 An anatomical drawing of a human tibia, adapted from [3]

The structure of bone is hierarchical in nature with different features that exist on many levels of scale. Where Figure 2.1 is concerned with the macroscale features or those that can be seen with the naked eye. Figure 2.2 demonstrates the microscale features which include osteons, lamellae, canaliculi, and haversian canals. The Haversian canal in the centre of the osteon has a diameter ranging from 50 – 90 μm , within which there is a blood vessel typically of 15 μm in diameter [9,10].

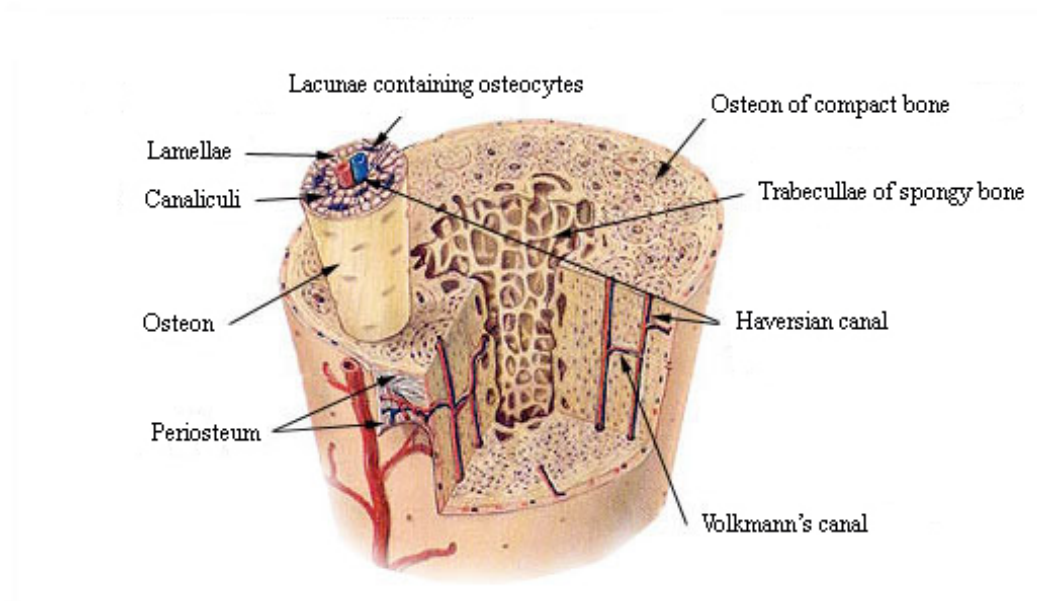


Figure 2.2 An illustration demonstrating the anatomical features from a section through a human long bone [9]

Beyond the microscale features are the nanoscale features consisting of collagen fibres that make up the osteons. These collagen fibres are made up of many collagen fibrils and in the gaps between these are the mineral crystals. The collagen fibres consist of arrays of tropocollagen molecules which are composed of three left-handed helices of peptides known as α -chains. These are subsequently bound in a right handed triple helix thus making up the collagen fibril with a diameter of 40 to 120 nm. These fibrils are wound into bundles of collagen fibre with a diameter of 0.2 to 12 μm as seen in Figure 2.3.

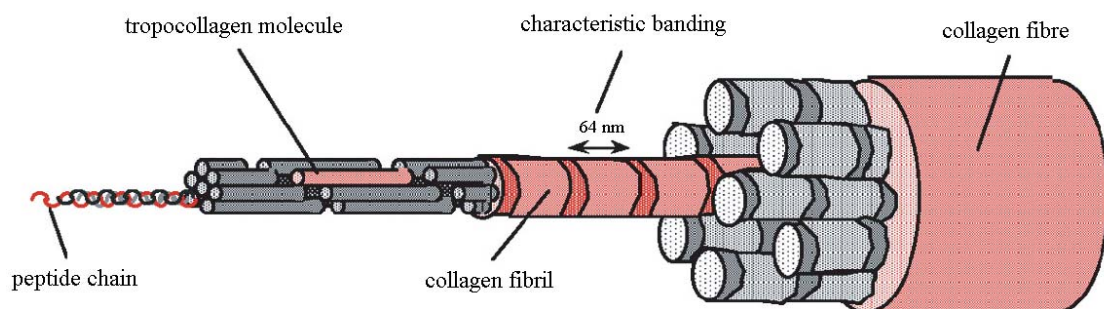


Figure 2.3 An illustration demonstrating the hierarchical organisation of collagen fibres [8]

Adult bone contains four cell types each with a specific set of functions. Osteoprogenitor cells are mesenchymal cells of bone. They differentiate into osteoblasts when new bone is required, or lie quiescent and are known as bone lining cells when bone is not needed. Osteoblasts are bone forming cells that deposit osteoid matrix onto the collagen fibres and control the subsequent mineralisation of woven bone into lamellar bone. Osteocytes are osteoblasts that have become entombed by mineralized matrix and may remain in this state for years and even decades. Osteocytes regulate the composition of bone matrix via ion-nutrient exchange thus maintaining the calcium and phosphate levels in serum. Osteoclasts are large, multinucleated cells able to break down calcified bone matrix. They originate from haemopoietic progenitor cells and can attach themselves to bone where they erode it via acidic digestion [7]. Bone is laid down in a highly ordered manner *in vivo*, where osteoblasts lay down bone in the space created by previous osteoclast resorption. Thus, the structure and morphological layout of the bone is preserved [11].

Bone can only be formed by deposition on a suitable surface that is within 200 μm of a blood supply so that it can receive nutrients via diffusion. These two criteria place limitations on the shape and size of developing bone which may form either by intramembranous ossification (in the case of skull and facial bones) or endochondral ossification (in the case of long bones). Intramembranous ossification starts after 6.5 weeks of gestation and occurs when a primary ossification centre develops in a slab of mesenchyme tissue. Here bone forming cells differentiate from mesenchymal cells and bone is formed without the need for cartilage. Endochondral ossification occurs by calcification of cartilage tissue. This occurs during growth of the foetal skeleton where the limbs need to grow in length and diameter. Bones are rigid and not able to achieve this; therefore cartilage is formed as an intermediary tissue and later calcified. Regions of cartilage persist on the bone ends and within the epiphyseal growth plate until bone stops growing in late adolescence [2,7]. Bone remodelling is a continual process of resorption and renewal that continues throughout the life of all mammals. It is defined as removal and replacement of bone tissue without altering its overall shape.

The mechanical properties of bone are remarkable and make it challenging to replicate. It possesses excellent strength, stiffness, and fracture toughness whilst also being porous and able to support the growth of cells and repair itself. Its properties derive from the size, shape, and organisation of the mineral and matrix phases throughout its structural hierarchy [12]. There is a large variation in the reported properties of bone due to many factors including its anisotropy, person to person variation, use of aged or osteoporotic bone, and the anatomical location of the tested specimen [1,13]. The compressive modulus for cortical bone lies in the range 5 – 35 GPa and compressive strength 50 – 250 MPa. The tensile modulus varies from 4 – 30 GPa and tensile strength 90 – 170 MPa [13-18]. It is important for any implant replacing bone to match both the strength (so it will not fail in service) and stiffness of the native bone to prevent problems with stress shielding (when the implant is too stiff) and excessive movement (when the implant has inadequate stiffness). Both may lead to resorption of the native bone and failure of the implant [13].

Table 2.1 provides a summary of the strength and modulus values for cortical and cancellous portions of human long bones [16]. It is immediately apparent that cortical bone is at least an order of magnitude stronger and stiffer than cancellous bone. This is due to the differing levels of porosity with cancellous bone having significantly greater porosity (30 – 90 %) compared with cortical bone (8 – 28 %). The minimum mechanical properties for a structural bone graft material are a compressive modulus of approximately 5 GPa, tensile strength ~ 90 MPa and compressive strength ~ 90 MPa.

Table 2.1 Summary of human long bone mechanical properties [13-18]

	Cortical bone	Cancellous bone
Compressive Strength (MPa)	50 – 250	1.5 – 10
Compressive Modulus (GPa)	5 – 35	0.05 – 0.9
Tensile strength (MPa)	90.6 – 170	-
Tensile modulus (GPa)	3.9 – 29.2	-
Torsion strength (MPa)	3.1 – 7.4	-
Torsion modulus (GPa)	5 - 71	-
Bending strength (MPa)	103 – 238	-
Bending modulus (GPa)	68 – 98	-
Bulk porosity (%)	8 – 28	30 – 90
Pore size range (µm)	5 – 200	1 – 900

Healing is the natural response to injury through which dead tissue is replaced by living tissue and bone possesses the ability to heal itself. Fracture healing occurs in two ways: with callus and without. Healing with callus typically occurs in tubular bones in the absence of rigid fixation. The precise number of defined stages in the healing process varies depending on author [19-21] but typically the process of fracture healing occurs in five stages. First is tissue destruction and haematoma formation where the damaged blood vessels form a haematoma within and around the fracture site, whilst bone at the fracture surfaces dies as a result of the loss of blood supply. The next stage is inflammation and cellular proliferation which occurs within 8 hours of the fracture. During this stage there is inflammation and proliferation of cells surrounding the fracture. The clotted haematoma is slowly absorbed and infiltrated by blood vessels and a callus forms around the fracture. Osteoclasts now begin to remove dead bone whilst osteogenic and chondrogenic cells create immature or 'woven' bone from the callus. Over time the callus is progressively mineralised eventually uniting the fracture. The woven bone is then consolidated into lamellar bone by the action of osteoblasts and osteoclasts. This process is slow and it may be months before the bone is strong enough to carry normal loads. Finally remodelling occurs over a period of years to remove excess bone laid down during the healing process and strengthen the union.

Healing without callus occurs when the fracture site is immobile as in the case of internal fixation. It occurs in the same manner except that a large callus does not form since it is not required to maintain the integrity of the fracture. The rate of fracture healing will depend on the type of bone involved (cancellous bone heals faster than cortical bone), the state of the blood supply (poor circulation results in slow healing), the patient's general health, and finally the age of the patient. Healing can be twice as fast in children as in adults. For the majority of simple fractures bone healing will proceed normally within a period of weeks or months. However problems with non union occur in up to 10 % of cases and there are many other instances in which larger bone defects occur that require surgical intervention [22].

All bodily organs including bone are susceptible to pathological conditions and age related degeneration that may require repair through surgical reconstruction. Defects in bone arise principally as a result of disease, trauma, infection or genetic abnormality [23]. When these

defects go beyond a 'critical' size (which depends on the age, health and lifestyle of the patient) they will not heal spontaneously and any void will be rapidly filled with fibrous tissue produced by fibroblasts. These are present throughout the body and are able to proliferate rapidly. Once this fibrous connective tissue is present it prevents any tissue repair or replacement from taking place. Thus, biodegradable membranes, scaffolds, and graft materials are essential to prevent undesirable tissue ingrowth and enable the body to heal critical sized bone defects.

There are an enormous number of diseases and bone disorders which may lead to the requirement for bone graft including neurological afflictions (poliomyelitis, cerebral palsy and spina bifida), endocrine disorders (osteoporosis, hypopituitarism and acromegaly), metabolic bone diseases (osteomalacia, rickets and hyperparathyroidism), abnormal bone development (achondroplasia or osteogenesis aclasis), bone disorders (cystic changes or tumours) or spinal conditions (degenerative disc disease, spondylolisthesis or scoliosis). Cancer often leads to the need for limb amputations although recent advances in the staging, diagnostic imaging and treatment of musculoskeletal sarcomas has led to an increase in the number of limb salvage operations (up to 90 %) as an alternative to amputation. The survival rate for limb sparing surgery has been shown to be similar to those treated with amputation. Local resection of the tumour and reconstruction has become the most common route for management of bone tumours [24-26].

In the case of traumatic injuries where the patient is in otherwise good health then healing of major injuries should proceed normally. Complications may occur when these injuries are combined with other diseases, infection or disruption to the blood supply (avascular necrosis, osteonecrosis, aseptic necrosis or ischemic bone necrosis). This usually occurs at the ends of long bones as a result of traumatic disruption to the blood supply, from long term use of medications (cortico steroids) or excessive long term alcohol consumption. Infection of bone (osteomyelitis) is classified into acute and chronic.

Acute osteomyelitis occurs when bacteria, typically staphylococcus aureus enter the bone via the blood stream. It causes severe pain and tenderness over the involved bone accompanied by a fever. The bacteria multiply in the bone causing pus to form which eats away at the

bone and causes an abscess. Treatment via antibiotics, surgical drainage and curettage is usually successful although chronic osteomyelitis may develop from unsuccessful treatment of acute symptoms, surgery or open fractures where the bone has become contaminated [27]. In severe cases the bone requires resection and replacement with graft material or other implant. If the infection persists amputation may be required.

In the same way that there a great number of diseases which affect humans there are also a large number of bone abnormalities that may arise from genetic or environmental circumstances. These may lead to under or over production of bone (fibrodysplasia ossificans progressiva), weak bones (osteogenesis imperfecta) or unusual growth of bones. Any one of these situations may require surgical intervention with the use of bone graft to correct.

Figure 2.4 illustrates the human skeleton and highlights the areas where bone graft procedures are commonly required. These regions include the specialisms of neurology, orthopaedics, ophthalmics, maxillofacial and dentistry and whilst bone grafts may be required anywhere on the skeleton the ends of long bones, the cervical and lumbar spine, maxilla and mandible, and extremities are the most commonly affected areas.

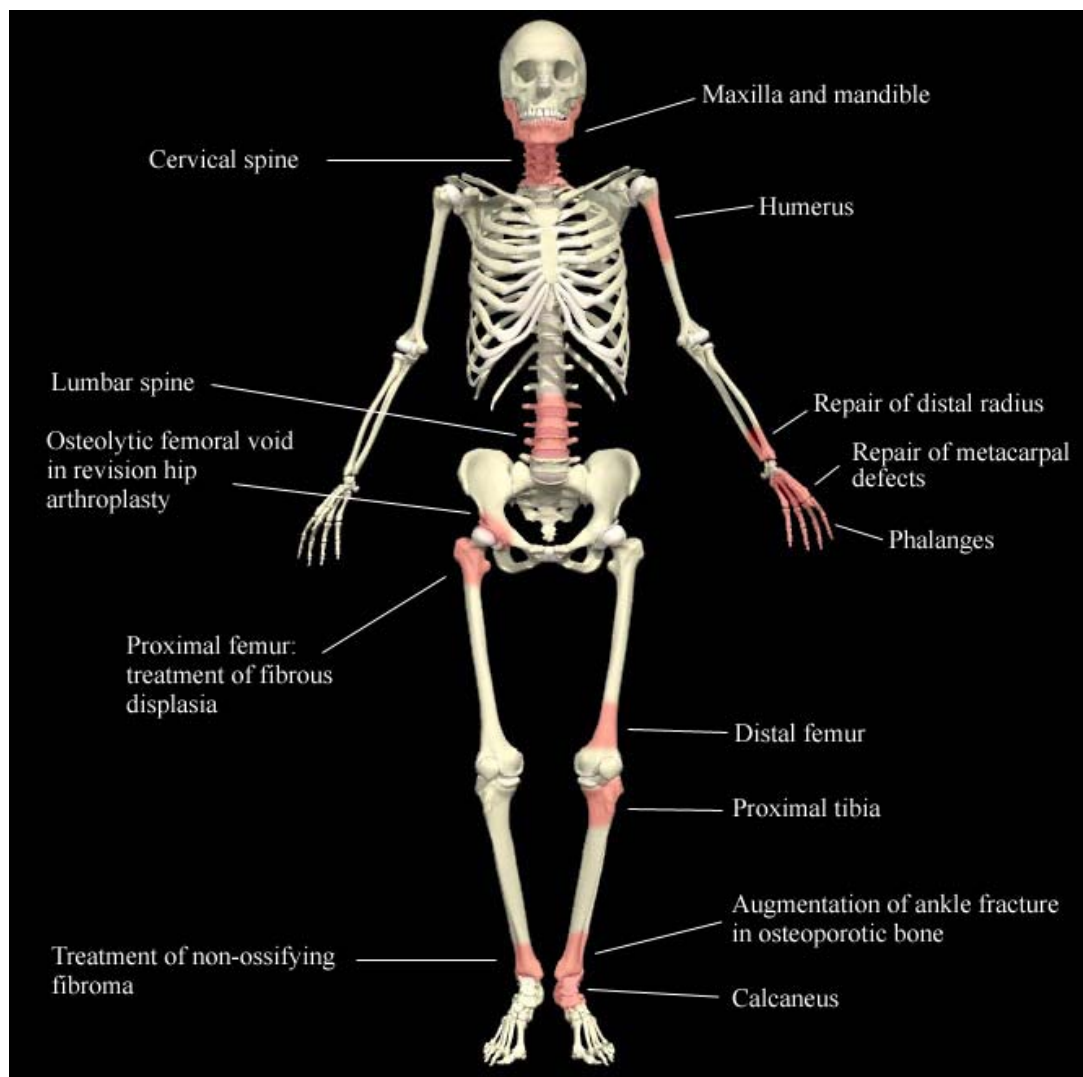


Figure 2.4 An illustration of a human skeleton highlighting the areas where bone graft materials are commonly required

2.3 Current bone grafting solutions

Historically, orthopaedic reconstruction has made extensive use of non degradable materials e.g. stainless steel, titanium, or alumina to replace bone tissue. These devices are associated with long term problems such as loosening, fracture, and the biological reaction to wear debris and metallic ion release [24]. In order to spare the patient from a retrieval operation and reduce the overall resource required to carry out this procedure, considerable effort is being directed towards the development of degradable implants. This modern approach is marked by a shift in emphasis from replacement to regeneration of tissues by use of materials which degrade over a period of time and are replaced by native tissue [28]. When a bone graft is required the primary route for the surgeon is to transplant bone from another site on the same individual for use at the defect site, this is known as autograft. When this is not available bone donated from another member of the same species (allograft), from another species (xenograft) usually porcine or bovine in origin, or synthetic materials may be used [29]. Since 1940 autografting has been used extensively in maxillofacial surgery but it was not until the 1980s that allograft bone banking, vascularised autograft and bone graft substitutes (BGSs) became routinely available [29,30].

Autograft is considered as the ‘gold standard’ in terms of performance. This technique promotes osteogenesis, osteoinduction and osteoconduction. Osteogenesis is the creation of new bone via cells and proteins within the graft, osteoinduction is the biologically mediated recruitment or differentiation of pluripotent cells into chondrocytes and osteoblasts essential for bone formation and osteoconduction is the facilitation of blood vessel ingrowth into a three dimensional (3D) scaffold [26,31,32]. Autograft has no associated risk of viral transmission, excellent success rates, offers structural support and is eventually remodelled into the surrounding bone through creeping substitution. Unfortunately, there are few sites from which bone can be harvested without serious complications. The iliac crest is most commonly used but bone can also be harvested from Gerdy’s tubercle, the distal radius, and the distal tibia. Its availability is limited, and often severely limited when it is required for the most challenging cases. Autograft harvest requires a separate surgical procedure with associated risks, costs and time [8]. Furthermore autograft is associated with 8.5 – 20 % risk of complications which include blood loss, nerve

injury, hernia formation, infection, arterial injury, fracture, cosmetic defects and chronic pain [33,34].

Allograft is available off the shelf from bone banks in a number of geometric forms and has excellent mechanical properties although these vary from batch to batch. It has been associated with delayed healing, poor remodelling [35], and disease transmission [36]. It is also expensive at around £250 for a femoral head (a revision hip arthroplasty may require 4 – 6 donor hips [8]) and often has limited availability [37]. Recent reports in the press describing the illegal removal of cadaver bones from diseased bodies for the allograft black market have raised serious concerns about the quality and safety of this product [38].

The US Navy Tissue Bank was established in 1951 and since then strenuous efforts have been made to improve the safety of bone banking. These include the exclusion of donors with systemic or infective disease and screening for human immunodeficiency virus (HIV) and other viruses. There have been reported cases of HIV transmission and bacterial contamination from allograft bone. As a result, bone banks now undertake secondary sterilisation although this degrades the mechanical properties of the bone. Both allograft and xenograft are highly immunogenic and can stimulate a potent incompatibility reaction. This can be improved by processing the bone, for example by freezing, freeze drying, gamma irradiation or chemical means. This eliminates any osteogenic capacity leaving only an osteoconductive scaffold. Xenograft has similar performance to allograft but with the additional risk of animal derived diseases including bovine spongiform encephalopathy (BSE) [29].

The drawbacks with conventional grafting methods have led to a great deal of research and development into synthetic alternatives known as bone graft substitutes (BGSs) or bone scaffolds. These can be broadly classified by their constituent material: polymer (synthetic and natural), ceramic, glass or a composite of two or more. The most common polymeric materials in use belong to the polyester family and a subset of this the poly(α -hydroxyacids). These contain polylactide (PLA) and polyglycolide (PGA) which have excellent mechanical properties and can be combined to alter the rate of degradation. They degrade to monomeric acids and then carbon dioxide via respiration and the citric acid cycle in the

kidneys [39,40]. These degradation products are acidic and may lead to a local decrease in pH around an implant and subsequent cell lysis. For this reason they are often combined with calcium phosphate filler materials e.g. hydroxyapatite (HA) or tricalcium phosphate (TCP) which serve to reinforce the matrix and neutralise the surrounding environment due to their basic degradation products [41-43].

The calcium phosphates have also been used on their own because of their excellent biocompatibility and osteoconductivity. Recent work has determined that macrostructure, microstructure, and chemical composition are critical to their osteoinductive potential although the precise mechanisms behind this are not fully understood [33,44,45]. Of the glassy materials, the most famous is Bioglass® (45S5) developed by Hench *et al* in 1969 and available in resorbable and non resorbable variants [46]. It exhibits a strong bond to bone, has been shown to upregulate the expression of genes related to osteoblast activity [47,48], and has found extensive use in maxillofacial and dental applications. Its moderate mechanical properties limit its use as a BGS for load bearing applications.

The principal advantages of BGSs are unlimited supply, easy sterilisation and storage, predictable mechanical properties, excellent bone ingrowth and moderate cost [49]. There is an ever expanding choice of BGSs available on the market, typically in the form of powders, granules or blocks. These are summarised in

Table **2.2** which elucidates the manufacturer and brand name, material, published information on porosity and strength and approved indications. Establishing the cost for each BGS proved extremely challenging since the price paid varies between institutions and as such they are commercially sensitive. The majority of these BGS materials are indicated as fillers for bony defects which are not intrinsic to the stability of the skeleton, those that are able to offer some structural support for the skeleton are dense materials [50-73]. Few are indicated for use at infected sites or in the presence of systemic disease. Load bearing capacity is not essential for all indications particularly if the material is mixed with bone marrow aspirate and allowed to clot before use. This forms a highly osteoinductive bone graft with excellent handling properties, able to fill large non structural defects e.g. acetabular defects after revision hip arthroplasty and posterolateral lumbar fusions.

Table 2.2 BGS materials available in the market in 2009

Manufacturer & brand name	Availability	Material	Strength	Porosity	Structural	Not intrinsic to stability	Use in infected area	Systemic disease	Ref's
AAP									
Cerabone	granules and blocks	Bovine derived HA	Low	100 – 1500 μm	N	Y	N	N	[50,74]
Ostim	Injectable paste	HA	Moderate	N/A	N	Y	N	N	[50,74]
PerOssal	Porous morsels	Nano HA	N/A	High	N	Y	Y	N	[50]
Apatech									
Actifuse	Granules, mouldable paste	Si substituted HA	N/A	High	N	Y	N	N	[51,74]
Berkeley advanced biomaterials									
Bi-Ostetic	Blocks and granules	60% HA 40% β -TCP	N/A	high	N	Y	N	N	[74,75]
Cem-Ostetic	Injectable paste	Nano HA	Low	N/A	N	Y	N	N	[75]
GenerOs	Granules	B-TCP	N/A	high	N	Y	N	N	[52,75]
Biocomposites									
Stimulan	Pellets or injectable paste	Calcium Sulphate	N/A	N/A	N	Y	Y	N	[53]
Allogran N	pellets	HA	N/A	N/A	N	Y	N	N	[53]
Allogran R	pellets	β -TCP	N/A	N/A	N	Y	Y	Y	[53]
Gene X	Injectable paste	Biphasic CaP	N/A	N/A	N	Y	N	N	[53,54]
Biomet									
Endobon	Blocks or granules	Bovine derived HA	Low	45-85% 100-1500 μm	N	Y	N	N	[55]
Calcibon	Paste or granules	Carbonated calcium deficient HA	4-7 MPa comp.	150-550 μm	N	Y	N	N	[55]
Collapat II	Fleece	Collagen & HA	N/A	N/A	N	Y	Y	Y	[55]
Biogran	300 μm granules	45S5 Bioglass	N/A	N/A	N	Y	N	N	[55]
Mimix	Injectable paste	Tetra calcium phosphate & α -TCP	20 MPa comp.	200 μm	N	Y	N	N	[55,74]
OsteoStim	Granules	Calcium sodium phosphate	N/A	N/A	N	Y	Y	N	[55,74]
CAM implants									
CamCeram	Blocks and granules	60% HA 40% β -TCP	Low	High	N	Y	N	N	[56,74]
Ceramisys									
ReproBone	granules	60% HA 40% β -TCP	N/A	> 80 %	N	Y	N	N	[57,74]

PermaBone	granules	HA Non resorbable	N/A	N/A	N	Y	N	N	[57,74]
Ceraver									
Calciresorb	granules	β -TCP	N/A	N/A	N	Y	N	N	[74,76]
Cerapatite	granules	HA	N/A	N/A	N	Y	N	N	[76]
Calciresorb 35	granules	65% HA 35% β -TCP	N/A	N/A	N	Y	N	N	[76]
Ceraplast	Injectable paste, pellets	Calcium Sulphate	N/A	N/A	N	Y	N	N	[76]
Curasan									
Cerasorb	Blocks and granules	β -TCP	N/A	high	N	Y	N	N	[74,77]
DePuy									
α -BSM	Injectable paste	Calcium phosphate with Ca:P = 1.45	N/A	low	N	Y	N	N	[58,74]
Healos	Sheets	Type I bovine collagen & HA	N/A	N/A	N	Y	N	N	[59,60]
Dot GmbH									
BONITmatrix	Granules	13% silicon dioxide (w/w) HA & β -TCP (60:40)	N/A	100 – 1000 μ m	N	Y	N	N	[61,74,78]
Exactech									
OpteMX	Granules, wedges, blocks	60% HA 40% β -TCP	N/A	70 %	N	Y	N	Y	[74,79]
IsoTis									
OsSatura BCP	Granules	80% HA 20% β -TCP	N/A	75%	N	Y	N	N	[63,64]
OsSatura TCP	Granules	β -TCP	N/A	75%	N	Y	N	N	[80]
Kasios									
TCP	granules, blocks and wedges	Pure β -TCP	N/A	200-500 μ m 60–80 %	N	Y	N	N	[65]
TCH	granules, blocks and wedges	75% HA 25% β -TCP	N/A	200-500 μ m 60–80 %	N	Y	N	N	[65]
JectOs	Injectable paste	55% DCPD 45% β -TCP	N/A	< 5 μ m 40 %	N	Y	N	N	[65]
Kyocera - Japan Medical Materials									
Osteograft-S	Blocks or granules	HA	N/A	N/A	N	Y	N	N	[66,74]
Mitsubishi Pharma									
Biopex	injectable paste	HA	N/A	N/A	N	Y	N	N	[74]
Novabone									
Putty	Injectable putty	45S5 Bioglass	N/A	N/A	N	Y	N	N	[67,74]
PerioGlass	particles	45S5 Bioglass	N/A	N/A	N	Y	N	N	[67,74]
MPB	Blocks and granules	45S5 Bioglass	N/A	High	N	Y	N	N	[67,74]
Olympus Terumo									
OSferion	block and granules	B-TCP	N/A	100- 400 μ m 75%	N	Y	N	N	[68,74,81]

OSferion 60	block and granules	B-TCP	15 – 20 MPa	100-400µm 60%	N	Y	N	N	[81]
Bonaceram P	blocks and granules	HA	N/A	50-300 µm 35-48%	N	Y	N	N	[81]
Bonaceram K	blocks and granules	HA	N/A	Dense	Y	Y	N	N	[81]
Olympus spine (Orthogem)									
Tripore	blocks and granules	HA/TCP	N/A	N/A	N	Y	N	N	[74,82]
Orthovita									
Vitoss	blocks and granules	β-TCP	N/A	100 – 1000 µm 90 %	N	Y	N	N	[74,83]
Cortoss	Injectable paste (Non resorbable)	Bisphenol-A dimethacrylate & baria-boroaluminosilicate glass	N/A	N/A	Y	Y	N	N	[74,83]
Ossacur									
Colloss	Cotton like	Collagen-lyophilisate	N/A	N/A	N	Y	N	N	[55,84]
Targobone	Cotton like	Collagen-lyophilisate	N/A	N/A	N	Y	Y	N	[85]
OsteoBiologics (now Smith & Nephew)									
Polygraft	Granules, cylinders, blocks	PLGA, calcium sulphate, PGA fibres	N/A	high	N	Y	N	N	[69]
Pentax									
Apaceram	powder and block	HA	N/A	N/A	N	Y	N	N	[74,86]
Smith and Nephew									
Jax CS/TCP	granules	Calcium Sulphate or β-TCP	N/A	N/A	N	Y	N	N	[87]
Styker									
HydroSet	Injectable cement	HA	N/A	N/A	N	Y	N	N	[74,88]
BoneSource	injectable cement	HA	No	No	N	Y	N	N	[74,88]
BoneSave	granules	80% β-TCP 20% HA	No	No	N	Y	N	N	[74,88]
Synthes									
Norian SRS	injectable paste	Carbonated apatite	N/A	N/A	N	Y	N	N	[74,89]
ChronOs	Granules and blocks	β-TCP	N/A	N/A	N	Y	N	N	[74,89]
Therics									
TheriLok TheriWedge	Granules, wedges, blocks	β-TCP	N/A	N/A	N	Y	N	N	[73]
TheriGraft	injectable putty	β-TCP	N/A	N/A	N	Y	N	N	[73]
Wright									
Osteoset®	Pellets and	Calcium	N/A	N/A	N	Y	Y	N	[90]

	injectable putty	Sulphate							
Cellplex	blocks and granules	TCP	N/A	N/A	N	Y	N	N	[74,90]
Zimmer									
CopiOs	granules and blocks	Calcium phosphate and type I collagen	N/A	N/A	N	Y	N	N	[72,91]

There is currently a need for structural synthetic bone graft materials that can be used as a substitute to allogeneous or autogenous graft materials in large defects, for example in resections for infection or tumour. In these instances bone grafts can be as large as 20 cm and their location (joints, spine, and long bones) require them to be able to bear load and be used with instrumentation to maintain the stability of the skeleton. A graft material capable of replicating the properties of allograft without its inherent risks would represent a major step forward in bone grafting. Furthermore, a BGS material with cortical bone matching mechanical properties may prove beneficial in other indications e.g. interbody spinal fusion where high strength and osteoinductivity are required to ensure rapid fusion.

An important area for consideration is how the healing environment alters according to anatomical location e.g. metaphyseal defects, long-bone fractures, interbody spine fusion or posterolateral spine fusion. Each will have different levels of difficulty in forming new bone, metaphyseal defects may only require an osteoconductive material whereas a posterolateral fusion will not succeed with a purely osteoconductive material as a result of the poorer blood supply. A poorly vascularised site will lead to problems with nutrient diffusion into the graft and affect the maximum size of the defect that can be successfully treated [31]. Therefore, it is important to validate that a material will work as intended for each site into which it is implanted [26].

In challenging cases it is often not enough to use a purely osteoconductive material and new techniques are required, for example, tissue engineering. This requires a new and multi-disciplinary understanding of materials that considers many new factors which include: developmental biology, genetic engineering, and cell biology as well as the surgical techniques required for their use. A satisfactory outcome when repairing any defect is dependent on restoration of an adequate blood supply and the ability to maintain implant

stability and controlled loading whilst repair is underway. Large structural defects present the greatest clinical challenge and in order to improve the chances of successfully repairing them it is necessary to consider the use of tissue engineering [92]. This is examined in the following section.

2.4 Tissue Engineering

Tissue engineering (TE) is the regeneration of tissues through an in depth understanding of the complex mechanisms and processes occurring in the human body by combining knowledge from many disciplines [93]. Engineers, materials scientists and chemists examine methods to create a bone-like scaffold whilst life scientists examine the body's response to them at the same time as searching for methods to accelerate and improve the likelihood of successful healing. In this respect there are five main strategies being pursued: (i) *in situ* targeting of connective tissue progenitor cells (PCs), these originate from stem cells, have finite potential to self renew and generally give rise to one or more differentiated phenotypes, (ii) homing of connective tissue PCs, (iii) transplantation of connective tissue PCs, (iv) transplantation of culture expanded cells, and (v) transplantation of genetically modified cells.

In situ targeting (i) is the promotion of desired tissue formation by stimulating activation, proliferation, and differentiation of PCs. A BGS aims to prevent the encroachment of adjacent tissues and provide a surface on which cells can attach. Examples of targeting include the use of acellular BGSs combined with locally delivered growth factors [94,95], stimulation by mechanical or magnetic means and use of systemic pharmacological methods. Growth factors were discovered by Marshal Urist when he found that demineralised bone matrix (DBM) can induce the transformation of mesenchymal stem cells into osteoblasts which then form bone [96]. These osteoinductive agents are known as bone morphogenetic proteins (BMPs) and are members of the transforming growth factor beta (TGF- β) superfamily. There are currently two BMP products approved by the Food and Drug Administration (FDA), Stryker Biotech osteogenic protein OP-1 (rhBMP-7) indicated for anterior lumbar interbody fusions (ALIF) and open tibial fractures, and Medtronic Sofamor Danek Infuse[®] bone graft (rhBMP-2) indicated for recalcitrant long bone nonunions and

revision posterolateral spinal arthrodeses. These have a potent osteoinductive effect and can be used alone or more commonly in combination with a carrier material. BMP materials are costly although recent trials have shown that the high upfront cost is offset by a decreased length of hospital stay as well as a reduction in post surgery complications [97]. A potential complication of BMP use is leakage to surrounding tissues resulting in bone formation at unintended sites. Hence delivery and containment of the BMP is essential for success.

Homing (ii) is the recruitment of cells from the circulatory system. Recent studies suggest that therapies may become available which direct osteoprogenitor cells to the site of bone repair via the circulatory system. Transplantation of autologous bone (iii) is of particular benefit in regions which have been compromised by previous trauma, infection, irradiation, scar or poor blood supply. Bone marrow aspirate (BMA) can be used to extract the relevant cells without the inherent risks of taking autologous bone, this can be combined with acellular BGSs to enhance the rate of healing. Mesenchymal stem cells from a number of human tissues including muscle, adipose, and bone marrow can be expanded *in vitro* (iv) and used to regenerate bone, muscle, tendon and cartilage [98]. The cell expansion is able to generate a large number of PCs but at significant cost and risk in terms of contamination with bacteria or reduction in the proliferative capacity of the cells. Cells lack the ability to form three-dimensional (3D) structures instead they randomly migrate to form a two-dimensional (2D) layer of cells [99]. Therefore bioreactors are used to culture the cells onto 3D matrices [100]. It is also possible to use the human body as a natural bioreactor either by implanting the scaffold into a highly vascularised ectopic (muscular) site which will result in the rapid vascularisation of the scaffold or by injecting a hyaluronic acid gel into a surgically created void between the periosteum and native bone. This will be converted to bone over a period of weeks [101,102]. This technique is currently applied clinically for repair of cartilage defects and clinical trials are underway for repair of bony defects.

The transplantation of cells which have been genetically modified (v) to secrete osteogenic proteins is known as gene therapy. It has shown tremendous promise for treatment of massive bone loss but recent clinical trials led to two deaths, an outcome not acceptable for the treatment of non fatal musculoskeletal conditions [103,104]. In many cases where promising results have been obtained for bone healing via the previously mentioned

strategies there is a lack of clinical evidence with few randomised clinical studies and no cost *versus* benefit analysis [22]. A more elegant solution is to harness the natural power of the body to heal bone defects by creating a BGS with inherent osteoinductive properties. Recent work has found that growth factors or biocatalysts are not necessary in tissue engineering. This is primarily because the surface properties of the material can be tailored to affect the cell response to the implant [105] and secondly because human blood contains all of the cells and signalling molecules that are necessary for the healing of bone defects. Any object implanted into the body will generate an immune response and hence inflammation. Following this a number of cells, specifically PCs which are able to differentiate into any type of cell. It is the function of the BGS to recruit relevant cells and control the process of cell differentiation such that it is colonised with cells and eventually bone.

An important area of current research is concerned with investigating how cells respond to an implant as a result of its surface properties. These may be inherent to the material or created through surface modification techniques. Research to date makes it clear that material surface properties, such as roughness, wettability, surface mobility, chemical composition, electrical charge, and crystallinity can have a profound effect on cell response [41]. The cellular response to most synthetic biomaterials is greatly influenced by surface chemistry. Surfaces only acquire biological activity after a layer of protein is adsorbed onto the surface which provides anchorage sites for cells, nutrients, and signalling epitopes that control cell behaviour [106]. It is believed that the chemical properties of a surface directly influence cell behaviour via plasma membrane contact. Different cells types react differently to material surfaces therefore tailored surfaces can be developed to suit a range of different *in-vivo* applications. The following section highlights the essential requirements of a BGS.

2.5 Specifications for a BGS

The specification for an ideal BGS is covered extensively in Submission 3. The creation of a 'bone like' graft material is not a simple task, there are a number of important aspects that must be considered. A synthetic graft material requires suitable mechanical properties to resist the dynamic stresses and strains imposed upon it according to its anatomical location and skeletal movement. It must have a porous surface and completely open porosity with fully interconnected pores to facilitate the ingrowth of bone, initially via angiogenesis and then through the normal bone remodelling process. Porosity is also necessary for the diffusion of nutrients and gases as well as removal of metabolic waste from cell activity [107,108]. Many aspects of porosity have been found to influence cell response to a scaffold including the volume fraction, size, nature and interconnectivity of the pores, as well as the density and stiffness of the struts between pores [8,109].

The minimum pore size is regarded to be 100 μm due to cell size, migration requirements and nutrient transport. However, pores 300 μm and larger are recommended in order to facilitate enhanced formation of *de novo* bone and blood capillaries [110]. It is essential that these pores are fully interconnected to facilitate ingrowth of blood vessels [49,99,107,111,112]. In addition to macroporosity, defined as pores greater than 10 μm , microporosity has been demonstrated to influence osteoinduction. Increased microporosity enhances bone formation in calcium phosphate BGSs, although the precise biological mechanisms remain unclear [113,114]. In an *in vivo* (yucatan minipig) comparison of two different HA structures, one with an orthogonal array of 330 μm holes and the other with similarly sized radial holes and a central channel of 1.2 – 2.0 mm, the larger channel was found to have an intact piece of bone within it after 9 weeks of implantation demonstrating that channels of this size may be beneficial for BGS materials [115].

The measurement of porosity and the analysis of explanted bone scaffolds can be carried out using microcomputed tomography (μCT). This technique has recently been developed from conventional CT imaging and has become a valuable tool to study the process of tissue engineered bone growth [116]. It is possible to construct a 3D model of a bone sample with a resolution of 2 μm thus enabling the structure of the bone to be visualised as well as blood

vessels within the bone itself. This technique has shown itself to be useful not only for visualising bone but also for assessing the in-growth of *de novo* bone into an explanted scaffold after *in vivo* experiments [117-119].

The materials that comprise the BGS should be biocompatible, biodegradable, osteoinductive, osteoconductive and not elicit any unsatisfactory immune responses. The rate of degradation needs to occur in a predictable manner in sequence with bony ingrowth and ideally be adjustable to account for patient age, health, smoker or non smoker, anatomical location, and proximity to a good blood supply [108]. A material that maintains strength for a period of time and then completely disintegrates is less preferable to one which steadily declines in strength. An ideal timescale for degradation is regarded to be between 6 and 24 months depending on the likely healing rate. This is dependent on the age and health of the patient, the implant site and its proximity to a good blood supply and the size of the defect. The ability to sterilise the implant without compromising its properties is vitally important to eliminate the risk of infection. Finally it is important to understand the clinical indication or intended use for a BGS since this will effect the requirements for the implant.

Any material implanted into the human body is immediately subjected to a barrage of proteins, saccharides, lipids, and other solutes found in all bodily fluids. The larger cells arrive later when the smaller molecular processes are already well underway. All biomaterials react in some way to physiological fluids, none are inert. In the past, biomaterials have been concerned with minimising their impact on the bodily environment or their biocompatibility. Now, tissue engineering is concerned with a bioactive approach. In this way biomaterials can be used to directly influence physiological processes and enhance the rate of healing. In addition to possessing a structural function a BGS should mimic the *in vivo* environment to promote cell proliferation, differentiation, and maintenance of phenotype as well as function. This means that when a biomaterial is placed adjacent to a tissue to be regenerated it must induce the migration and proliferation of the relevant cell types [31].

2.6 The bone graft market

The worldwide orthopaedics market is currently enjoying consistent expansion (4% per annum) principally as a result of an ageing generation of post war ‘baby boomers’ who are now reaching the age where orthopaedic products are required to maintain their quality of life [120]. This has coincided with increased patient expectations in terms of the quality of life they can expect as they grow older and the increasingly extreme activities that are undertaken by older people. Furthermore, the population is now living significantly longer thereby increasing the likelihood that some form of orthopaedic product will be required in their lifetime.

There are approximately 600,000 bone graft procedures carried out annually in the US. Some 50% of these are in spinal arthrodeses, and 35 – 40 % in general orthopaedic applications [24]. In 2008 the global orthobiologics market was worth £1.65 billion and growing at 9 % per annum. At this time BGSs represented approximately 20 % of the total value of the bone graft market, although this has been rapidly increasing due to greater experience and confidence in their use. Allograft and demineralised bone matrix (DBM) together made up the largest group of the orthobiologics market (~ 40 %) and growth factors are an ever increasing presence, up from 22 % in 2006 to 30 % in 2008 [121,122].

The introduction of the BMPs has been met with great enthusiasm by orthopaedic surgeons although their use has not yet been optimised and they are often used as a last resort. High doses of growth factor are required to produce adequate bone formation, typically in doses up to a million times greater than its normal concentration in bone. Naturally there are concerns about both the safety and cost of such an approach [103]. These concerns are thought to be partially attributable to the collagen scaffolds used to deliver them which make inefficient protein delivery systems, calcium phosphate ceramics on the other hand are reported to be excellent delivery vehicles [104].

The global market for spinal devices was worth £3.8 billion per annum in 2008 and growing at 13 % per annum making it a highly attractive segment in which to target a new medical device [122]. A high strength degradable BGS which could be developed into a novel and improved spinal implant has the potential to be both highly beneficial for the patient and

achieve excellent sales. The following section examines the empirical methodology employed for this project with the aim of creating an innovative BGS material.

Chapter 3 Methodology

3.1 Introduction

An extensive review of the manufacturing methods attempted for the creation of an ideal BGS was carried out and is presented in Submission 1. There are two main approaches to this problem: those using Rapid Prototyping (RP) techniques and those using more conventional methods such as injection moulding or solvent casting. It is noteworthy that the majority of these techniques are engineering solutions to a biological problem. It was apparent to the author in the early stages of the project that the ideal solution would be to replicate the process by which bone is formed *in vivo*. To this end time was spent understanding developmental bone processes and whether it was feasible to create bone by first making a protein and collagen matrix, then seeding it with cells which could be encouraged to deposit HA crystals onto it. In this way the natural process where a child's cartilaginous bone ossifies into adult bone could be replicated. Unfortunately, this approach would require a team with a diverse range of skills to be successful and so a more conventional engineering approach was followed. This led to the initial approach of examining the readily available RP machines for their suitability to manufacture a novel BGS.

3.2 Experimental work using rapid prototyping methods

The RP machines available at Warwick consisted of Stereo Lithography (SLA), three Dimensional Printing (3DP), and Selective Laser Sintering (SLS). All of these had been attempted previously to manufacture BGSs but at this time none were in use commercially. This was not considered an obstacle for this project since there was still scope for innovation using these processes and RP processes were and remain a highly fashionable research area.

Many researchers have attempted to replicate the natural structure of trabecular bone since it has an ideal porous geometry [123]. Biomimicry is a term that has been adopted to describe the mimicking of natural phenomena and in this instance refers to the manufacture of bone in such a way as to mimic its natural structure [39,124-128]. The process of mimicking the native structure of cancellous bone has been simplified greatly by recent advances in three dimensional (3D) imaging. μ CT is defined as being capable of achieving an isotropic voxel spacing of $< 100 \mu\text{m}$ and recent studies have generated 3D datasets of bone with a resolution of $2 \mu\text{m}$ [129]. It enables a 3D data set to be generated quickly and non destructively, a process which until recently required histomorphometry. This is an extremely time consuming process involving considerable expertise in the preparation of histological slices and use of image recognition software [117,130,131]. In any μ CT system there are a number of factors that affect the resolution. These are the inherent resolution of the detector, the focal spot size, the amount of geometric magnification, the stability of the sample rotation mechanism, and the algorithm used to construct the CT images [118]. Clearly, μ CT is a powerful technique not only for visualising the natural bone with remarkable detail but also for visualising implants that have been tested *in vivo* in order to establish whether blood vessels and bone have been able to grow within the scaffold.

A μ CT dataset of a 10 mm diameter core sample from a lamb femur was obtained from Skyscan (Kontich, Belgium) and the images of each slice were combined into a 3D model and exported as an STL file using Mimics (Materialise, Leuven, Belgium). The STL file is then converted into the file format for the relevant RP machine using Magics (Materialise) and the 3D model was then constructed. Initial experimentals were intended to determine which RP processes were capable of direct replication of the bone sample and thus be suitable for further research. A number of RP techniques were attempted including stereo lithography (SLA), three dimensional printing (3DP), selective laser sintering (SLS) and selective laser melting (SLM).

SLA was capable of replicating the dataset with little trouble although its requirement for support structures to cope with overhanging features means there are some additional elements in the model. Figure 3.1(a) is an image of an SLA model at four times scale showing the intricate detail of the model. This process is capable of achieving a $20 \mu\text{m}$

resolution, similar to the actual μ CT data [132]. At the time of conducting these experiments the major stumbling block for adoption of SLA was the lack of availability for UV curable biopolymers. Research is still underway to find a suitable UV curable biopolymer for direct implantation but none are commercially available at present [133,134]. SLM is able to produce intricate models of high melting point metals direct from powder. This is a new process and it was thought that it could be developed to produce degradable magnesium alloy or ceramic implants direct from powder. The mechanical properties of magnesium are well suited for BTE but it degrades rapidly *in vivo* with the formation of large quantities of hydrogen gas which must be eliminated from the body [135].

SLM is a recently introduced process which is similar to SLS but employs a more powerful laser capable of melting metals. This process was attempted using stainless steel to determine if it was suitable for further research. Figure 3.1(b) is an SLM model in stainless steel at twice normal scale. This demonstrates how the inherent resolution is beginning to affect the accuracy of the model. When the data is produced at 1:1 scale the pores and solid parts blend together to form an almost continuous component.

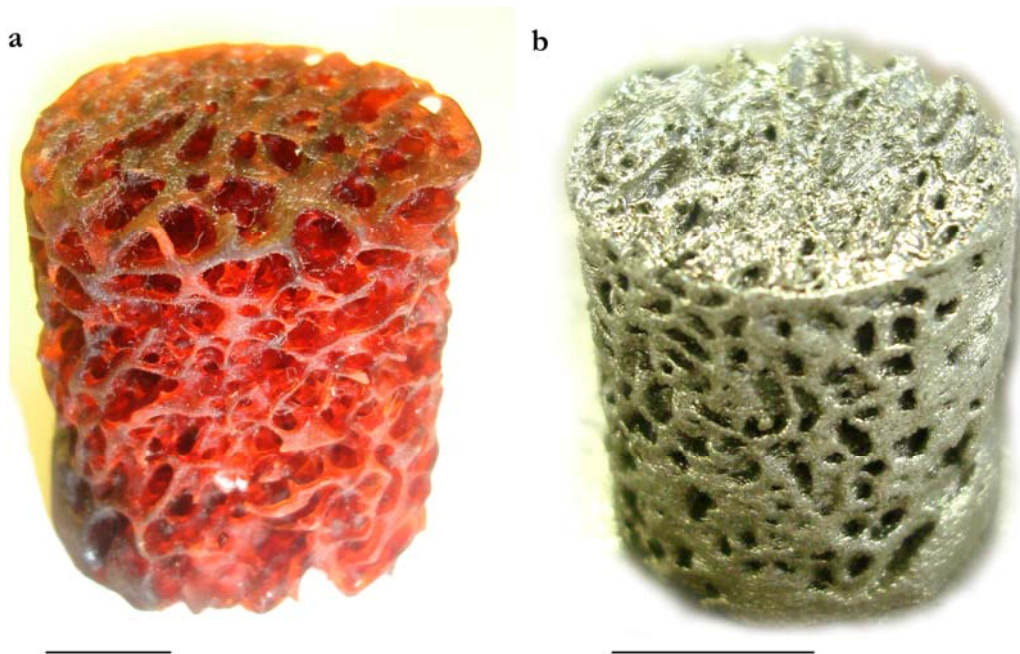


Figure 3.1 Images of (a) lamb femur μ CT data replicated via stereo lithography scale x 4 and (b) selective laser melting scale x 2 [scale bar = 10 mm]

3DP was employed to create an alumina replica of the bone sample. Alumina powder is mixed with polyvinyl alcohol (PVA) powder which acts as a binder. Initial attempts using this method were carried out at five times normal size as the resolution of the machine was not capable of resolving all of the microscale detail in the bone data. The resolution is a function of the powder size and morphology as well as the nozzle size of the print head. The models produced were very weak and fractured during firing. It proved difficult to achieve suitable binder burnout such that the gases produced did not fracture the model. The problems associated with 3DP meant that it was abandoned as a research direction.

Further experimental work concentrated on selective laser sintering (SLS) which at this time was a new technique, and few researchers had investigated its use for manufacture of BGSs [136]. Hence this was a promising technique for innovative research. For this reason it was decided to use SLS to create a series of samples, each set using different machine parameters. These samples would be tested both mechanically and biologically to establish their suitability for use as a BGS. The material chosen for use with SLS was polycaprolactone (PCL) a commonly used biopolymer. PCL is an aliphatic polyester that has been tested extensively for use in tissue engineering. It has a low melting point of 58 – 63°C and a low glass transition temperature of -62°C. It degrades by microorganisms as well as hydrolytically *in-vivo*. It is a regulatory approved biodegradable polymer proved to be tissue compatible by use as sutures and long term drug delivery systems [137]. The degradation time of PCL is quite slow when compared to other biodegradable polymers and as such it is suitable for BTE. Unfortunately it turned out to be impossible to manufacture a PCL BGS via SLS for a number of reasons described fully in Submission 4.

These experiments with RP techniques highlighted both the positive and negative aspects relevant to producing a BGS and are summarised in Table 3.1. Positive aspects of all RP methods included their ability to seamlessly integrate with medical imaging systems and enable production of complex patient specific implants with specifically designed porosity. These would possess adequate strength and be suitable for direct implantation after ensuring their sterility. Rapid prototyping techniques were originally developed for one off manufacturing of components for design verification and function testing. These processes

have now developed to such an extent that they are termed rapid manufacturing or direct manufacturing processes and can be considered for mass production of BGS materials. 3DP is currently in use commercially for manufacture of highly porous blocks and wedges [65,138].

The disadvantages of RP methods vary according to the individual process and are mentioned below. SLS machines are expensive to purchase, require a long cool down time for the powder bed, waste large amounts of raw material (a real problem with expensive biomaterials) and the final products have a loose powdery surface. SLA machines are cheap to purchase but expensive to run in terms of the resin required. More significantly there are no high strength UV curable biopolymers commercially available. They also require additional support structures within the 3D model that need to be removed prior to post curing with UV light. From the experiments carried out as part of this research it became apparent that RP techniques may not be the ideal solution for manufacture of a high strength and economically viable BGS. Thus, attention was focused onto more conventional processes.

Table 3.1 Summary of Rapid Prototyping processes

Process	Materials	Advantages	Disadvantages	Ref's
Stereo Lithography (SLA)	UV curable polymers	Integration with medical imaging High resolution – 20 μm Direct production of ceramics is possible Low cost machine Quick build speed	Expensive raw materials Availability of suitable UV degradable biopolymers Models require removal of support structures Models require a UV post cure	[108]
Selective Laser Sintering (SLS)	Polymer	Integration with medical imaging Good mechanical strength Sintering of powder particles provides microporosity No support structures required	Expensive machine Resolution determined by powder size and laser spot size – typically 1 mm High process temperature degrades polymer Highly sensitive to raw powder Loose powdery surface Lengthy post processing time High energy consumption Large amounts of waste raw material	[108]
Selective Laser Melting (SLM)	Metals, polymers or ceramics	Integration with medical imaging Good mechanical strength No support structures required	Expensive machine Resolution determined by powder size and laser spot size – typically 2 mm Lengthy post processing time High energy consumption	
3D printing (3DP)	Polymer or ceramic	Integration with medical imaging Suitable for a wide range of materials Biocatalysts and cells can be incorporated into scaffold No support structures required Low cost process	Resolution determined by powder size and print head Use of toxic solvents Lack of mechanical strength Manufacture of ceramic components is challenging	[139,140]

3.3 Experimental work using conventional methods

The experimental work using RP techniques with μ CT bone data crystallised an idea to create a simple, regular and porous structure. The requirement for high porosity infers that the implant will be significantly weaker than a solid block of material. Therefore any porosity should be structurally ordered as for example in a space frame lattice. In this way the material can be arranged in a structurally efficient manner. Replicating the structure of cancellous bone is not necessarily the ideal method of achieving this as recent work has established that a great deal of the strength in bone comes not from the trabeculae but from the glue like material in the voids which bind the elements together [141]. Figure 3.2 illustrates a simple block with an array of holes in each face and it was the intention to replicate this using a number of conventional techniques.

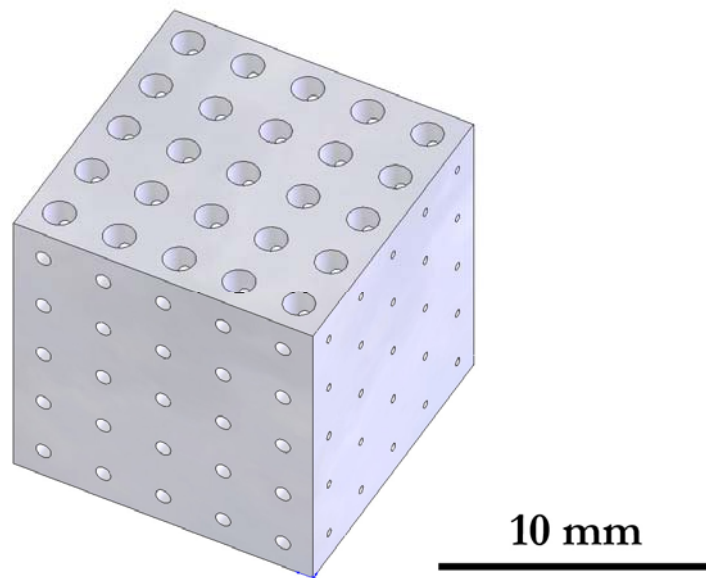


Figure 3.2 A 3D CAD model demonstrating a cube with structured porosity

Conventional machining was attempted first. An array of 1 mm holes with a 2 mm pitch were drilled into one face of PCL and PCL/HA composite blocks. The low melting point of PCL ($\sim 60^{\circ}\text{C}$) made it difficult to machine satisfactorily. Further experiments were carried out to establish if a pure HA blocks could be machined in a similar fashion. Three sets of samples were fabricated by compressing HA powder and then sintering them at different temperatures. The first set of samples were left as compressed (HA0), the second set were sintered at 600°C (HA600), and the final set were sintered at 1150°C (HA1150). Of

these, only the HA600 set proved possible to machine although only with great care. Machining of the holes is a time consuming process and so a number of other methods were considered to create an array of holes in a block of material, one of which was to use a laser. Pulsed laser drilling, also known as percussion laser drilling uses a number of laser pulses to create a via or hole in a piece of material. When the laser irradiance is kept below a threshold value the work piece material is melted and not vaporised in which case the molten material is ejected from the hole by an assisting gas [142,143]. There were two lasers available for use at Warwick: Carbon Dioxide (CO₂) and Neodymium doped Yttrium Aluminium Garnet (Nd-YAG).

A series of experiments were carried out to determine if lasers could create an array of holes in different materials. Three sets of biopolymers were used PCL, PCL/HA composite, and polylactic acid (PLA). Each of the samples was moulded into a flat sheet approximately 5 mm thick. The results of drilling a series of holes in these materials with a wide range of settings demonstrated that PCL was not suited to laser drilling due to its low melting point. PCL/HA proved more suitable with well defined holes, although it still showed excessive melting. Polylactide (PLA) is a degradable polyester used commonly in medical implants. It has a melting point of 185°C and proved straight forward to laser machine. The holes were perfectly circular, neat on entry and exit and exactly 350 µm in diameter. Thus PLA was selected for further trials and an injection moulding tool was manufactured to mould 10 mm cubes of material. These cubes were then assembled into a jig and the laser programmed to drill an array of 25 holes in each face.

Each face required sixteen seconds to laser drill the 25 holes. Laser drilling of all three faces was accomplished in under two minutes. The results from the laser drilling of PLA cubes are shown in the scanning electron microscopy (SEM) micrographs in Figure 3.3. The striking feature in these images is the precision of the holes. These experiments demonstrated that this technique can be used to create porous blocks of biopolymer with a regular and organised porosity.

The experimental attempts to manufacture a porous block of material utilising novel methods have raised some interesting points. Machining is not an efficient method of

producing a porous block of material and gave poor results in PCL, PCL/HA composite and HA. Laser processing of PCL yielded poor results but PLA proved highly satisfactory and when formed into a cube of material and laser drilled resulted in a highly satisfactory and rapid method to create a porous cube. Laser drilling of HA blocks proved impossible although whilst discussing the results of these trials with Dr. Kajal Mallick we stumbled upon the idea of a simpler method to create a porous ceramic structure.

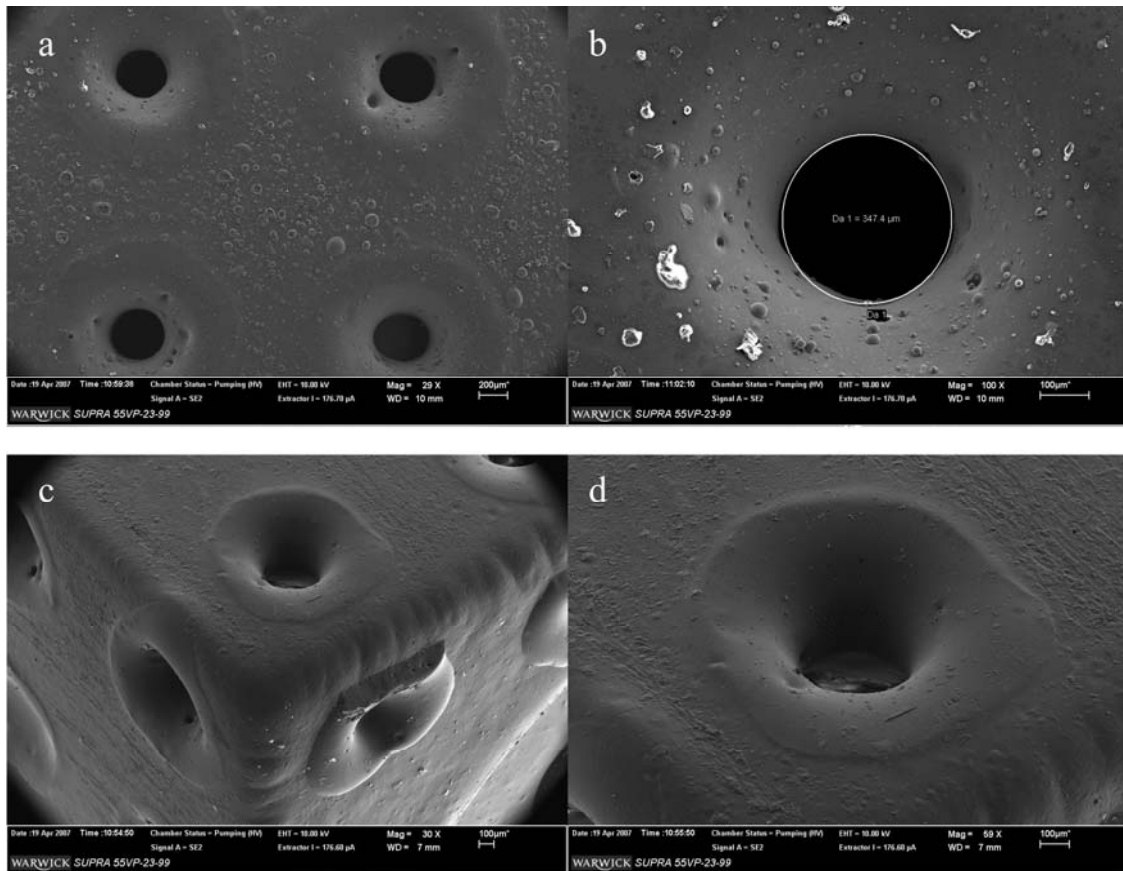


Figure 3.3 SEM micrographs of a laser drilled PLA cube (a) a view of the top surface of the cube showing some of the melt debris on the surface of the PLA as well as the regular spacing and circular nature of the holes (b) is a close up of one of these holes demonstrating a hole diameter of 347 μm (c) is a view on one corner of the cube and shows the holes generated by laser in each of the surfaces (d) is a magnified image of the top hole in image (c)

The idea was to use a monolithic ceramic structure that would provide the basic scaffold. Additional porosity could then be added by laser drilling if necessary. The ceramic monoliths would be manufactured using a similar process to that used for the ceramic 'brick' in an automotive catalyst. Using this existing mass production process would enable a highly porous yet strong implant to be manufactured at low cost thus providing a significant advantage over existing materials.

3.4 Extrusion of ceramic monoliths

A ceramic monolith is described as a porous, unitary, ceramic body. Its method of fabrication yields both remarkably high porosity and strength, a combination highly sought after in BGS materials. The process to manufacture ceramic monoliths for use as the substrate in automotive catalytic converters is well established. Ceramic powder is mixed with binders and lubricants and then kneaded under vacuum to yield a clay like paste free of any air inclusions. This paste is then forced through a die to create the form as seen in Figure 3.4. The 'green' component is air dried at 30 - 100°C. The drying phase is an important part of the process where the water is eliminated from the green component resulting in shrinkage. This is where cracks may form that can be large enough to break the monolith. The temperature and humidity of this process must be controlled carefully to dry out the monolith slowly and uniformly to achieve high compaction with no cracking. The monolith is then cut to shape and heated to burn off the binders, subsequently it is fired to sinter the ceramic particles together [144].

The innovative and novel aspect of this research is to make use of an existing manufacturing process and successfully adapt it to a new field of application. The initial aim was to establish if calcium phosphate ceramics including hydroxyapatite (HA) and β -tricalcium phosphate (β -TCP) could be extruded into monoliths suitable as BGS materials. The extrusion process enables the longitudinal porosity to be controlled by the extrusion die and the lateral porosity to be controlled by the initial paste formulation and processing conditions.

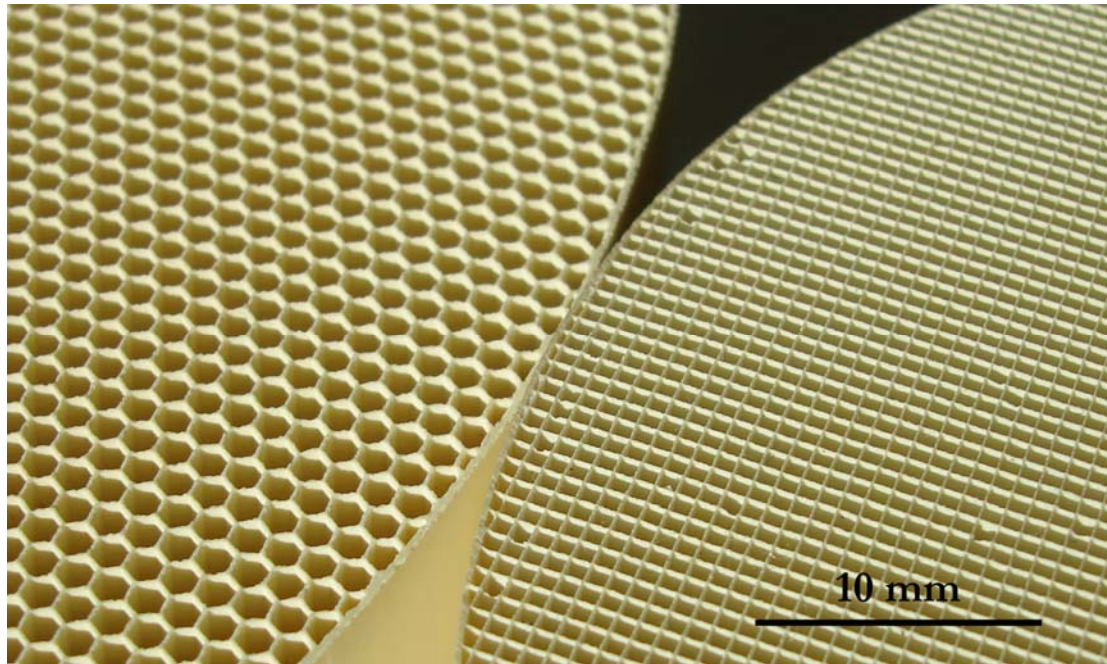


Figure 3.4 An image demonstrating ceramic monoliths with hexagonal and square cells

A device capable of extruding a ceramic paste through a die to form a monolith was designed and manufactured, as seen in Figure 3.5. The precise design details are described in Submission 6. A series of experiments were then carried out using a range of paste formulations composed of HA powder, binder and water. None of these resulted in the successful extrusion of a monolith and it became clear that industrial expertise would need to be sought. In order to facilitate this process it was necessary to have a patent to protect the idea and funding to cover costs for equipment and expertise. A patent was filed which can be found in Submission 5 and a number of bids for research funding were written the principal one can be found in Submission 6.

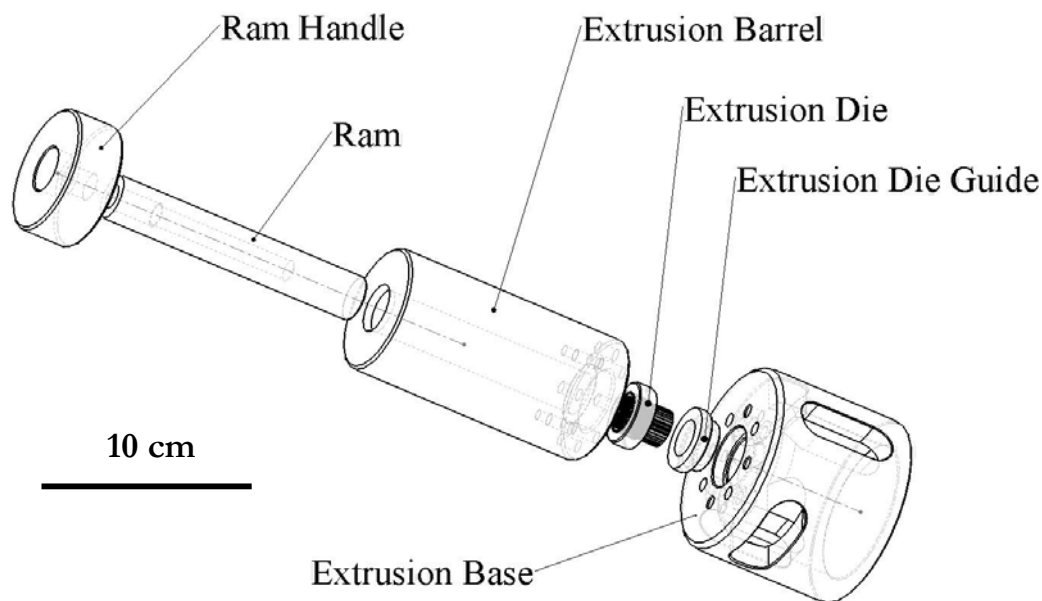


Figure 3.5 A CAD model of the ceramic monolith extrusion apparatus

Once the patent had been filed a number of companies were approached in search of an industrial collaboration. A rigorous process to find a suitable partner was carried out which is described in detail in Submission 6. Briefly, a two page proposal was created and then distributed to over 15 companies with expertise in this field. Two of these companies expressed an interest in collaborating. After a two month period of negotiation and discussion a leading international manufacturer of engineering ceramics were chosen as our partner. This led to proof that calcium phosphate ceramics could be extruded into monoliths and on only the second trial a highly satisfactory monolith was obtained (Figure 3.6). The next step was to manufacture a range of different monoliths and subject them to a series of mechanical and biological tests in order to determine their suitability as a BGS material. The original aim was to examine a wide range of variables including the material, cell pitch, wall thickness, wall porosity, and sinter temperature. After discussions with our partner it was apparent that the time to manufacture approximately 100 samples of each variant would require significant time and be difficult to fit into their schedule. Hence, it was decided to concentrate on two easily adjusted variables, the paste formulation and die dimensions.

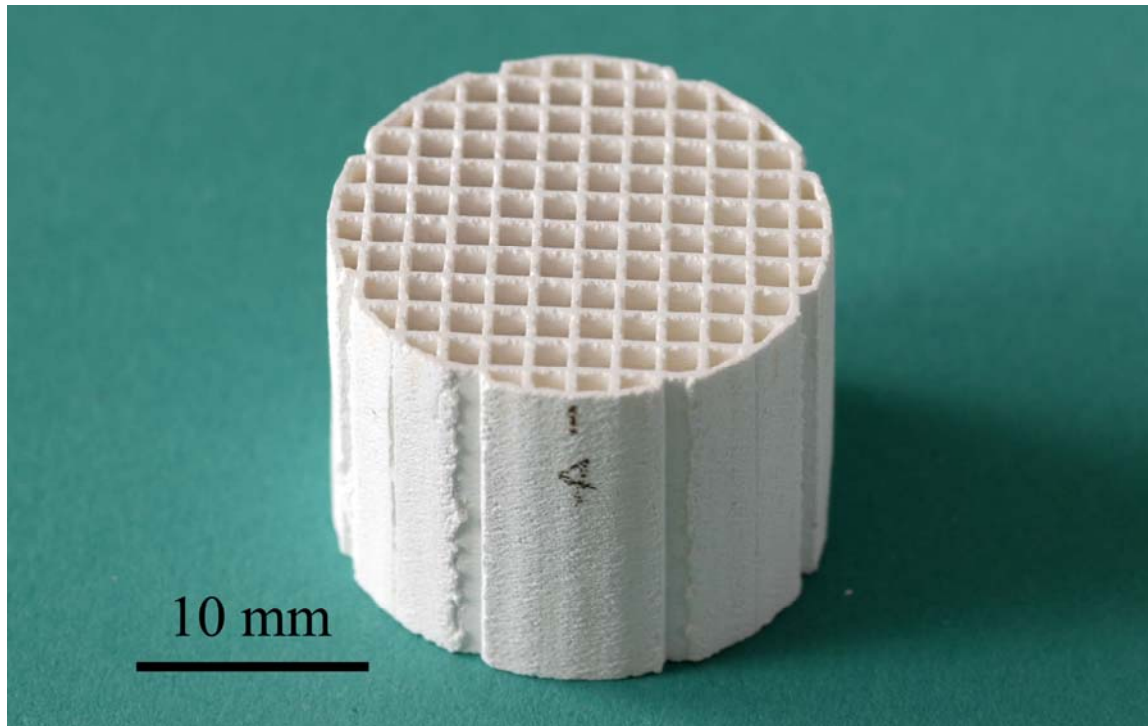


Figure 3.6 An image of the second industrial extrusion attempt with a 50% HAP 100 and 50% HAP 200 paste through a 28/70 die

The material chosen for the trials was HA since this would provide an excellent benchmark against existing BGS products. The monoliths were produced using two different paste formulations. Paste 1 was composed of 50:50 mix of two different raw powders HAP 100 and HAP 200. Figure 3.7 is a series of SEM images of the raw powders, HAP 100 has a mean particle size of 24 μm and HAP 200 has a mean particle size of 9 μm . Paste 2 contained HAP 200 only. The other variable that was simple to adjust, and thought to have an effect on the mechanical and biological properties of the scaffold was the die specification. The die is used to alter the cell pitch (CP) and wall thickness (WT) of the extruded monoliths. Two different dies would be used for these experiments, the 28/70 and a finer 12/300 die. The 28/70 designation refers to the WT in thousandths of an inch (mil) and the number of cells per square inch (CPSI) (Figure 3.8).

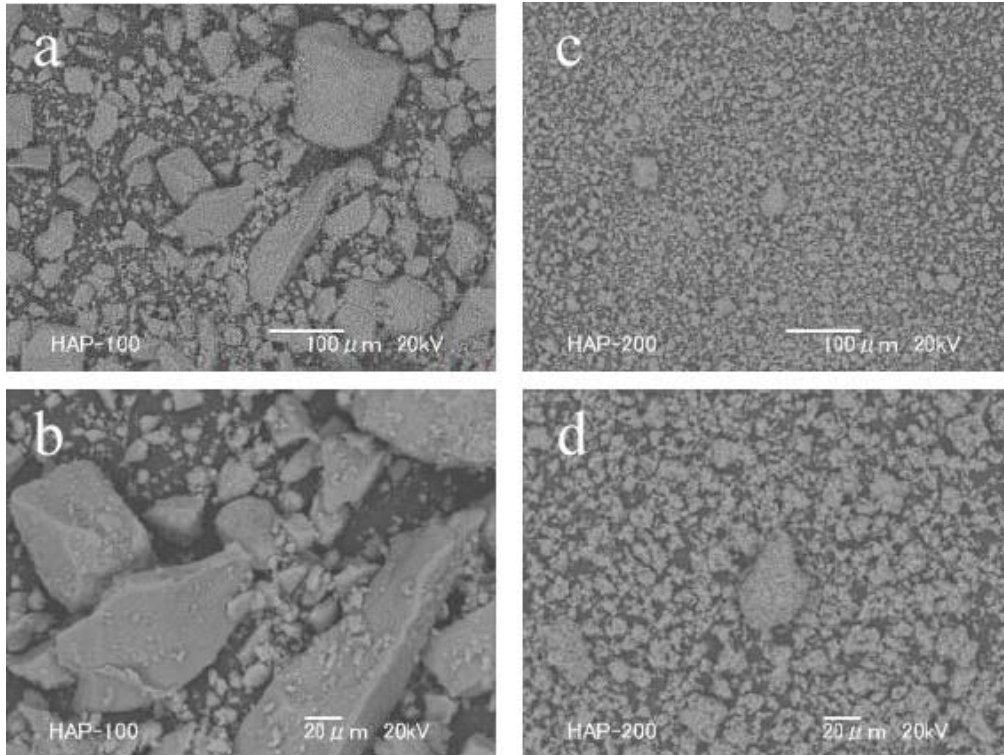


Figure 3.7 SEM images of raw HA powder (a) and (b) are HAP 100, images (c) and (d) are HAP 200

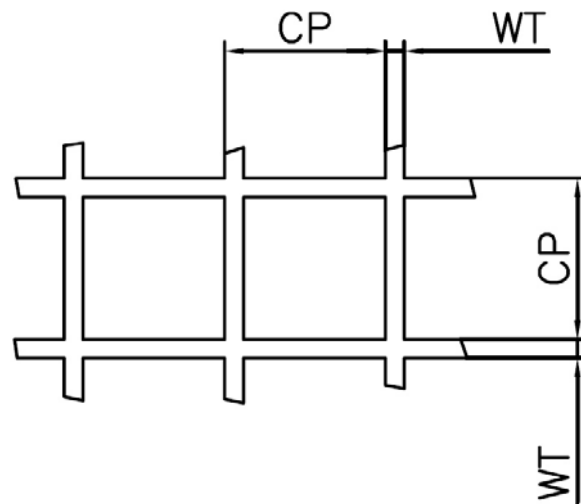


Figure 3.8 A schematic view of monolith cells demonstrating cell pitch (CP) and wall thickness (WT)

In order to reduce the overall number of experiments it is possible to use Taguchi methods or design of experiments (DOE). These methods allow the effect of changing a large number of variables to be established without having to test each unique combination of variables. DOE can be extremely powerful when undertaking experiments that are likely to have reliable results with each experimental iteration. Unfortunately, biological experiments are associated with large variances and so the confounding that often occurs in DOE would lead to results which cannot be easily interpreted. For this reason it was decided to carry out a full factor two factorial experiment as shown in Table 3.2. An extra sample with high porosity was also added to help further understand the effects on mechanical and biological properties. One hundred samples of each sample type were manufactured for the mechanical and biological evaluations.

Table 3.2 HA monolith configuration details

	DIE 1 (12/300)	DIE 2 (28/70)
PASTE 1 HAP 100/HAP 200 50:50	A 1150°C Sintered	B 1150°C Sintered
PASTE 2 HAP 100/HAP 200 0:100	D 1200°C Sintered	E 1200°C Sintered
PASTE 2 HAP 100/HAP 200 0:100	C 1150°C Sintered	

3.4.1 Physical and mechanical characterisation of HA monoliths

Each sample type A, B, C, D and E were subjected to a series of tests to establish their physical properties. These included:

- A-axis compression strength and modulus, the A-axis is the primary axis in line with the extrusion direction (measured using 3 cells by 3 cells, 20 mm in height for the 28/70 samples, and 15 mm diameter and 5 mm height for the 12/300 samples)
- 3 point bending strength and modulus (measured over a 10 mm span with a sample size of 20 mm (length) x 4 mm (width) x “wall thickness”)
- Wall porosity and median pore diameter (determined using mercury porosimetry)
- Material composition (determined by X-Ray diffraction (XRD))
- Microscopy to visualise the macro and micro porosity

3.4.2 Biological characterisation of HA monoliths

The biological characterisation of the HA monoliths examined:

- Cell attachment to scaffolds (assessed by actin fibre patterns)
- Expression of osteoblastic markers (alkaline phosphatase (ALP) and osteocalcin (OC))
- Cell proliferation (assessed by MTT assay)

A wide range of cell types have been used for cell culture studies including human fibrosarcoma (HT1080) [145], human osteosarcoma cells (SaOS-2 & MG-63) [146-151], neonatal rat calvaria osteoblasts [152,153], L929 fibroblasts [154,155], mesenchymal stem cells (MSC's) [156,157], and bone marrow stromal cells (BMSC's) [158-160]. For these experiments two different human osteoblastic cell lines were available: MG63 and SAOS₂, both of which were examined for their suitability. Both MG63 and SaOS-2 cell lines expressed ALP and OC mRNA and secreted detectable levels of ALP and OC protein into the media. The MG63 cells were chosen for future studies principally because of their higher growth rate and thus subsequent reduction in overall experimental time.

Successful attachment to a BGS is demonstrated by appropriate cell growth, cellular proliferation, and formation of actin fibres. Figure 3.9 is a confocal microscopy image of MG63 and SaOS-2 cells growing on the monoliths and demonstrates the lower cell numbers seen in SaOS-2 cell culture. MG-63 cells are commercially available cells derived from a human osteosarcoma cell line and they provide an appropriate model for studying cell proliferation and adhesion on engineered surfaces. In a comparison between human osteoblast and MG-63 osteosarcoma cells [161] numerous differences were found but they are still a valuable tool for analysing bone cell behaviour. It is important to mention that there are strict guidelines governing the use of human osteoblast cells and so MG-63's provide valuable information without the requirement for ethical approval.

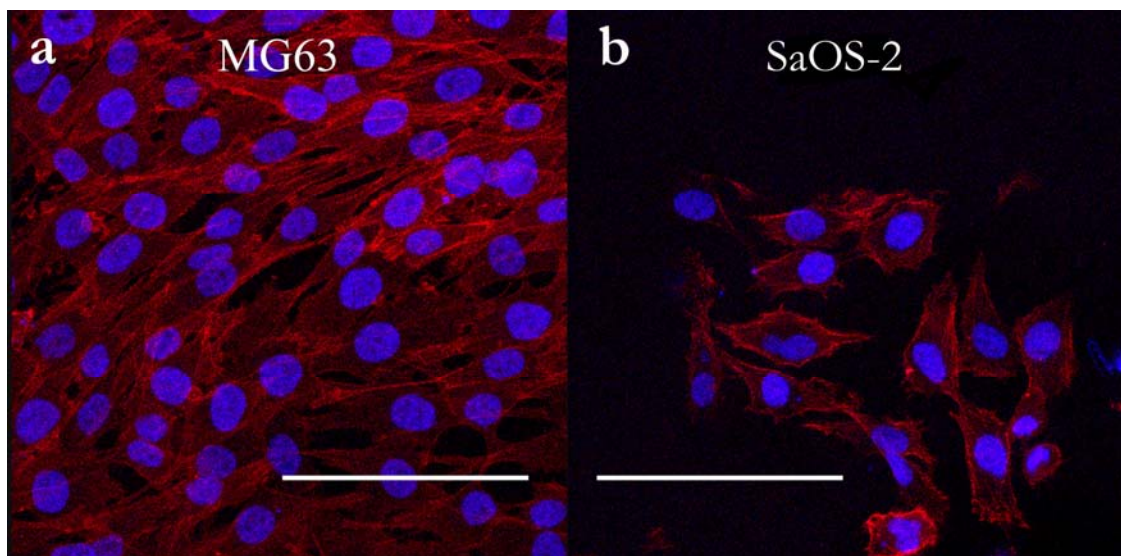


Figure 3.9 Confocal microscopy images (x40) of Actin fibre staining. (a) MG63 cells and (b) SaOS-2 cells stained with DAPI (blue, nucleus) and phalloidin (red, actin fibres) [scale bar = 50 μ m]

MG63 cells were grown on 3D scaffolds and ribonucleic acid (RNA) was extracted after six and thirteen days in culture. The expression of ALP and OC was analysed using the reverse transcriptase polymer chain reaction (RT-PCR) process and gel electrophoresis. Figure 3.10 is an image of a gel demonstrating the relative levels of AP and OC expression compared with the 18S control after six and thirteen days in culture. The 18S controls differences in RNA quantity and PCR process. The intensity of the bands were measured and the results from OC and AP divided by the 18S values. These results are plotted in Figure 3.11 and Figure 3.12.

At six days expression of OC and AP are similar for all samples and the control. After thirteen days some changes may be apparent (sample size = 1). Expression in the control remains constant whilst samples A, B and E demonstrate increased osteoblastic gene expression compared with C and D. This suggests that A, B and E are better than C and D at encouraging the osteoblastic phenotype. Ideally, gene expression tests would be carried out on all samples in parallel with cell proliferation. However, the time consuming nature of these experiments coupled with a limited number of samples led to the decision to use cell numbers (measured by MTT) as the primary performance measure for the samples.

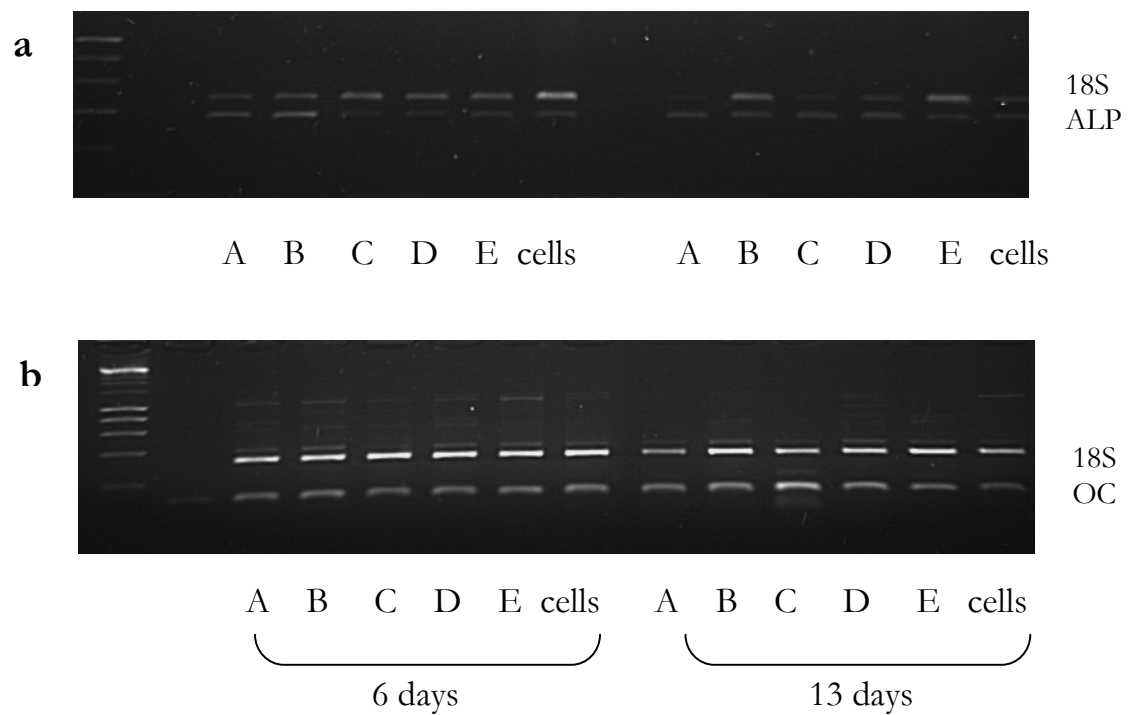


Figure 3.10 Images extracted from a plate reader demonstrating expression of ALP (a) and OC (b) mRNA in MG63 cells after 6 and 13 days in culture

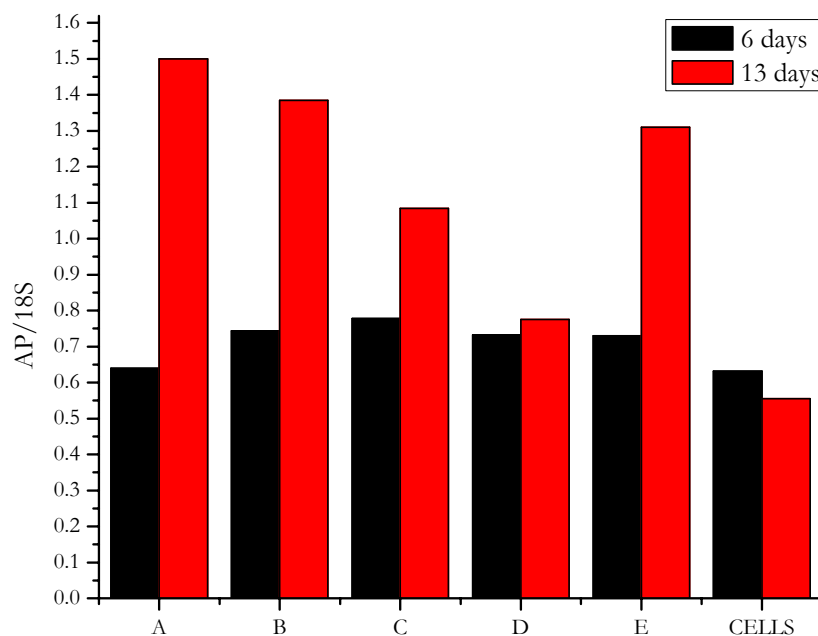


Figure 3.11 Relative AP expression for HA samples and the control at 6 and 13 days in culture

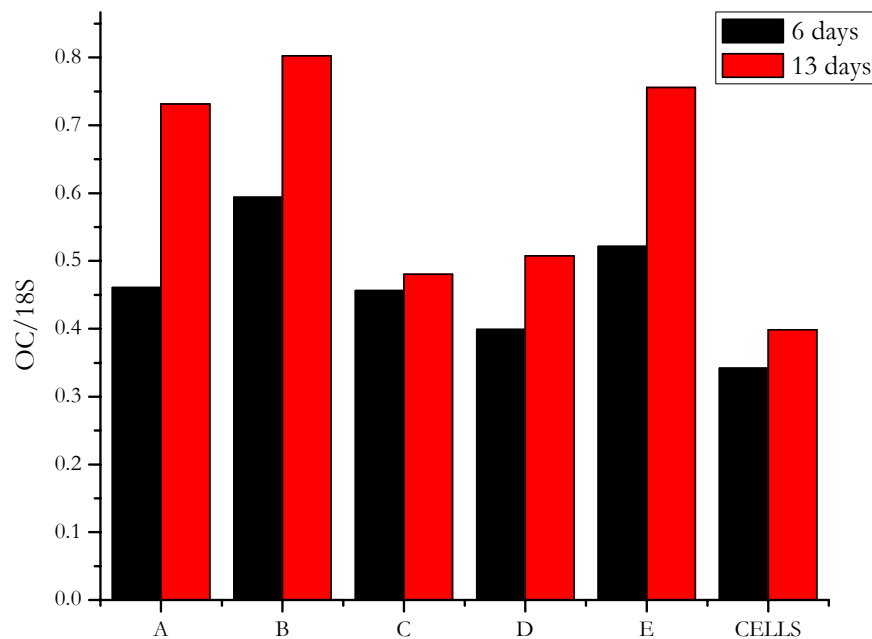


Figure 3.12 Relative OC expression for HA samples and the control at 6 and 13 days in culture

The cell proliferation test procedures were the same in each case. The experiments were carried out in triplicate, samples (A – E) were loaded into 12 well culture plates. MG63 cells which had been maintained in culture under standard conditions were subdivided and seeded onto the sterile scaffolds with 1×10^5 cells. After culture at 37°C for a set period of time (3, 6, 9, 13 days) the samples were subjected to the standard (3-(4,5-dimethylthiazol-2-yl)-2,5-diphenyltetrazoliumbromide) (MTT) assay to assess cell proliferation. A detailed description of this process can be found in Submission 6.

Chapter 4 Analysis and characterisation of HA monoliths

4.1 Results of physical and mechanical characterisation

The results for the physical characterisation are shown in Table 4.1, each test examined five specimens of each sample type. Samples A, B, and C were sintered at 1150°C and samples D and E at 1200°C. In each case the cooling rate was the same at 30°C/hour. The cell configuration of each scaffold is different to the actual die due to the overall shrinkage of the material during sintering. The wall thickness of samples A, C and D varied from 0.28 to 0.33 mm and for samples B and E between 0.58 and 0.63 mm. The cell pitch for samples A, C and D varied from 1.08 to 1.16 mm and for samples B and E between 2.48 and 2.53 mm. Figure 4.1 demonstrates the differences in monolith structure due to the different extrusion dies.

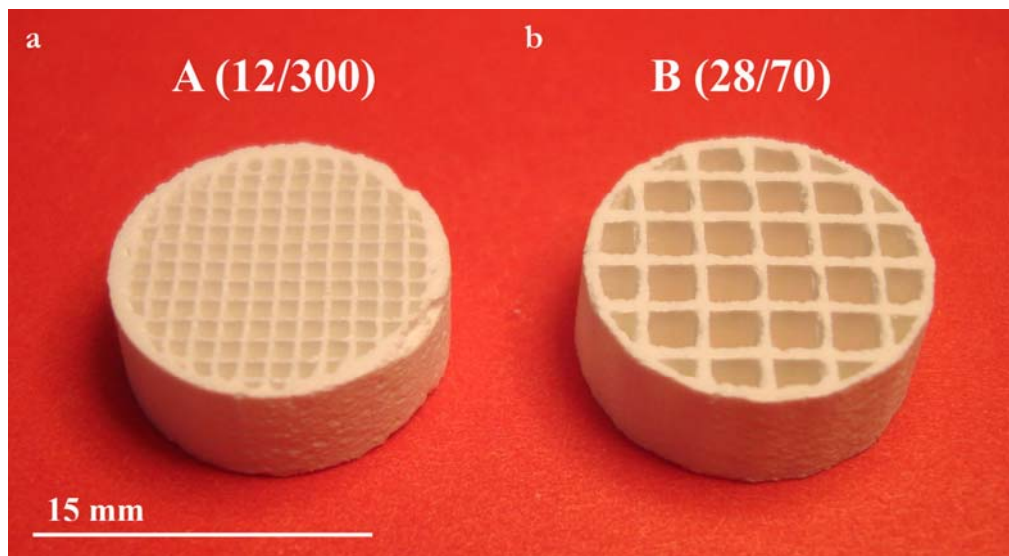


Figure 4.1 Image comparing the influence of die on the sample. (a) Sample A using a 12/300 die and (b) sample B using the 28/70 die

Samples A and B have a wall porosity of $\sim 14\%$, samples D and E $\sim 22\%$ and C $\sim 33\%$ as measured by mercury porosimetry. The high wall porosity of sample C is responsible for its low strength (142 MPa). Figure 4.2 is the mercury porosimetry plot for each sample demonstrating the nature of the porosity in each scaffold, all having median pore diameters of $0.20 - 0.43 \mu\text{m}$. Bending strength tests were carried out on the wall thickness associated with DIE 2 ($1.08 - 1.16 \text{ mm}$) for the three different sintering and paste conditions as shown in Table 4.1. Mean values for bending strength ranged from $33 - 46 \text{ MPa}$ and bending modulus from $29 - 57 \text{ GPa}$.

Table 4.1 Physical properties for the samples undergoing biological testing

Sample number	A	B	C	D	E
HAP100/200 (by mass)	50/50		0/100		
Binder (mass %)	10		15		
Kneading water (mass %)	46		50		
Firing temperature ($^{\circ}\text{C}$)	1150	1150	1150	1200	1200
Cooling rate ($^{\circ}\text{C}/\text{hour}$)	30	30	30	30	30
Cell configuration (mil/CPSI)	11/548	23/105	13/475	11/533	25/101
Wall thickness (mm)	0.28	0.58	0.33	0.28	0.63
Cell pitch (mm)	1.08	2.48	1.16	1.10	2.53
Wall porosity (%)	-	15	33	-	22
Bending strength (MPa) (σ)	-	46 (3)	33 (5)	-	46 (7)
E modulus bending (GPa) (σ)	-	57 (4)	29 (4)	-	46 (5)
A-axis compressive strength (MPa) (σ)	265 (29)	243 (40)	142 (8)	233 (52)	263 (63)
E modulus A-axis comp. (GPa) (σ)	4.1 (0)	4.4 (0.1)	3.2 (0.1)	3.9 (0.5)	4.2 (0.3)
Median pore diameter (μm)	0.23	0.25	0.40	0.43	0.35
Pore Volume (cc/g)	0.036	0.047	0.124	0.066	0.079
Bulk Porosity (%)	54.4	59.5	63.1	58.3	61.6

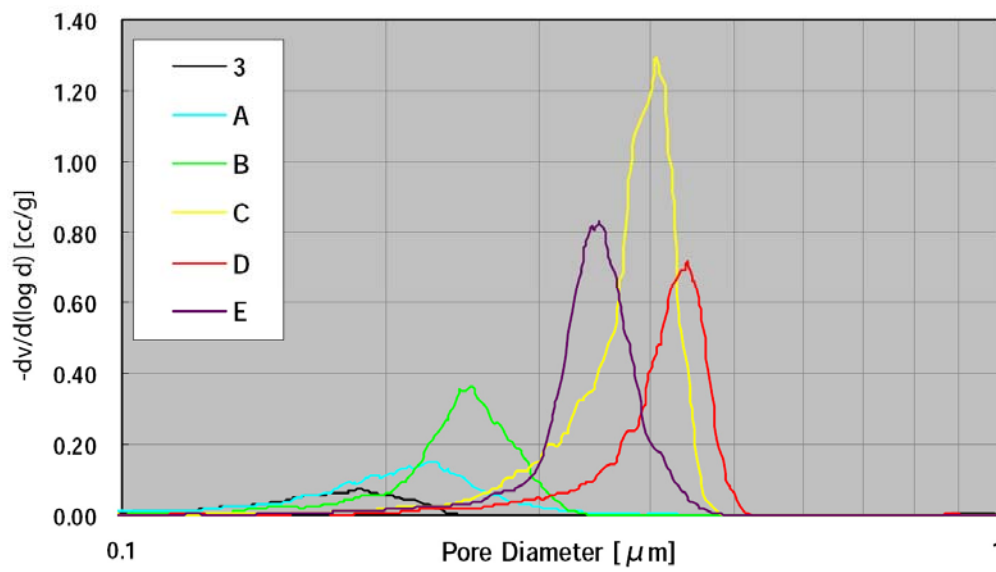


Figure 4.2 Mercury porosimetry plot of wall porosity for HA monolith samples A, B, C, D and E

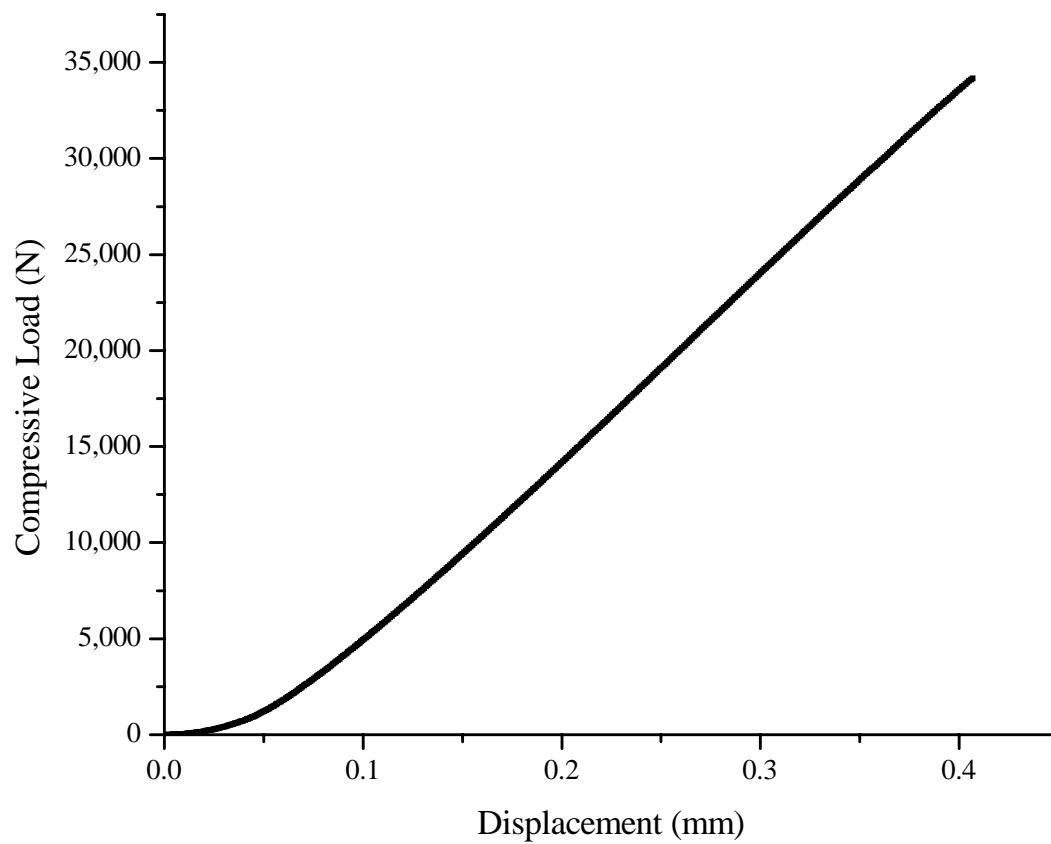


Figure 4.3 A-axis Force *versus* displacement plot for sample A in compression

A typical force displacement plot for scaffold A is shown in Figure 4.3. The scaffolds fail in an explosive fashion with little warning. It is worth noting their virtually constant modulus all the way to failure. The A-axis compressive strength and modulus have been plotted onto a graph which compares their properties versus other common biomaterials both porous and dense (Figure 4.4). The results clearly demonstrate that scaffolds A, B, D, and E all have similar mechanical properties, whilst C is approximately 50% weaker. All are excellent with a strength within the range of cortical bone and a peak modulus of 4.4 GPa which is just below the lower range of cortical bone (5 – 35 GPa) [13-18]. These values are superior to any porous degradable bioceramic currently available.

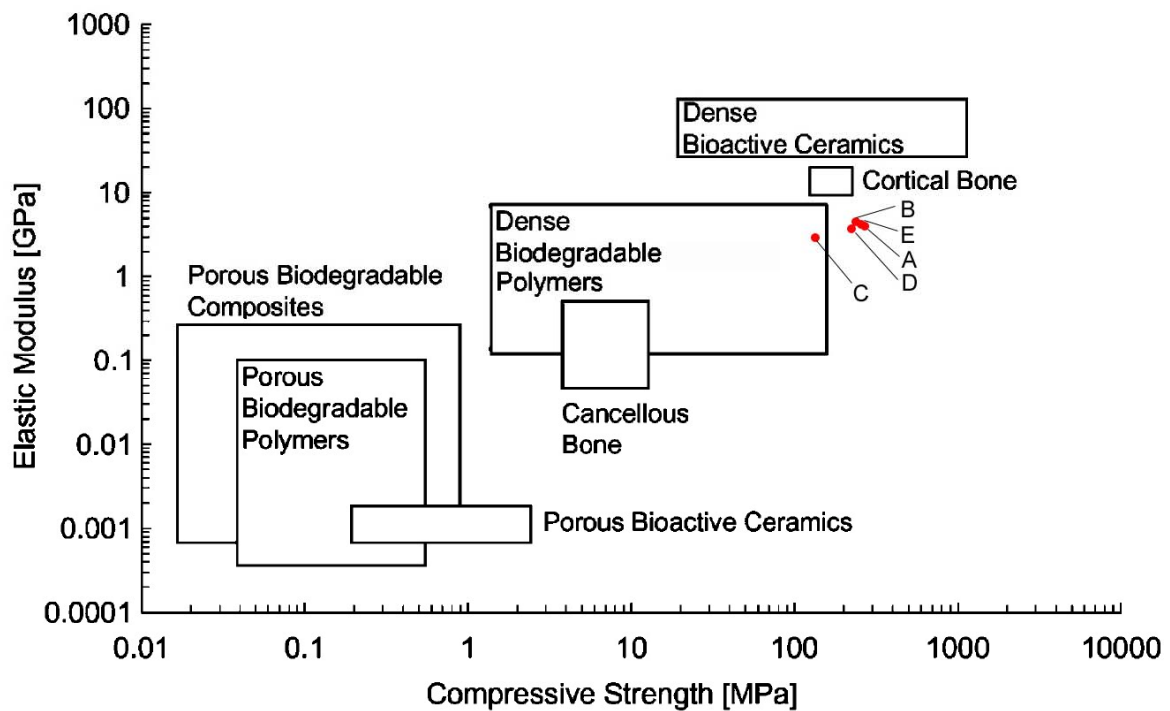


Figure 4.4 A plot of compressive strength and elastic modulus comparing a range of biomaterials with bone and HA monoliths, adapted from [47]

The material properties, particularly the crystallinity and stoichiometry (minimal defects in the final composition) of the material have a large effect on both the degradation rate and osteoconductivity of the scaffolds and so a great deal of attention needs to be paid to the fine details of material analysis. The compositional analysis is crucial in order to establish

whether the manufactured components meet the requirements for stoichiometry and crystallinity. To this end a XRD analysis of each material is shown in Figure 4.5 and demonstrates that each material used is 100% phase pure and crystalline HA.

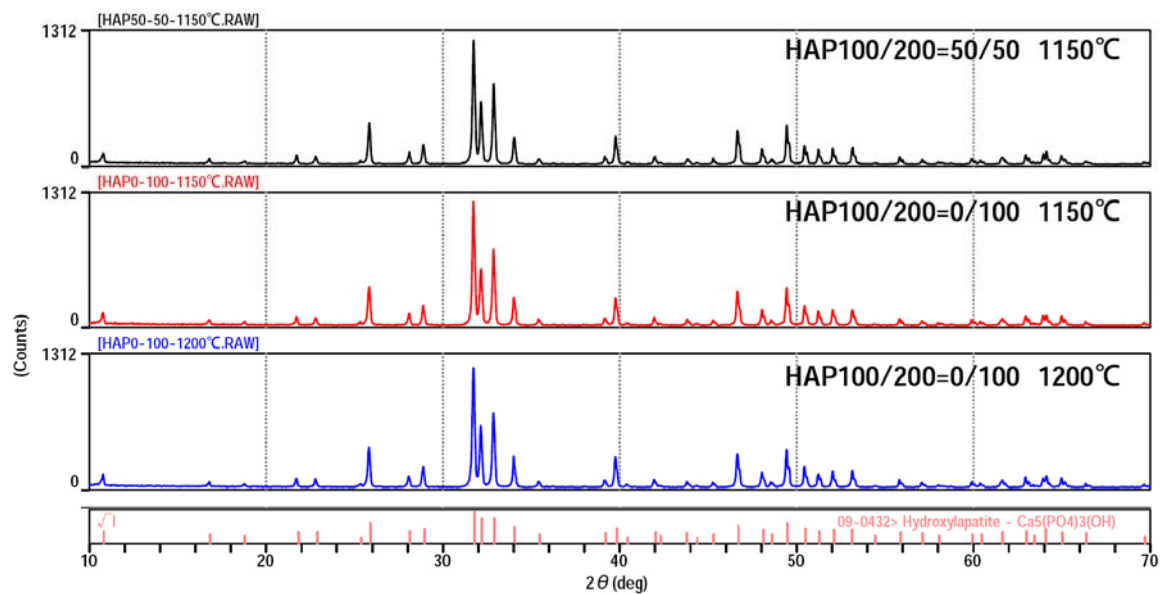


Figure 4.5 XRD plot for HAP 100/200 50:50 sintered at 1150°C (top), HAP 100/200 100:0 sintered at 1150°C (middle) and HAP 100/200 100:0 sintered at 1250°C (bottom) compared with HA standard

SEM analysis of scaffold A reveals the microstructural details of the material. Figure 4.6 (a) reveals the mix of large and small particles characteristic of the HAP 100/200 powder mix. Figure 4.6 (b) shows the boundary between a large and dense HAP 100 particle and the smaller HAP 200 particles which are sintered in a porous matrix. Figure 4.6 (c) clearly demonstrates the micro sized particles of HA ($\sim 1 \mu\text{m}$) that form the matrix. Figure 4.6 (d) is a highly magnified image of the porous area demonstrating that the particles are well sintered which explains the observed excellent compressive strength. Figure 4.7 is a series of SEM images of a fixed and polished example of sample A. Again the large HAP 100 particles are evident in a matrix of micron sized HAP 200 particles.

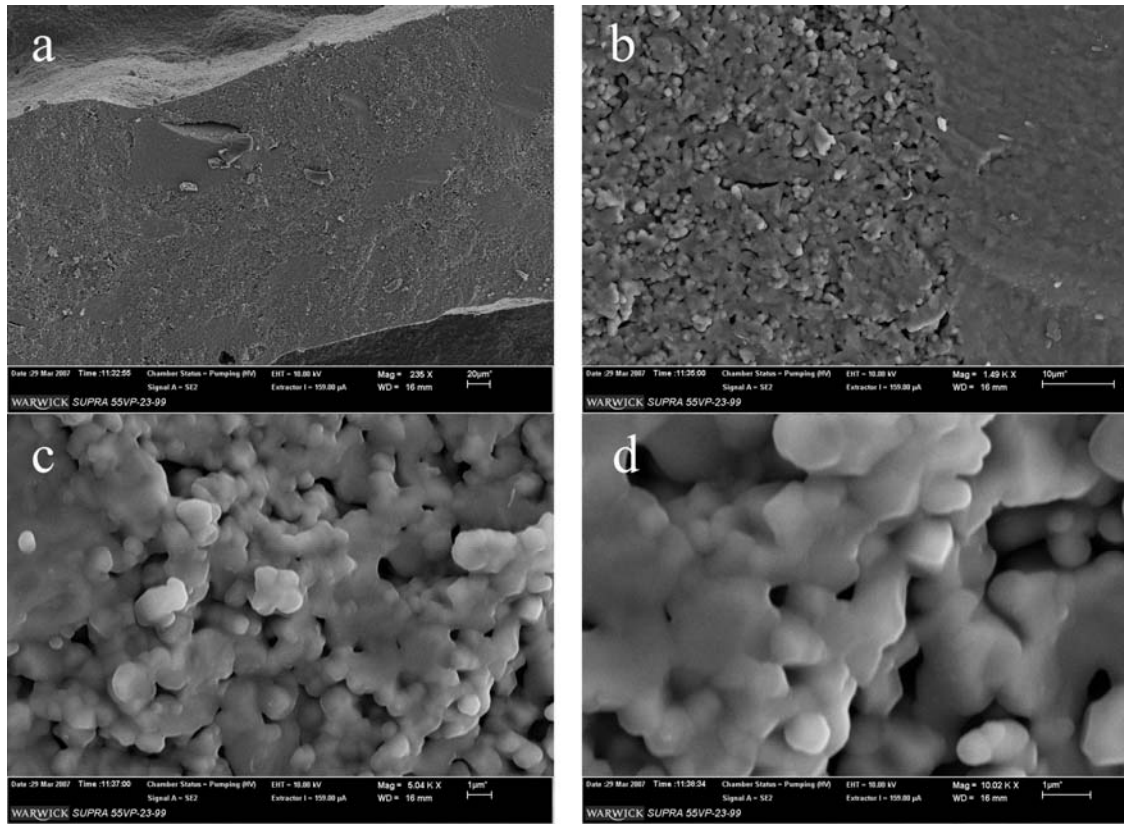


Figure 4.6 SEM images on the end of a cell wall for scaffold A, (a) illustrates the entire wall thickness with large particles from HAP 100 visible [scale bar = 20 μm] (b) illustrates the boundary between one of the large particles and the smaller particles of HAP 200 [scale bar = 10 μm] (c) illustrates the porosity of the monolith [scale bar = 1 μm] and (d) illustrates how the particles have been sintered together [scale bar = 1 μm]

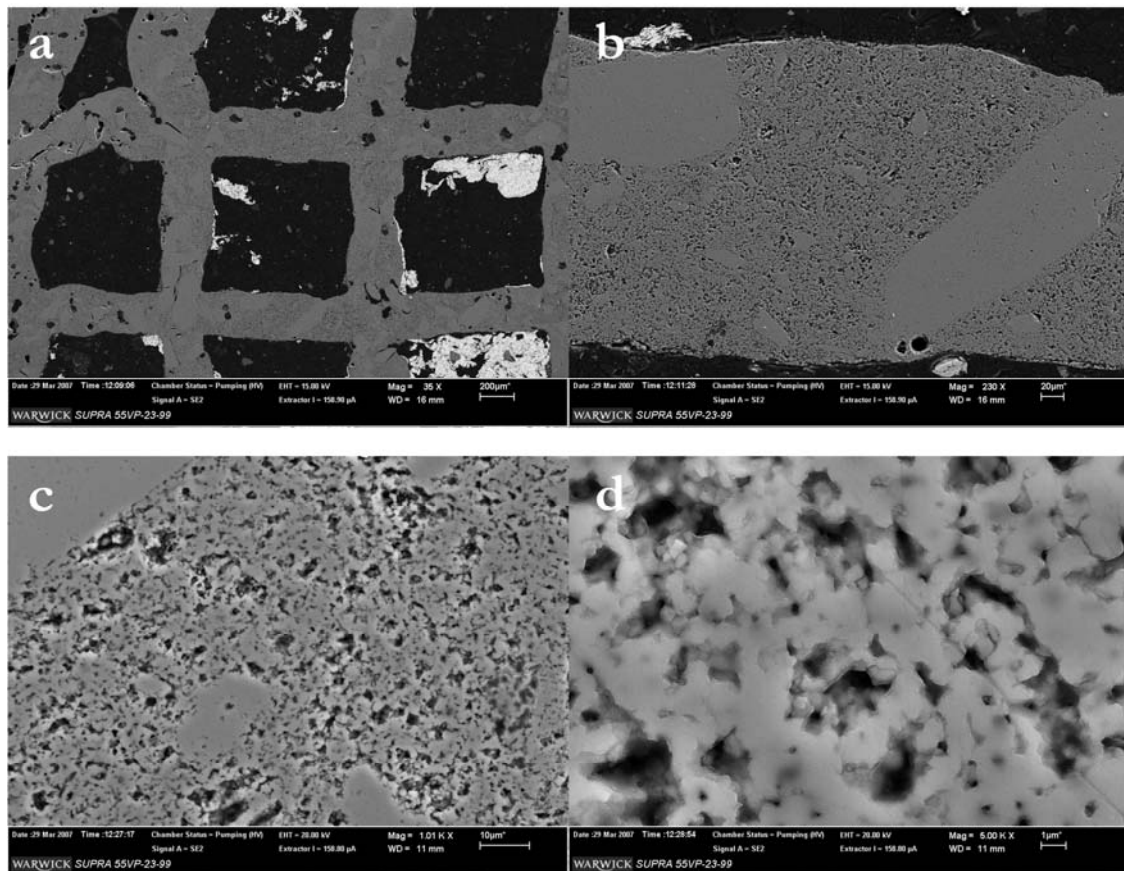


Figure 4.7 SEM images on the end of a polished cell wall for scaffold A, (a) illustrates a number of monolith cells [scale bar = 200µm] (b) illustrates the entire wall thickness with large particles of HAP 100 visible (c) illustrates the wall microporosity [scale bar = 10 µm] (d) illustrates the porosity in more detail [scale bar = 1µm]

4.2 Results of biological characterisation

4.2.1 Results of biological experiment 1

The MTT assay results from experiment 1 are presented in Figure 4.8, the lines represent the mean of the three tests. The most striking result is that sample C did not support the growth of MG-63 cells. The other samples demonstrate excellent cell proliferation during the experiment although cell growth has stabilised after 9 days of growth. A and B appear to have the greatest cell proliferation followed closely by D and E.

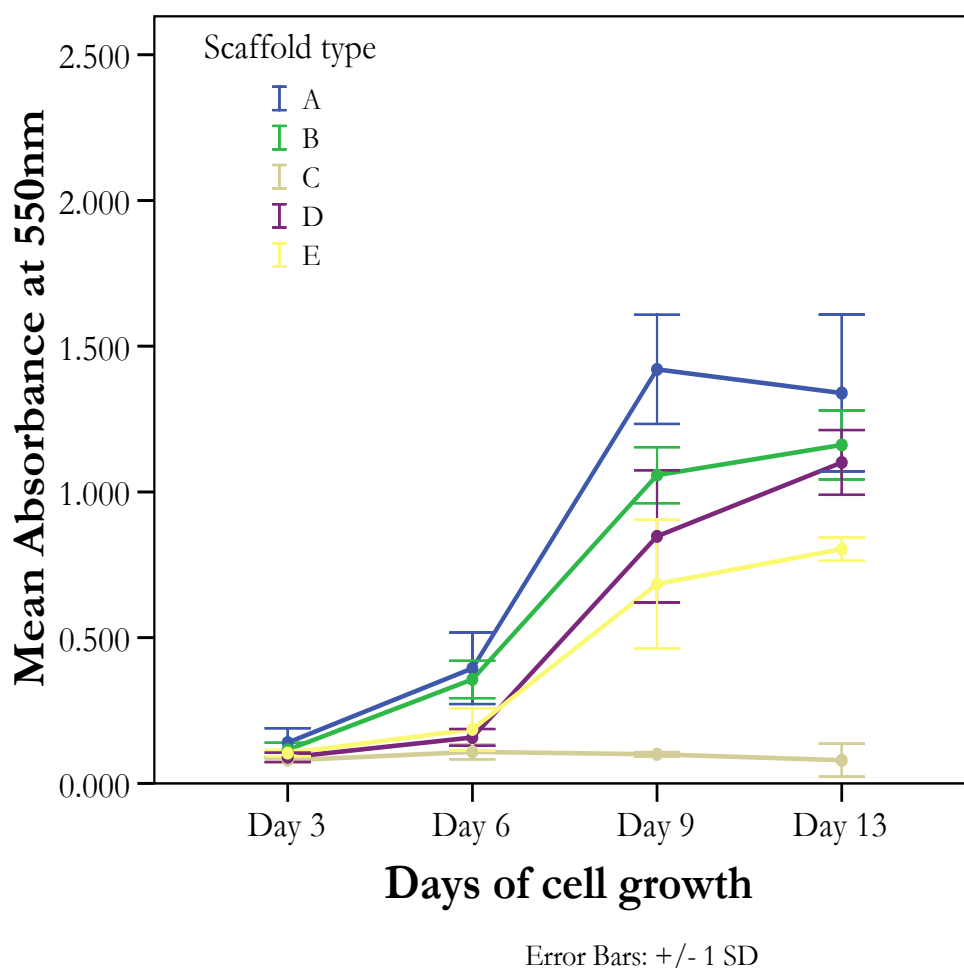


Figure 4.8 Graph of MTT assay results for each sample in biological experiment 1

The results for sample C demonstrate zero cell growth. A possible reason for the lack of cell growth of sample C was to be found in the colour of the cell culture media which was different for each sample. A and B were shown to have a light pink colour whilst C, D and E were bright pink. The colour of the media is affected by its pH and so the pH of the media for each sample was measured. The results shown in Figure 4.9 demonstrate that sample C is having a significant effect on media pH. The poor performance of sample C was postulated to involve a water soluble toxic substance present on the scaffold surface. In order to confirm the validity a second, identical experiment was set up but this time each of the scaffolds was equilibrated, or soaked in media for 24 hours prior to seeding with cells.

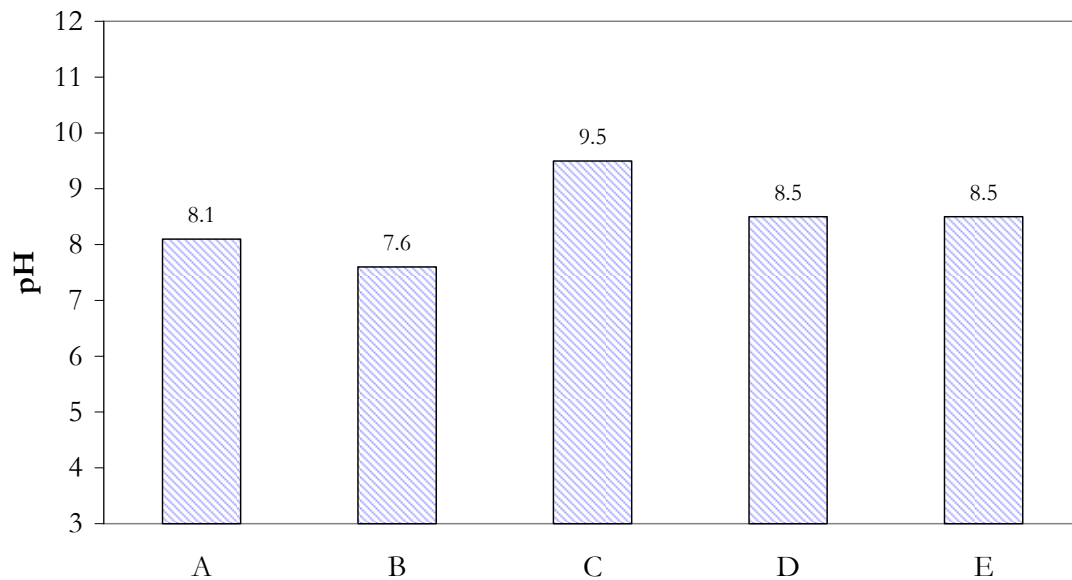


Figure 4.9 Graph of media pH after equilibrating the samples in media for 24 hours

4.2.2 Results of biological experiment 2

The MTT results from experiment 2 are presented in Figure 4.10. It can be seen that sample C now performs similarly to all of the other scaffolds. The mean results from each scaffold cross over one another and show remarkably similar rates of cell proliferation. It is useful to consider the performance of these samples versus the empty control. MTT assays were carried out to assess the number of live cells remaining in each culture plate well for all of the samples and the control. Figure 4.11 demonstrates the large number of cells growing in the empty well versus samples A to E. A more valuable result can be obtained by summing the assay results for the cells on the samples and the cells remaining in the culture wells, these are presented in Figure 4.12.

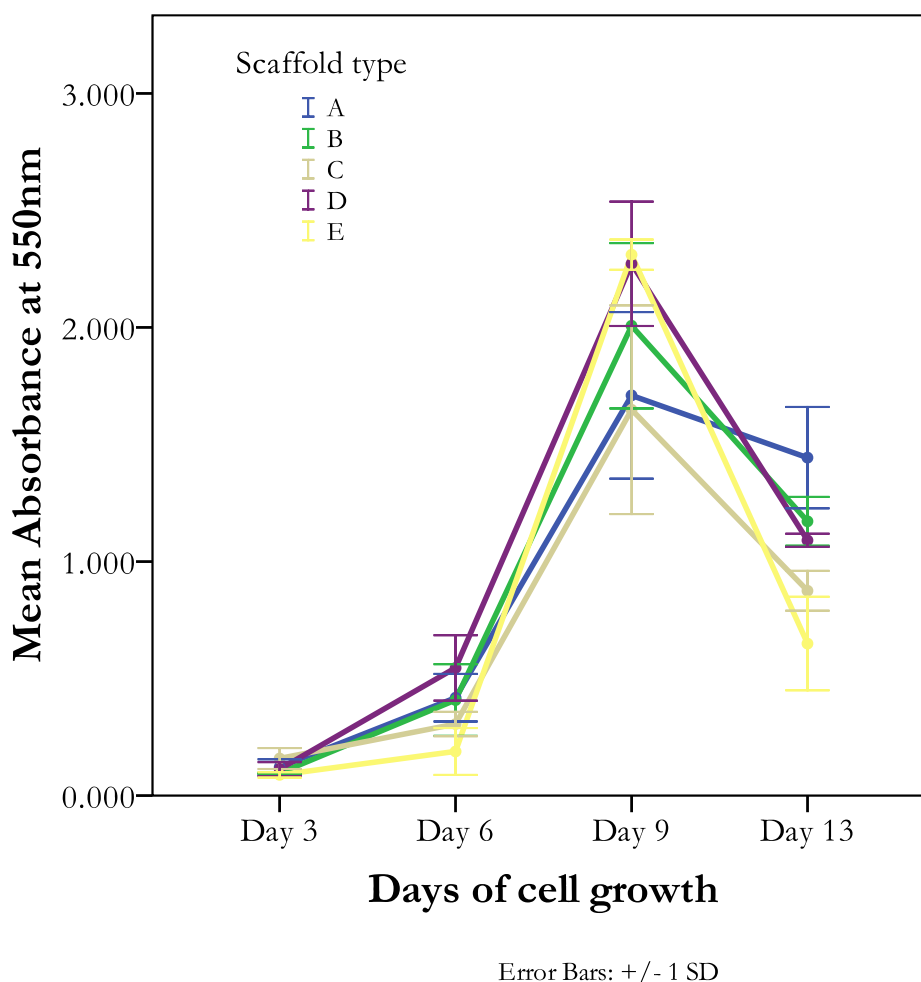
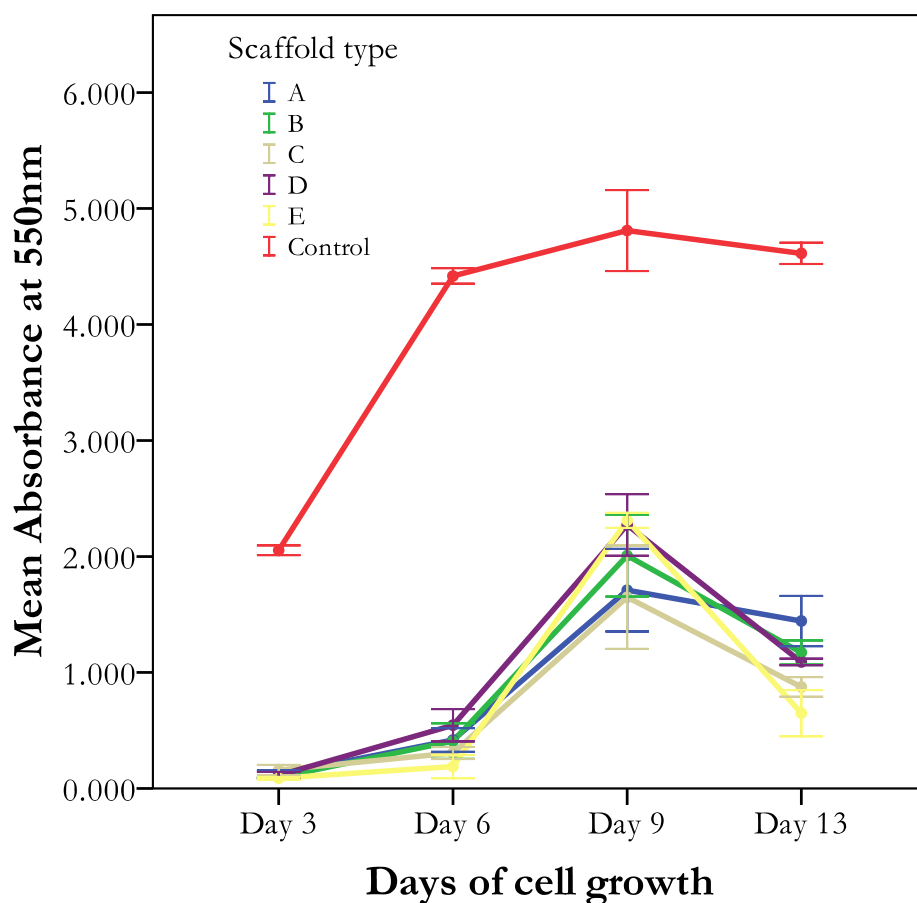


Figure 4.10 Graph of MTT assay results for each sample in biological experiment 2



Error Bars: ± 1 SD

Figure 4.11 Graph of MTT assay results for each sample in experiment 2 versus the control

Figure 4.12 demonstrates the total number of cells in culture and highlights that the total number of cells in culture for samples A, B and D is greater than the control up to day 9 and samples C and E have less cells than the control. All samples show a steep decrease in total cell count from day 9 to 13 and perform worse than the control at day 13. This is most likely as a result of the difficulty in supplying the cells on the monoliths with nutrients because of their 3D structure. This graph demonstrates a difference in the total number of cells in culture between samples A and B (paste 1) and C, D and E (paste 2). Samples A and B have a higher total cell count which may reflect the ability of the material to support osteoblast proliferation.

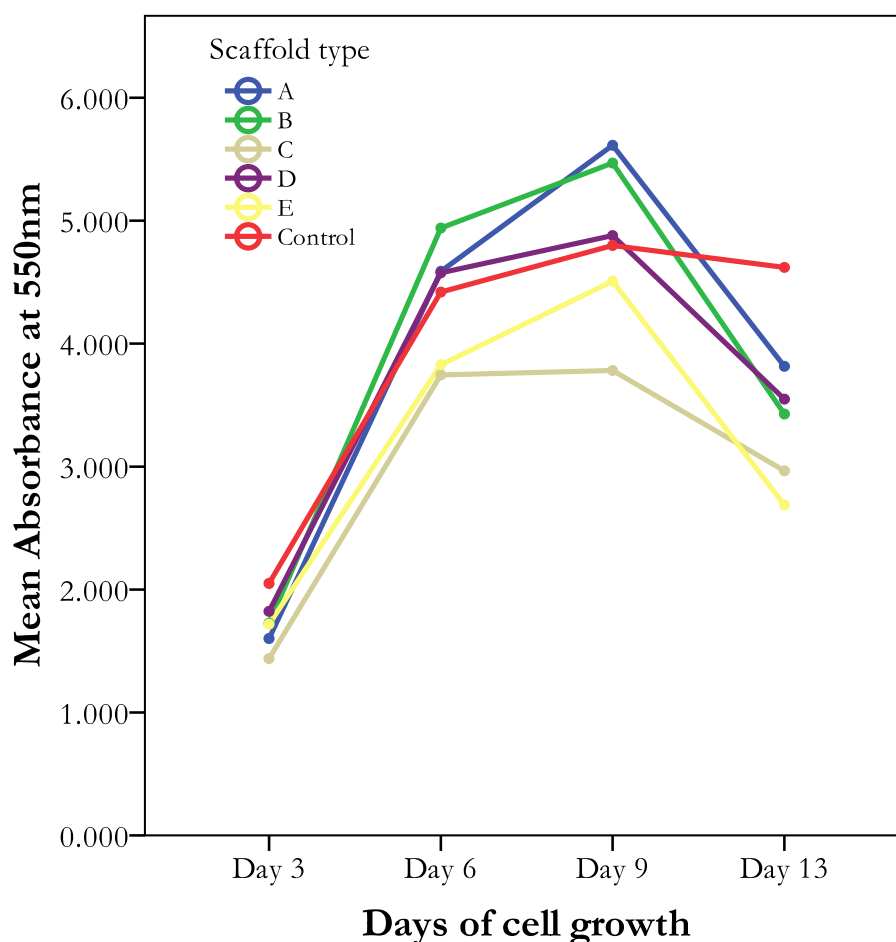


Figure 4.12 Graph of summed MTT assay results for cells on samples and cells in wells from experiment 2

4.2.3 Comparison with an existing BGS material

In order to gain an appreciation of how the HA monoliths performed when compared with an existing BGS material it was deemed prudent to carry out the same tests on a market leading product. Orthovita Vitoss[®] was chosen as it has been in the market place for many years and would provide a useful indicator of performance. Vitoss[®] is a β -TCP ceramic foam used as a void filler for bony defects. Equilibrated and non equilibrated samples of Vitoss[®] were seeded with cells in an identical fashion to previous experiments. When the results for Vitoss[®] and the HA monoliths are compared the cell proliferation for samples A, B, D and E compare favourably for both unwashed and washed samples. However, these

experiments were not carried out at the same time. Therefore, in order to confirm these results it was necessary to carry out a further experiment to compare them directly. Figure 4.13 presents the data from unwashed samples and Figure 4.14 presents the washed sample data. Washing of the samples in media for 24 hours appears to have a detrimental effect on the Vitoss[®] samples but a positive effect on the HA monoliths. Figure 4.15 shows the purple formazan attached to the scaffolds after incubation in MTT. Each of the HA monoliths has extensive cell growth on the horizontal surfaces with some penetration into the channels and around the periphery of the scaffold. Equally the Vitoss has good cell growth on the horizontal surfaces but no cell penetration into the foam. It also has little growth on the underside of the cylinder. Overall, the results show a remarkable similarity between the HA monoliths and Vitoss[®] although the phenomenon relating to the surface of the HA monoliths required further investigation.

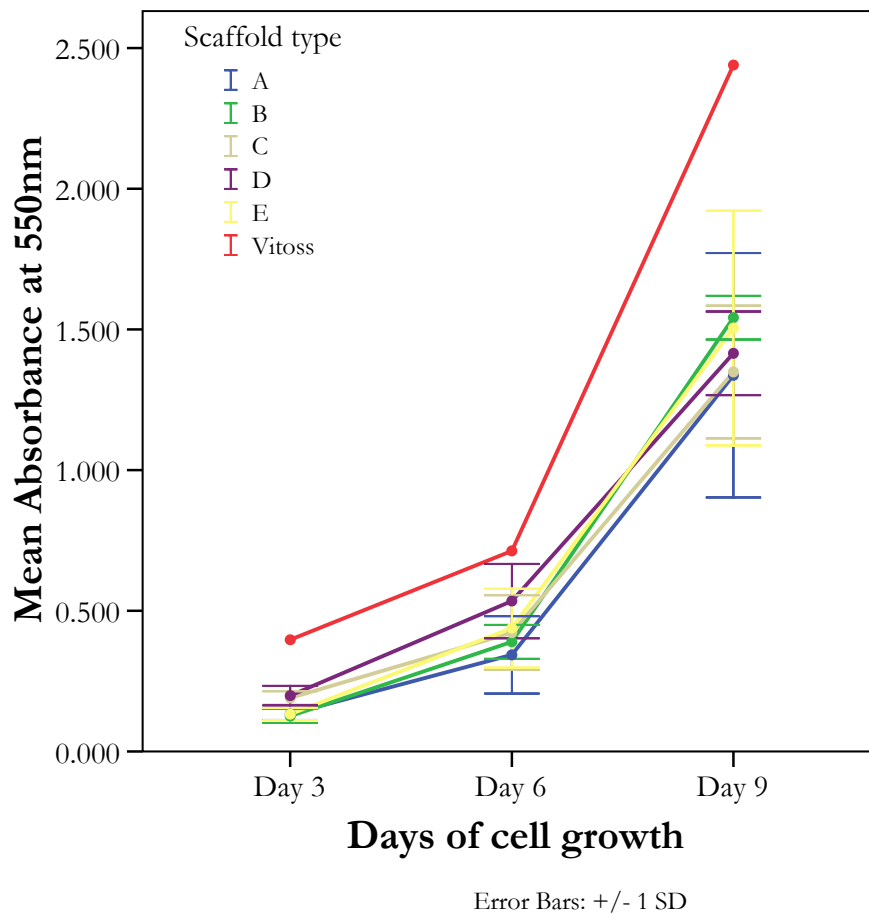


Figure 4.13 MTT results comparing unwashed HA monoliths with β -TCP Vitoss

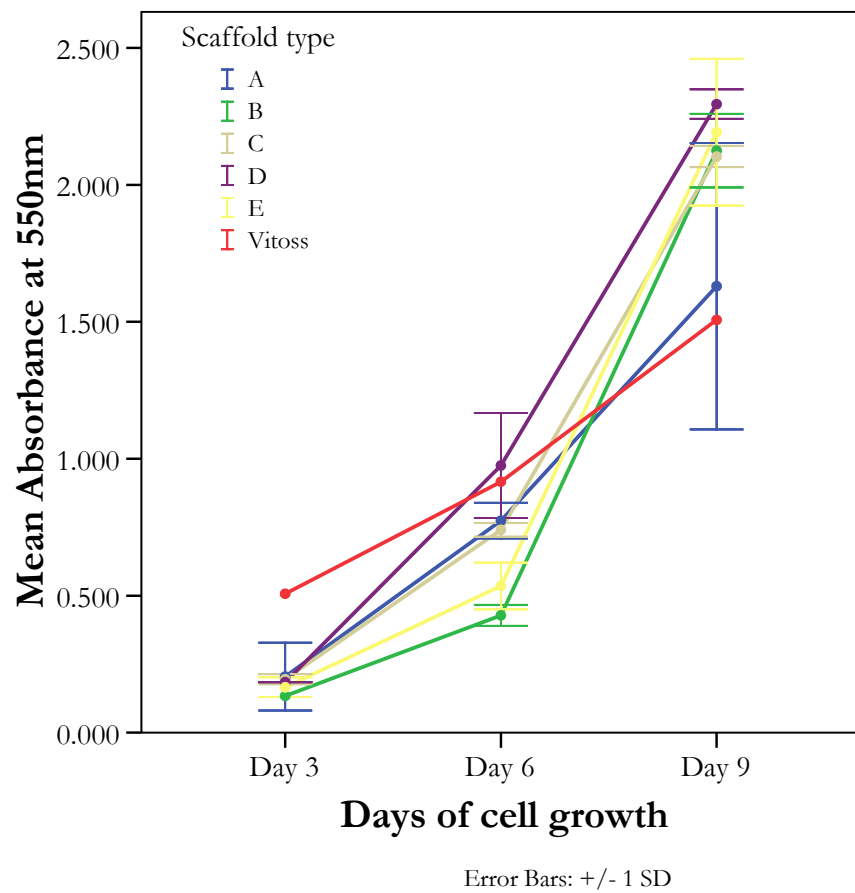


Figure 4.14 MTT results comparing washed HA monoliths with β -TCP Vitoss

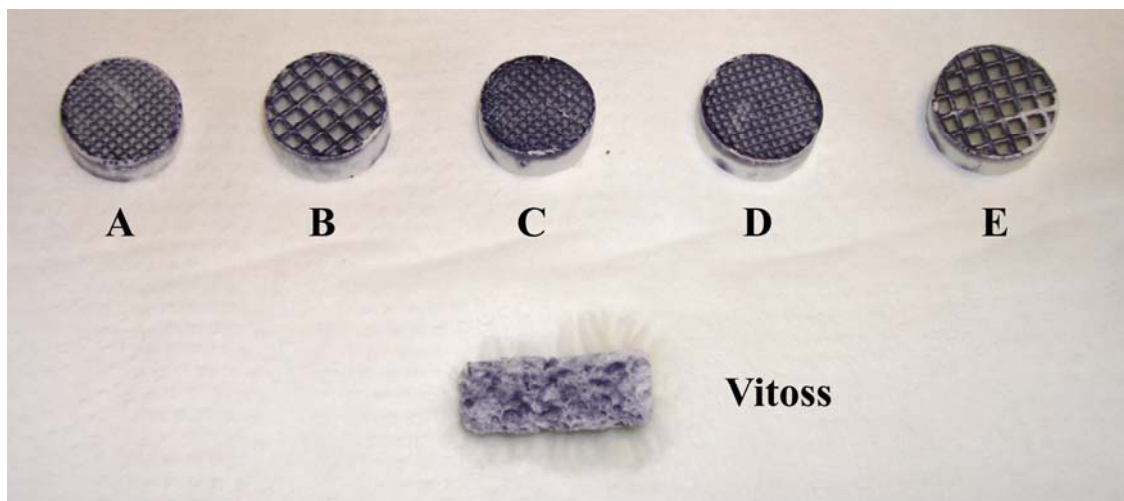


Figure 4.15 Image demonstrating the formazan staining on HA monoliths and Vitoss[®] after 9 days of cell culture and incubation in MTT for 30 minutes

4.2.4 Further sample analysis

Gas chromatography mass spectrometry (GCMS) is used to identify different substances within a test sample. To establish if there are any contaminants in the manufactured monoliths, samples A – E, a sample of Vitoss, and a blank sample were placed in glass bottles with 400 ml of methanol and allowed to soak for 24 hours. After this time a 100 µl sample of the methanol from each bottle was placed into a separate tube on the GCMS and analysed. The results for sample C are seen in Figure 4.16 where the X axis represents the time taken for the molecule to exit the column (retention time) and the Y axis is the relative intensity. Six of the peaks are identified although only two of these peaks are identified with greater than 85 % confidence. These relate to hexamethylcyclotrisiloxane and octamethylcyclotetrasiloxane.

When the results for each sample are combined and these peaks examined in further detail it is evident that samples C, D, and E all have higher concentrations of these chemicals than samples A and B which in turn have higher concentrations than Vitoss or the blank sample. Figure 4.17 shows the hexamethylcyclotrisiloxane peak for each sample clearly demonstrating that samples C and E have high concentrations with Vitoss and the blank sample very low in comparison. Hexamethylcyclotrisiloxane and octamethylcyclotetrasiloxane are both based on a ring of Silicon to Oxygen bonds and are a possible cause of the basic media present in the initial biological experiments although it unclear if the poor cell proliferation is due to the alkalinity of the media or the chemical itself. There are a number of possible sources for this contamination which include the raw material, the mixing/kneading process, the die and the furnace. Our industrial partner has examined the paste in detail and found no contamination that may have led to the siloxane contamination. One of the most probable areas where contamination may have occurred is during the firing process. As an example of this one set of samples that were manufactured had a pink tinge to them most probably as a result of iron contamination during firing. These were discarded but they highlight that very small levels of contamination can have a profound effect on the final material. It is clear that the production of medical implants such as these should use stringent control of raw materials and processing conditions including the use of clean rooms and dedicated furnaces which are free from contamination.

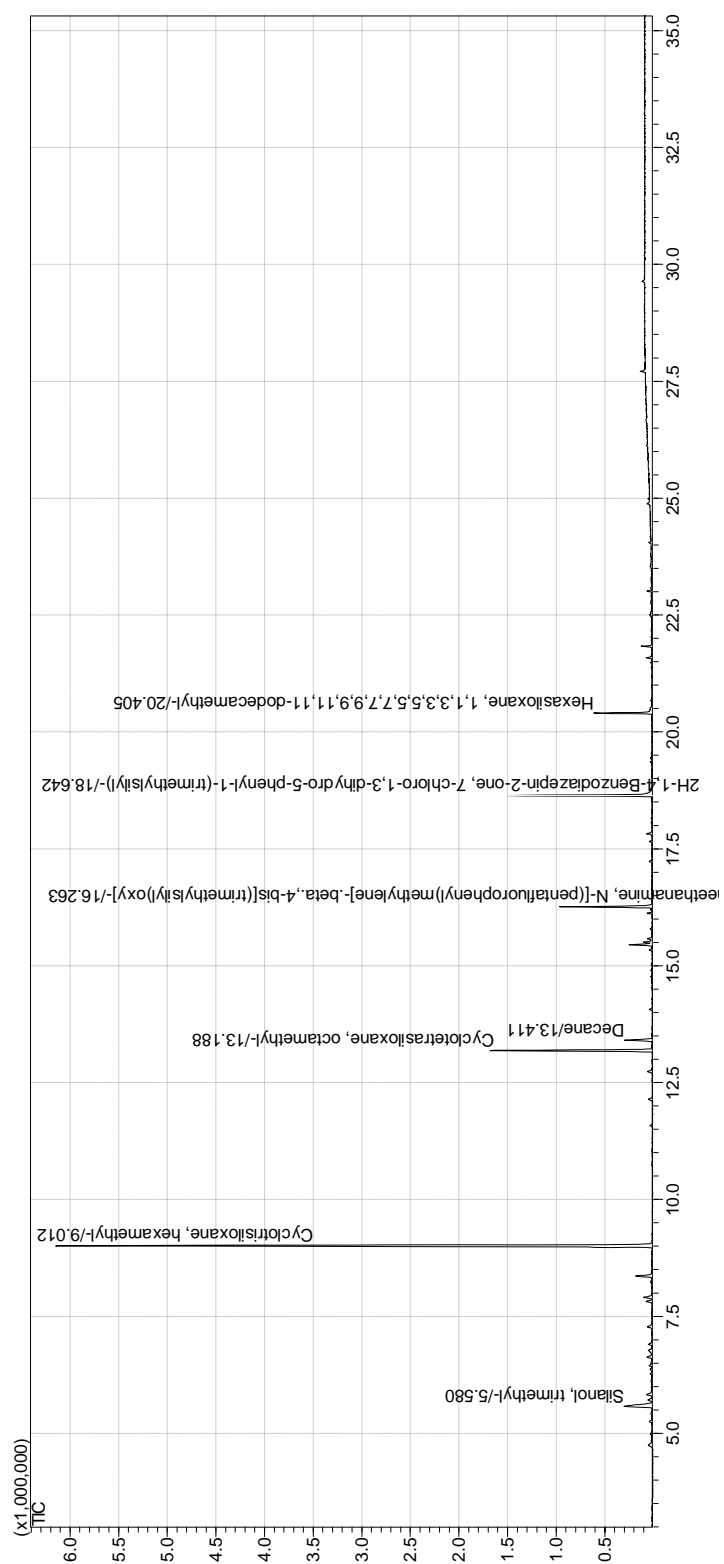


Figure 4.16 A GCMS plot for sample C with a methanol solvent

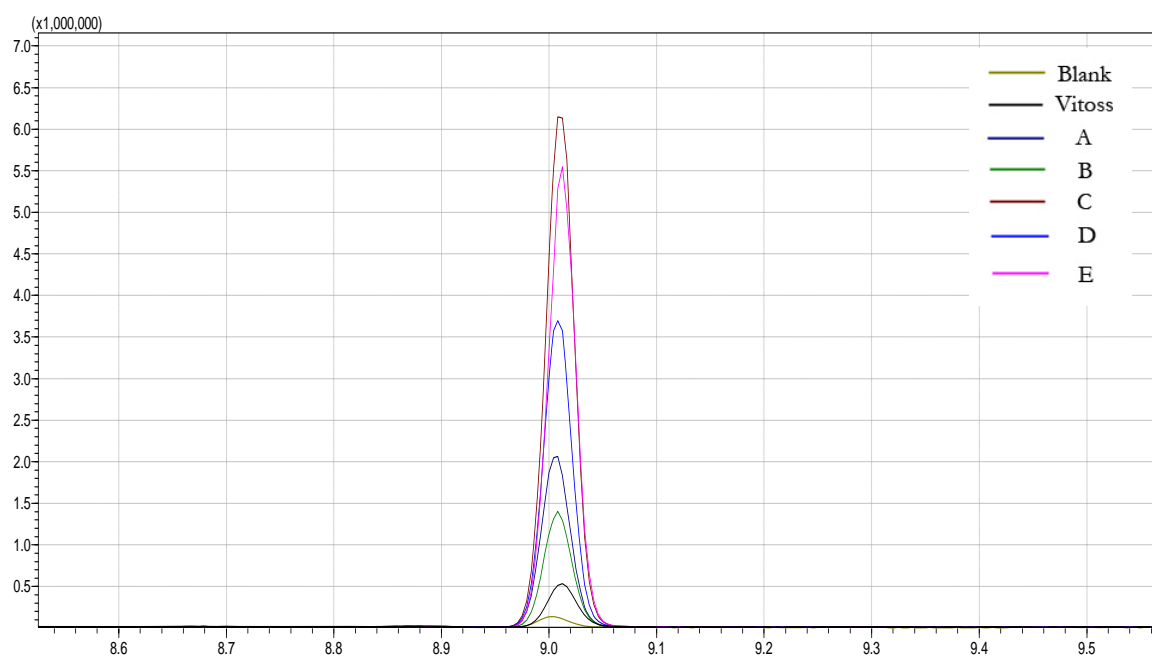


Figure 4.17 A magnified comparison of the GCMS hexamethylcyclotrisiloxane peak for A – E and Vitoss

Chapter 5 Clinical and expert opinion

5.1 The key benefits of calcium phosphate monoliths

The most important aspect of the extruded HA monoliths is the manufacturing process. Extrusion of ceramic monoliths is a highly consistent mass production process that can be used to produce consistent, high quality implants economically. The process enables any bioceramic to be formed into a highly porous and yet strong implant. Initial experiments using HA have produced monoliths with a bulk porosity of between 54 % and 63 % combined with a high compressive strength of 142 – 265 MPa and compressive modulus of 3.2 – 4.2 GPa. These values compare favourably against cortical bone (Table 5.1) and are significantly higher than Vitoss[®] a BGS material currently in the market [13,17,18].

Table 5.1 Comparison of strength and porosity for HA monoliths versus bone

	Monoliths	Bone	Bone	Vitoss
Material	Hydroxyapatite	Cortical	Cancellous	β -TCP
Compressive Strength (MPa)	142 – 265	50 – 250	1.5 – 10	0.1 – 0.6
Compressive Modulus (GPa)	3.2 – 4.4	5 – 35	0.05 – 0.9	0.001 – 0.01
Bulk porosity (%)	54.4 – 63.1	8 – 28	30 – 90	88.0 – 92.4
Channel size (mm)	1.08 – 2.53	-	-	-
Pore size range (μ m)	0.2 – 0.5	5 – 200	1 – 900	1 – 1000

The open structure of the HA monoliths provides an open channel structure that can be rapidly vascularised thus providing nutrients to cells throughout the entire scaffold not just at the surface as with conventional foamed ceramics. In addition, the channel walls are microporous providing an excellent environment for cell attachment and proliferation.

A further advantage of the open channel structure is the ease with which nutrients can be delivered throughout the scaffold in a bioreactor for tissue engineering applications. The linear channels in the material allow for cell culture media to be easily passed through it such that cells can be grown within the material rather than around the periphery. Furthermore the open structure allows for simple application of a coating to the implant. This may be a biopolymer (natural or synthetic) or other bioceramic (including bioactive glasses). A coating can be used to improve the mechanical and the biological properties of the sample. The coating could be impregnated with antibiotics to prevent infection or growth factors to enhance the rate of healing.

The open cell structure of the extruded monoliths allow it to be packed with demineralised bone matrix (DBM) or morselised autogenous bone both of which are highly osteogenic materials. In this way any implant will have structural integrity provided by the ceramic scaffold, contain osteogenic material and maintain its location at the implant site until full healing has occurred.

These monoliths can be manufactured in sizes suitable for use in massive (greater than 50 mm) structural grafts. Furthermore it can be formed directly after extrusion to conform with the geometries of irregular shaped bones in the skeleton. These may include curved extrusions to replace curved bones e.g. the hip or a rib as seen in Figure 5.1(a). It is also possible to mimic the ends of long bones using reduction extrusion as seen in Figure 5.1(b). In this way the internal structure of the graft will be maintained and have the greatest possible mechanical strength.

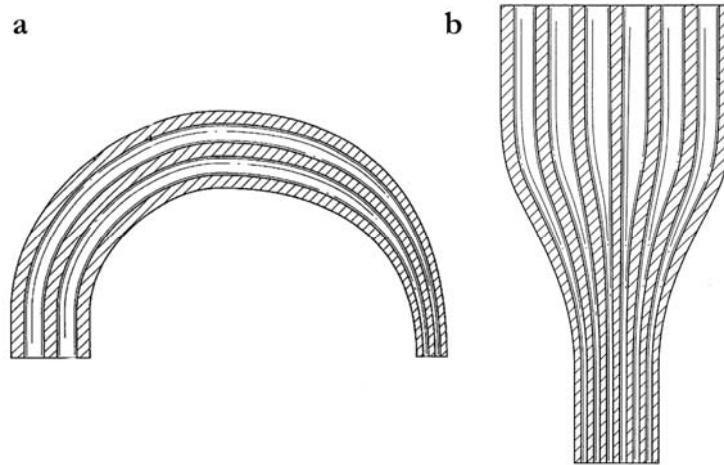


Figure 5.1 Illustrations of sections through curved (a) and reduction extruded (b) monoliths that can be utilised to mimic the natural form of bone, adapted from [162]

Extruded monoliths can also be machined using conventional techniques into patient specific implants, and can be easily shaped, using hand tools, by the surgeon in theatre. It can also be manufactured with a functionally gradient structure (FGS) such that the porosity and strength can be altered across the section of the extrusion to suit a particular application. Figure 5.2 demonstrates some typical monolith extrusion profiles (triangles, squares and hexagons) and in the bottom right a FGS where the structure is mimicking the cross section through a long bone. In this case the centre of the implant is highly porous and the density of material increases towards the periphery.

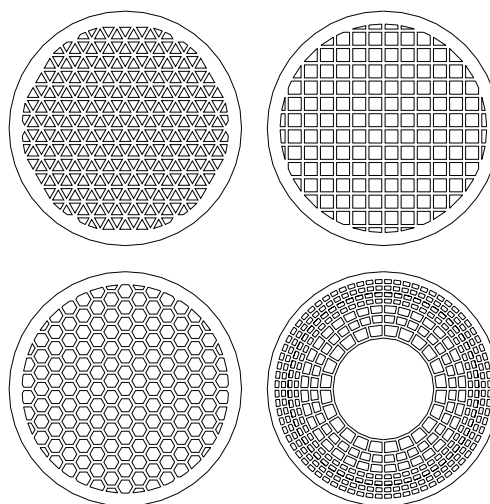


Figure 5.2 An illustration demonstrating four readily achievable extrusion profiles

5.2 Clinical input to this research

A vital part of any medical engineering project is to involve the end customer right from the beginning in order to develop new products which are clinically beneficial. In this case surgeons represent the end customer as it is them who must be convinced of the efficacy for any new product. To this end every opportunity to present this work to clinicians has been seized as well as seeking advice from experts in the field to identify the indications where ceramic monoliths may prove clinically beneficial. During the course of this research the author has written a number of bids for funding to support this research. One of these successful bids was used to pay a medical device expert to review the results of the work on HA monoliths. A summary of the main comments from a number of experts in the field are organised into specific topics and set out below:

Indications where monoliths may be beneficial

- “Treatment of long bone segmental defects, approximately 50 mm in size and larger”
- “Spinal applications that require high compressive strength. Current blocks suffer from low strength and bone incorporation is generally poor”
- “An implant that was strong enough to cope with the mechanical loads around the spine and have the patients own cells present in the scaffold to increase the rate and likelihood of successful interbody fusion was considered to be ideal”
- “For large defects it is important the BGS can be retained with screws, hence understanding its performance with screws is important to understand for both attachment of soft tissues and structural location at the defect site”
- “Spinal applications are attractive, particularly if good surface area contact can be provided to prevent subsidence, and if the implant modulus could be tailored to be less rigid than current materials. Problems with current spinal implants include the small contact area which leads to subsidence into exposed bone and subsequent loss of correction and intervertebral spacing. As well as the rigidity of current implants being a problem, reduced modulus may help to stress the bone and give faster ingrowth and incorporation”

- “Replacing the bone removed during bone tumour surgery”

Tissue Engineering

- “There was a strong desire for any BGSs to be suitable for use with growth factors”
- “Equally there was a desire for tissue engineered products cultured with autologous cells prior to surgery in order to increase the chance of successful integration”

Barriers to uptake

- “Previous experience of calcium phosphate ceramics will mean that surgeons will be sceptical of their high strength”
- “Spinal applications are a possibility but there may be a ‘leap of faith’ required from surgeons”
- “Clinical data is essential to clinicians, in particular demonstration of bony ingrowth/incorporation into large defects”

Resorbability

- “Synthetic materials remain in the body for a significant time after implantation. The material should be capable of significant resorption. A composite of HA/TCP is preferred to pure HA”

General points raised

- “There is significant interest in new BGSs and especially biological solutions”
- “There is a possible move back to autograft in the future for budgetary reasons”
- “A clinical or science champion is essential”
- “It is important to have an approved product (CE marked) in order to achieve success”

Highlighted concerns

- “The maximum size of defect that could be treated in terms of actually getting nutrients into the scaffold and then ossifying it”
- “The product as it stands appears suitable for use in long bone segmental defects but may not have adequate strength for spinal applications”
- “The compressive strength of the material is very good but further consideration needs to be given to understanding and improving the tensile strength and fracture toughness”

Addressing these concerns will require further research. The maximum defect size that can be treated by a BGS will depend on a number of factors including patient health, their weight and whether they smoke. Healing of large defects will almost certainly require use of growth factors and depend on establishing an adequate blood supply to the region. The literature contains examples of massive allografts up to 24 cm in length healing successfully [163-165]. However the survival rate of massive allografts at 216 months is reported to be only 56.6 %. The majority of these fail because of infection, a problem which may be eliminated by use of synthetic materials [164].

The use of HA monoliths for spinal implants is an interesting possibility and their compressive strength is adequate as described in Chapter 4. In spinal applications the cost of implant failure is high, hence current spinal cages are made of titanium, carbon fibre, or polyetheretherketone (PEEK). Maintenance of disk height during spinal fusion is closely related to favourable outcome but is often impossible to achieve because of subsidence. This is a particular problem when the vertebral endplate is resected [166]. In this case an implant which induces rapid formation of a bony bridge between the vertebrae and then degrades over time will not suffer from subsidence and loss of correction as occurs in existing rigid non degradable implants [167].

A spinal implant would need extensive strength and fatigue testing to prove its suitability. Also further understanding of the fracture toughness, tensile and shear properties will need to be obtained in order to increase confidence in their suitability as a high strength bone graft. A number of comments were made regarding the suitability of HA for use in BGSs as it is thought to degrade too slowly *in vivo*. The material is easily altered and future work should concentrate on maintaining the strength achieved while increasing osteoinductivity and degradation rate. There is also an issue related to altering the beliefs of surgeons and making them consider the use of new and innovative materials and methods. Surgeons are a conservative group of people unwilling to take any risk. Therefore new products will need to prove their efficacy before being applied clinically.

Chapter 6 Design of an implant utilising ceramic extrusion

6.1 Introduction

Feedback from clinicians and experts in the medical device field highlighted the spine and particularly spinal fusion as an indication where extruded calcium phosphate monoliths may be clinically beneficial. The cost of lower back pain in the US exceeds £50 billion annually mostly through indirect costs as a result of lost wages and productivity. This provides enormous incentive to prevent spinal problems occurring and reduce their effects when they do. Particularly since 5% of the patients who present with lower back pain are responsible for 75% of the total costs [168] and are therefore easy targets for large improvements.

The spine consists of 30 bones connected together through compressible intervertebral discs which provide its flexibility. It is divided into four main parts: the cervical spine (C1 – C7), thoracic spine (T1 – T12), lumbar spine (L1 – L5) and the sacrum (S1 – S5) as can be seen in Figure 6.1. Again there are a wide range of conditions that may cause back pain but two common conditions are spondylolisthesis where one vertebra shifts forward over another and spondylosis where the intervertebral discs degenerate. Other conditions such as bulging and herniated discs can be seen in Figure 6.2. Once the intervertebral disc has degenerated there is little option but to fuse the vertebra in a technique called spondylosyndesis (interbody fusion). When fusion is successful it should eliminate back pain and other any neurological symptoms.

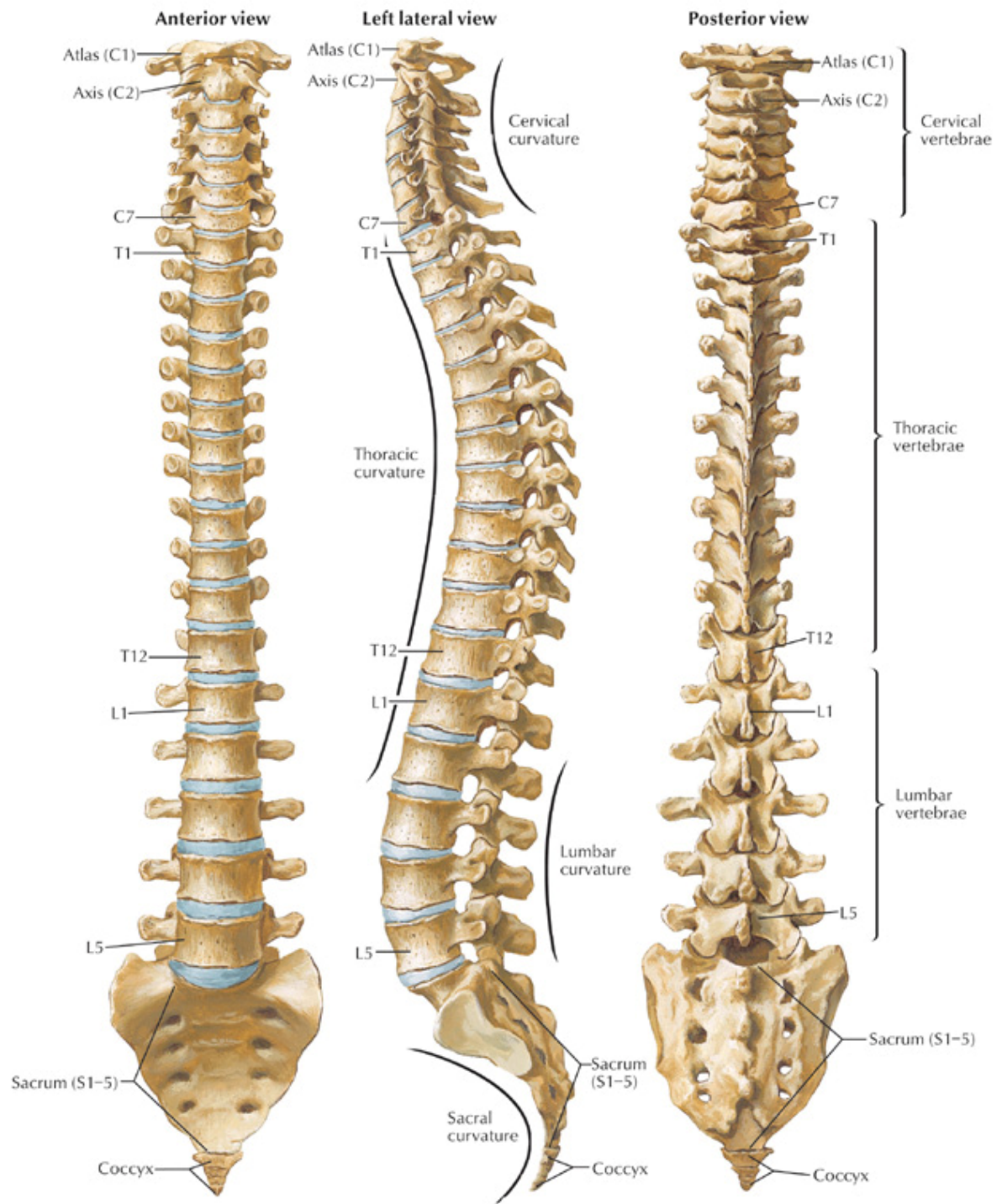


Figure 6.1 Illustration of the anatomy of the human spine [169]

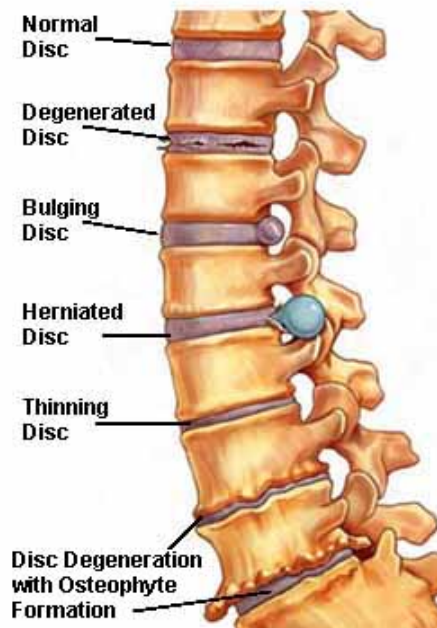


Figure 6.2 Conditions that may lead to the requirement for spinal fusion [170]

The approach taken for interbody fusion will vary according to patient and surgeon but the posterior approach is commonly used. Posterior lumbar interbody fusion (PLIF) is a complex procedure requiring the removal of the intervertebral disc, decompression of the spine, insertion of a spinal cage and bone graft into the space and finally the use of pedicle screw fixation to prevent any movement of the fused segment. An essential element of a successful interbody fusion is large quantities of bone graft material [171]. Figure 6.3 demonstrates the basic procedure for an L4 – L5 PLIF and is described below. First the L4 spinous process is removed (a), then the L5 superior facets (b), then the ligamentum flavum to expose the nerves (c). The nerves are retracted and the intervertebral disc material removed (d) then a chisel is used to flatten the vertebra end plates (e). Now the spinal cage is inserted (f) and located centrally (g) before a large quantity of autologous bone graft is inserted (h). Finally this process is repeated for the other side of the vertebra until the final view appears as in (i). The final layout of cages and autograft bone is shown in Figure 6.4 demonstrating the large quantity of bone graft material used.

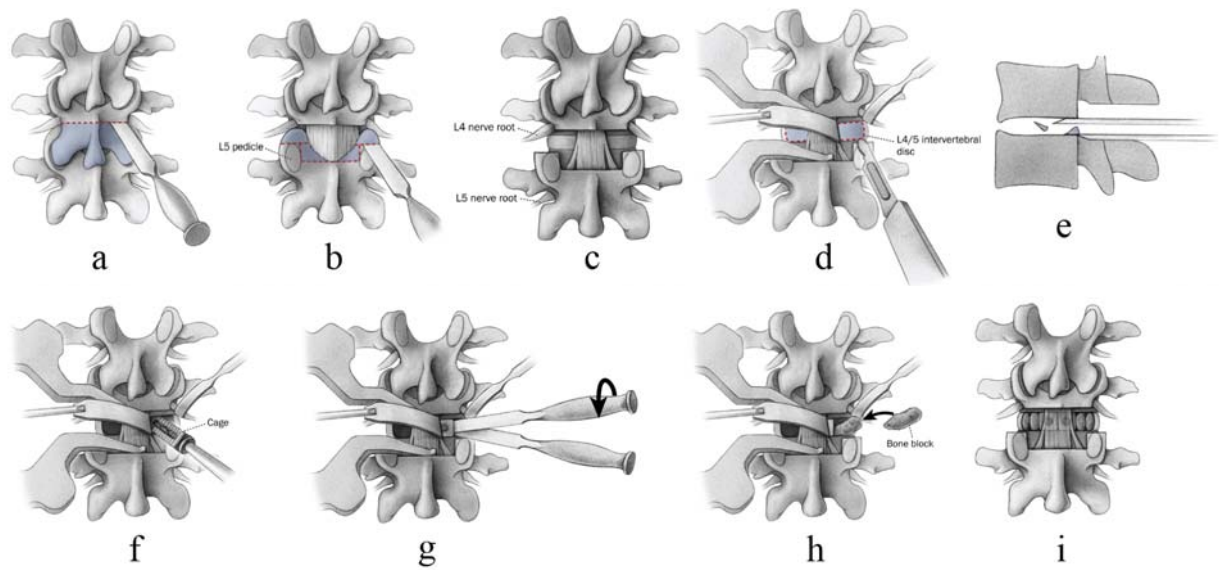


Figure 6.3 The procedure for posterior lumbar interbody fusion, adapted from [171]



Figure 6.4 The final layout of spine cages and autograft for a PLIF procedure [171]

Once the cages and bone graft have been inserted into the intervertebral space instrumentation in the form of pedicle screws is used to rigidly fix the two vertebrae together. Cervical or lumbar fusion can also be carried out using an anterior approach through the front of the body. The perceived advantages of an anterior lumbar interbody fusion (ALIF) or anterior cervical interbody fusion (ACIF) are that the muscles in the back around the spine are not damaged or cut during the procedure which avoids muscle

weakness. Furthermore the use of minimally invasive techniques with the anterior approach can reduce patient recovery time [170]. Each of these approaches are used frequently depending on the preferences of the surgeon and as such there are a large number of devices available that cater for both. The largest companies involved in producing interbody fusion devices are Stryker, Medtronic Sofamor Danek and Synthes. An image showing some of the devices produced by these companies is shown in Figure 6.5. These take a wide range of forms and are all beautifully engineered devices.



Figure 6.5 Image demonstrating a range of spinal interbody fusion devices [172-174]

6.2 Important design features

There are a number of important features that an interbody fusion device must incorporate in addition to all of the standard requirements for an implant as set out in the MDD:

- A tapered implant can be useful and is used to restore the natural curve (lordosis) to the spine
- Two cages are often used to give enhanced stability and make it simpler to insert the device particularly during PLIF
- The device should be as porous as possible to promote bone ingrowth and complete fusion
- The implant needs to be available in a number of heights from 11 – 17 mm and ideally with a taper of between 0° and 8°
- The implant should be radiolucent so that its position can be verified by X-ray during the procedure and checked for accuracy
- Typical materials are titanium, stainless steel, carbon fibre and PEEK for high strength and a modulus similar to the natural bone
- High maximum strength and resistance to fatigue are essential
- Any device needs to have secure attachment to instrumentation used to locate it
- The device must resist being squeezed out of its ideal location, serrations and spikes are often used to accomplish this

Most of these requirements are simple design problems that can be solved with good design practice. The issue of maximum strength and fatigue resistance are inherent to the material selected for the device. Titanium, carbon fibre and PEEK are used extensively because of their biocompatibility and strength. None are biodegradable and may lead to subsidence, loosening, migration and metallic ion absorption. Porous ceramic materials have been avoided to date since the cost of failure will be high. So when considering the use of a calcium phosphate spinal implant a great deal of care needs to be taken over making sure that it will survive the worst case loading scenario.

The ultimate compressive strength of a vertebral body is reported to be 8,000 N. Typical PLIF and femoral ring allograft (FRA) spacers have a compressive strength of over 25,000 N [175]. Earlier testing of 15 mm diameter extruded HA monoliths showed them to have a compressive strength of 24,000 – 34,000 N. If a safety factor of three is chosen then the maximum load to failure should be greater than $8,000 \times 3 = 24,000$ N for any spinal implant.

The typical loads on the spine during a number of activities are significantly lower than this although the loads do not always act in the axial direction. The loads in the lumbar spine during ‘very fast’ walking are reported to be 2.5 times body weight. So for a 100 kg person the maximum load in the lumbar spine is likely to be 2,500 N [1]. One study examined loads in the lumbar spine of patients implanted with an instrumented vertebral body replacement which measured a maximum of 700 N load when sitting whilst carrying a weight at arms length [176]. This is a static situation and loads are likely to be higher during dynamic loading although it should be remembered that patients having undergone a lumbar fusion will not be instantly mobile.

Another consideration is the forces which are likely to occur during bending where only one side of the implant will be loaded thereby greatly increasing the stress within one side of the implant. Any ceramic device for spinal fusion would have to undergo extensive *in vitro* testing to establish its suitability prior to any implantation trials being carried out.

In addition to compressive strength it is important to consider the resistance to implant expulsion. Many of the existing devices have saw teeth or spikes to prevent expulsion. The maximum shear force that a human disc can withstand is approximately 150 N and any new device should easily exceed this. The pullout force is typically determined with a clinically relevant axial load (around 450 N) and then a simple pull out test. PLIF devices have been found to have a pullout of around 1200 N which is thought to be adequate. Teeth were found to increase the pull out load by more than 3 times and as such are an important feature of the design [175].

The final consideration is the fatigue life of the implant. Clearly the implant is intended to promote the ingrowth of bone within and around it which will reinforce it over time.

Mature fusion is usually seen at six to nine months although studies have shown that the technical success (indicated by fusion) tends to be greater than clinical success (indicated by a decrease in pain) [175]. Any device should be designed to degrade at a rate that is proportional to the ingrowth of load bearing bone. It is imperative that the device does not begin to degrade before the *de novo* bone is able to bear a proportion of the load. This is particularly important in patients who may heal more slowly such as the elderly and those suffering from systemic disease. Another point of note is that lumbar fusions with segmental pedicle screw fixation are reported to have a 100 % fusion rate whereas those without instrumentation are only 58.6 % successful. This demonstrates a need for additional fixation either from pedicle screws or from screws that go through the interbody implant and into the vertebrae [175].

Spinal fusion is reliant on the biological healing process which is dependant on many factors including the extent of the instability problem, the type of bone graft used, the surgical technique and the patient's anatomy and lifestyle. Many of the studies carried out have contradictory results most probably as a result of the large number of unknown contributory factors. From the items discussed above it is now possible to design a theoretical interbody fusion device. This is elucidated further in the following section.

6.3 Design of a lumbar interbody fusion device

The aim for this section is to design a PLIF device using the innovative manufacturing process for BGS material that has resulted from the author's research. This initial design will then be assessed by neuro surgeons and a number of design iterations carried out until an implant suitable for manufacture and testing has been designed. Figure 6.6 is a 3D image of the pelvis and lumbar spine generated from CT data available from the visible human project. The CT data is imported into Mimics where the bone is highlighted using thresholding and a 3D model of the bone is exported into a CAD program (Solidworks).



Figure 6.6 A 3D rendering of the bones in the pelvis and lumbar spine

Once the data is in the CAD system, measurements can be taken of the actual size of the vertebra (Figure 6.7) and this information used to design the PLIF device. In this case a monolith with a cell pitch of 2.5 mm and wall thickness of 0.5 mm was chosen to provide excellent open channel porosity designed to promote rapid fusion. The device is made in two halves to allow for easy posterior insertion and it has serrated teeth to prevent expulsion from the interbody space.

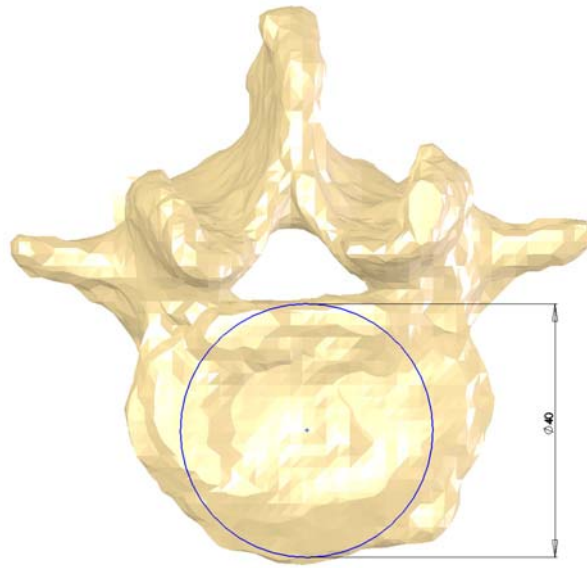


Figure 6.7 A CAD model of L4 vertebra and its approximate dimensions

The teeth for the initial design are only cut in one direction although there is evidence that suggests pyramidal shaped spikes hold the implant in place more satisfactorily. For ceramic implants there is little prior knowledge and so this would have to be determined empirically. Figure 6.8 is a CAD model demonstrating the preliminary design for a PLIF implant utilising ceramic monolith manufacturing methods. Some additional features visible are the chamfered lead in to ease insertion of the implant, and the teeth have rounded spaces between them rather than sharp corners so that there are no stress concentration points that may lead to early implant fracture. In addition, the surface area of the implant in contact with the vertebra has been maximised to prevent subsidence of the implant and the profile has been matched to the form of the vertebra.

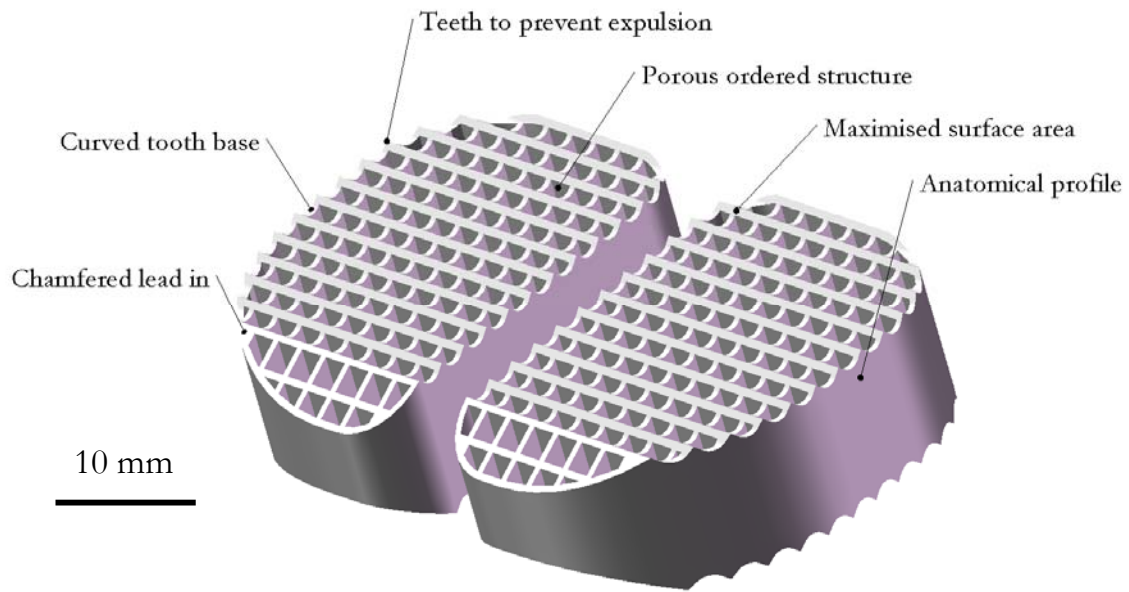


Figure 6.8 A 3D CAD model of a proposed PLIF device utilising ceramic extrusion

6.4 Planning for medical implant approval

The orthopaedics market is subject to increasingly strict regulatory scrutiny. The UK market is governed by the Medicines and Healthcare products Regulatory Agency (MHRA), the US market by the Food and Drug Administration (FDA), and the Ministry for Health, Labour, and Welfare in Japan [177]. This has led to an increase in the investment of money and time required to gain product approval and has led many of the small companies developing these products to seek strategic alliances with much larger companies to make use of their global marketing, purchasing, and logistics operations. The European market has recently adopted the European Medical Devices Directive which has harmonised regulations allowing any manufacturer with a CE marked product to sell anywhere in Europe.

Medical devices in Europe are regulated by the MDD (Medical Devices Directive) 93/42/EEC. Generally speaking the responsibility for ensuring compliance to this directive is down to the competent authority in each member state, typically the Ministry for Health. These competent authorities appoint notified bodies to administer the requirements of the

directive and compliance with this directive means that a product may carry the CE mark. In the UK the notified bodies are autonomous certification agencies such as the BSI or SGS.

Medical devices are classified according to the level of risk which they pose. The classes are I, II, IIA, and III, where class III devices pose the highest risk. BGS materials will be either Class IIB or III (Rule 8, Annex IX), the final classification will depend on the application and whether there is any biological effect or any degradation of the device. A simple hydroxyapatite (HA) device which degrades very slowly *in vivo* may be classified IIB but small changes to the material composition to make it degrade more quickly or have enhanced biological performance will mean that it would fall into Class III. Hence it is prudent to assume that a BGS material with ‘ideal’ properties will fall into Class III. This was confirmed by the Medicines and Healthcare products Regulatory Agency (MHRA).

Class III devices require both full quality assurance and an EC Design Examination. The full quality assurance means that the company selling the product needs to have a quality management system that complies with ISO 13485:2003. This is ISO 9000:2000 with additions specific to medical devices. The design examination is a review of technical documentation pertaining to the device by an expert in the particular field in question. Compliance with these requirements is assured by the notified body who can be selected based upon location, cost, and working relationship. Class III devices take longer and cost more than IIB devices to have certified.

There are a number of key documents required to meet the terms of the MDD. These are:

- Essential requirements review – this is normally in table form and sets out how each item in Annex I is addressed.
- Risk analysis – should be carried out according to ISO 14971 and set out all the risks along with appropriate management or mitigation actions.
- Biocompatibility – there are a range of standard tests set out in ISO 10993 which relate to biocompatibility. This section may amount to an extensive review of the literature with the possibility of using animal testing to give a high level of confidence

- Clinical evidence – the amount required depends on the device and its intended use. Use of materials that have already been proved to be biocompatible significantly reduces the amount of work required and may even eliminate the need for clinical testing in humans
- Sterilisation validation – the final product needs to be supplied sterilised and in suitable packaging. There are many ways of carrying out the actual sterilisation but it is important that the validation is carried out after the manufacturing process has been established since any changes may influence the level of residual micro-organisms and hence the efficacy of the device

There are a large number of harmonised standards in existence within the EU, none of which are a requirement but if met can be used to demonstrate that the essential requirements have been met. There are also a number of US and Japanese standards which would have to be conformed to if the product was to be sold in these markets.

Chapter 7 Overview

This research project has required a thorough understanding of the background material related to the specifics of bone tissue engineering. From the point of view of an engineer some of the biological and material science aspects have been hard to grasp and as such this research has focused principally on the engineering aspects and particularly on innovative methods to manufacture bone graft substitute materials. Extensive research into the properties of natural bone made clear the scale of the challenge to replicate its properties for an innovative BGS. There are even today significant gaps in our knowledge related to bone and the mechanisms that lie behind its remarkable properties. BTE is truly a multidisciplinary field and in time will be understood more completely thereby opening up the possibility to grow bone in the lab that mimics the properties of bone precisely. For now the best achievable result is to create a strong and porous material whose properties induce bone formation and which will degrade over time to be replaced by natural bone.

To this end the methodology for this project focused on gaining an understanding of a range of manufacturing methods and how they might be used to create a novel BGS. At the beginning of this project RP was a new and fashionable research area and so a number of these methods were attempted with limited success and a realisation that they were not the answer for production of an economically viable BGS. Extensive research in this area would certainly have resulted in innovative work. However, the problems highlighted by the manufacturing trials coupled with more practical problems such as machine availability led to a renewed enthusiasm for the conventional processes such as machining and injection moulding. The original premise that a block of material with ordered porosity would perform well both structurally and biologically led to a number of processes being attempted. The most successful of these was laser drilling of PLA cubes which resulted in a highly porous cube of material that could be shaped by a surgeon, in theatre, to match the

specific geometry of the defect. An unsuccessful attempt to create similar porosity in a HA block led to the realisation that extruded ceramic would have very similar properties and could be manufactured more efficiently. Further research revealed that extrusion of calcium phosphate ceramics for BTE had not previously been attempted. This catalysed a number of events including the design of a device to extrude ceramic paste, the writing of a patent to protect the idea and the writing of research grants to fund further research.

The extrusion of a ceramic paste to form a monolith is not a straightforward process and requires precise preparation as well as the correct machinery and processing conditions. The initial attempts by the author using an experimental extrusion device proved unsuccessful and served merely to demonstrate the inherent difficulties of the process and that expert advice was essential. A successful research grant for £30,000 from Warwick Innovative Manufacturing Research Council (WIMRC) meant it was possible to purchase suitable equipment and expertise to carry out further research. The previously filed patent enabled the author to safely discuss the idea with a number of companies interested in manufacturing HA monoliths. Eventually a collaboration with a manufacturer of ceramic monoliths for exhaust gas catalysis was set up which meant that the WIMRC grant could be used to pay for biological testing. This collaboration led to rapid proof that hydroxyapatite could be extruded to form a high strength and high porosity monolith that may be suitable for use as a BGS. Therefore an experiment was designed to establish the mechanical and biological performance of extruded HA monoliths. The expertise of our collaborator meant that a range of samples could be produced in large numbers such that a series of experiments could be carried out to establish the preliminary mechanical and biological properties of this innovative material. The patent has now gone through Patent Cooperation Treaty (PCT) stage and the International Preliminary Report on Patentability has shown all 45 claims to be novel.

The material chosen for the extrusion experiments was hydroxyapatite which has been used extensively in the clinical setting for many years. At the time of this decision it was thought that HA would make an excellent benchmark material. However, advice from clinicians after the experiments has made it apparent that HA is now unfashionable and its degradation rate considered to be too slow. An *in vivo* study followed up the implantation of porous HA

blocks into humans over 109 months and found them to be virtually unchanged [178]. Thus a commercial BGS is more likely to make use of a HA and β -TCP composite or an ion substituted HA both of which will degrade more quickly *in vivo* and have greater osteoinductive potential. The use of β -TCP may reduce the overall mechanical properties of the device, however ion substitution of HA has been reported to reduce its degradation time and increase its strength [179-182]. Recent work demonstrated that electrical polarisation of porous HA has a significant effect on osteogenic cell activity and may prove beneficial for HA monoliths [183]. Overall the HA used in this study was proved to be phase pure by XRD and its use has provided a useful benchmark material. Further work should examine the use of more degradable and osteoinductive materials.

The compressive strength and modulus achieved by these HA monoliths is remarkable given their high level of overall porosity ($> 50\%$). The compressive strength for samples A, B, D and E is 233 – 265 MPa which matches cortical bone. Sample C with high porosity walls had a compressive strength of 142 MPa in the lower range of cortical bone. The compressive modulus for scaffolds A, B, D and E is 3.9 – 4.4 GPa which, although lower than cortical bone (5 – 25 GPa), is still an exceptional achievement. Particularly when compared with other BGS ceramic foams, such as Vitoss whose properties are between two and three orders of magnitude lower. It is anticipated that the strength of the monoliths could be improved with further process enhancements which may include the use of finer dies. This will increase the CPSI and decrease the wall thickness of the monolith. This is known to increase the A-axis compression strength for a given material although the manufacturing process is likely to be more challenging.

The mechanical property values are calculated along the primary axis (A) of the monoliths and these will be lower when tested in other axes. The ideal use of this material will be for specific indications where the principal axis can be aligned with the requirements for the implant. Further consideration must be given to the fracture toughness, tensile and shear strength of the monoliths which were not measured on these samples because of their small size. Further work should examine these properties in more detail using larger monolith extrusions which will also be used to measure the B and C axis compressive strengths using cores from a larger monolith (Figure 7.1). Another consideration for a load bearing implant

is fatigue life. It will be necessary to generate a stress versus cycles to failure (S-N) curve for the monoliths such that the life of an implant can be predicted and designed to survive until a proportion of the load has been taken by native bone growing into the monolith channels. A fatigue test was carried out on sample A at three times the maximum load in the spine during fast walking (~ 7500 N) for 100 compression cycles. This resulted in no damage to the sample. Future work will need to extend this to many millions of cycles and carry out the tests in a wet environment as this is known to have a significant effect on fatigue life [184].

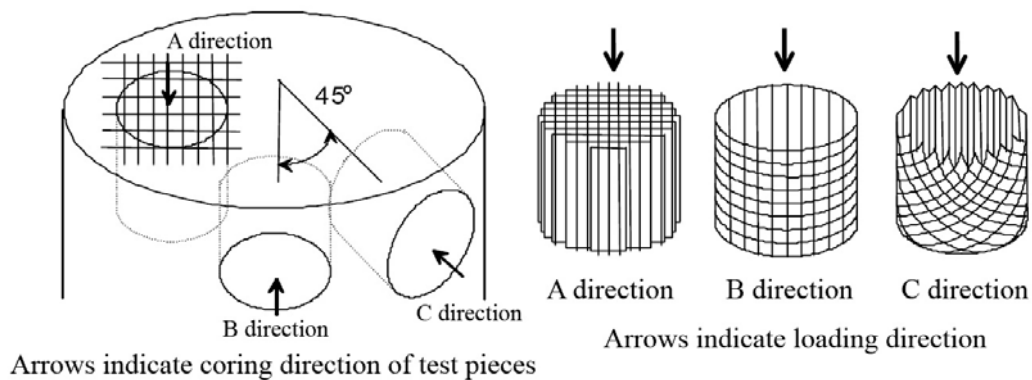


Figure 7.1 Diagram describing the A, B and C axis monolith orientations

The first biological experiment highlighted a problem with sample C regarding the proliferation of cells in culture. Not only were the cells not proliferating they were actually being killed in the tissue culture well. A possible explanation for this was that a water soluble toxic substance was present on the scaffolds. This was confirmed as equilibration of the scaffold in media for 24 hours prior to use eliminated this problem (as demonstrated by experiment 2). The results from experiment 1 do not show clearly that this cell death phenomenon was limited to sample C alone and in fact it was apparent on both D and E, although the effects were less pronounced. Samples C, D and E are all made from Paste 2 which is composed of 100% HAP 200. Results from the GCMS analysis of each sample type revealed the possibility that the samples were contaminated with hexamethyltrisiloxane and octamethylcyclotetrasiloxane in concentrations that reflected the levels of cell death seen in Experiment 1. The exact composition of each paste in terms of binders, lubricants and

other ingredients remains confidential. However the results from the GCMS have been analysed by our industrial partner who have determined that the contaminants did not originate in the paste. Thus they are likely to have been introduced during the firing process.

It is unclear if the cell death phenomenon is due to the pH of the media or directly because of the chemical present on the samples. The pH of the media following addition of the samples was: A - 8.1, B - 7.6, C > 9.5, D - 8.5, E - 8.5 and in the case of C the pH was greater than 9.5, an environment not conducive to a healthy cell population. The cause of this still requires further work to determine if the chemicals identified are the cause of cell death directly or via an increase in pH. Either way they need to be eliminated from the samples by careful preparation and rigorous quality standards. Any future work should produce the samples in a clean environment and use furnaces that have not been contaminated with impurities from other materials.

Biological experiment 1 suggested that there may be differences between the rates of proliferation on the different HA monoliths. However, because of the cell death problems outlined above more realistic results were obtained using equilibrated or washed samples (experiment 2) where the results for each sample are similar. It is clear that the MG63 cells proliferate well on each sample type and the differences noted on the washed samples in Figure 4.10 are unlikely to be biologically important. The decrease in growth rate between days 9 and 13 is not unusual and probably reflects the length of culture time as osteoblasts are known to change their proliferation rate in long-term culture. It is also worth noting that there is significant variation in the biological results. Even though each experiment was carried out in triplicate it is often necessary to carry out at least three sets of experiments in order to get a statistically accurate average. In this case there was insufficient resource to manufacture the large number of samples required for three separate sets of experiments. Future work to examine the effect of material composition on cell growth could be carried out more easily by using small flat samples of the material rather than extruded monoliths which are time consuming to produce in large numbers.

Confocal imaging of the cellular distribution did not suggest that there was a significant difference between the samples. It appeared as though the cells were not evenly distributed

throughout the monoliths and prefer to grow on the horizontal surfaces. They may not be migrating down the channels because it is difficult to ensure adequate flow of media into them. This suggests that analysis of the proliferation of cells on the monolith walls could be more appropriately carried out on calendered (extruded flat) sheets of material. Furthermore it may be necessary to investigate the use of a 3D culture system for future testing of the full scaffolds. Analysis of the expression of ALP and OC showed no significant difference and suggested that all the HA monoliths were similar in their ability to promote development of the osteoblastic phenotype. It was not possible to analyse the quantity of deposited calcium on the scaffolds directly due to the high calcium content of hydroxyapatite.

Overall the biological experiments proved that HA monoliths perform almost identically to Orthovita Vitoss[®] - a commercially available BGS, in terms of MG63 cell proliferation. The physical form of Vitoss[®] versus the HA monoliths is somewhat different and so these results are in no way definitive. They merely serve to suggest that both materials are similarly able to support the proliferation of osteoblastic cells. Furthermore the production process used for Vitoss is highly satisfactory in that there are no toxic substances present and indeed the initial state of Vitoss appears to promote cell growth. The biological experiments also highlight the limitations with two dimensional (2D) cell culture testing when comparing different 3D structures. It is a useful technique for examining cell-surface interaction but for 3D structures its value is limited. The structure of the monoliths will become much more important when testing *in vivo* or in 3D cell culture.

The monoliths created to date have enormous potential to be used as BGSs and later in BTE. These samples demonstrate many benefits over the existing market offerings including high strength and ordered porosity that will make them ideal for both BTE and as a delivery vehicle for osteogenic materials e.g. demineralised bone matrix (DBM). Monoliths are most suited for applications requiring high compressive strength. The tensile properties of the calcium phosphate ceramics are generally poor and when applied to massive bone grafts particularly long and slender struts there is a high chance of failure occurring. Equally the fracture toughness of HA is lower than many of the engineering ceramics. For this reason there is a need for research to improve the mechanical properties further through changes to the material composition, addition of filler materials (including fibres), increasing

the wall density of the monolith and by coating the monolith with additional polymer or ceramic layers. These coatings could further enhance the osteogenic potential by including BMPs that elute slowly as the polymeric coating degrades. These materials could be termed drug eluting monolithic bone substitutes (DEMBS).

The material properties of a BGS are of the utmost importance and further work should concentrate on identifying a suitable highly osteoinductive bioceramic through either ion substitution or creation of suitable composites with osteoinductive crystallinity and stoichiometry. The work to date demonstrates that adjustments to extrusion process parameters have minimal effects on cell proliferation. The most important aspects are the material itself and the elimination of any foreign substances on the implant. It has been speculated that osteoclasts modify the bone surface in such a way that osteoblasts know where to lay down new bone. It is a possibility that this surface could be analysed and then replicated on a BGS thus promoting bone growth. As new techniques are developed to help our understanding of material surfaces there is the likelihood that surfaces will be tailored to suit specific cell and tissue types. This research has a long way to go but advances are being made all of the time that create many exciting possibilities for the future of material development for tissue engineering.

The global orthobiologics market was worth £1.65 billion and growing at 9 % per annum in 2008. It is highly competitive and crowded with similar offerings for low strength void filling materials. Extruded calcium phosphate monoliths are uniquely positioned to provide a high strength, high porosity alternative to these materials. However, it is still highly conceptual and although opinion from experts and clinicians is highly favourable all recognise that this concept needs to be developed into a successful product capable of solving key clinical needs. To this end a device for use in posterior lumbar interbody fusion was designed and in the future will be developed in conjunction with clinicians to provide a degradable and osteoinductive device. This will outperform the existing non degradable, passive materials. There are a number of other indications where this innovative BGS may prove beneficial including long bone segmental defects particularly where high strength is required. It is expected that it will provide a viable alternative to allograft for massive structural grafts.

The ability to form large ceramic monoliths pre-firing into specific geometries that relate to particular bones in the skeleton is of particular benefit. The plastic paste that emanates from the die after extrusion can be easily shaped by various means to form a porous and high strength implant. This technique is likely to prove useful in forming the irregular bones in the skeleton including those found in and around the maxilla and mandible as well as at the end of long bones and in the spine. Ideally a range of standard forms would be available off the shelf rather than having to manufacture custom implants for individual patients. These could then be trimmed in theatre by the surgeon to suit the defect. In load bearing applications it will be important to consider the load conditions and align the internal structure of the monolith to resist this. In the case of the PLIF device designed during this project the load is primarily compression and the primary axis of the monolith is situated so that it aligns with the faces of the vertebrae and can allow a flow of blood through the implant to enhance the rate of healing. This situation would also be the case for segmental long bone defects where the structure of the monolith is aligned with the principal load axis and the flow of blood. It is likely that epiphyseal defects will heal more rapidly than mid shaft defects due to the improved blood flow.

The logical next step for this work would involve recruitment of a medical device company to add to our existing collaboration. It is expected that a medical company will have access to many experts who can quickly determine the indications where this innovative BGS is likely to succeed, help design suitable implants and catalyse the process of putting a product into the market place. There are still a number of process related problems that need to be solved; particularly contamination of the samples, but by far the greatest challenge will be attaining a CE mark. Achieving approval of a device is greatly simplified by using an existing material as in this case. This is likely to eliminate the need for human clinical trials to gain approval and therefore greatly reduce the time to market. The CE mark will be obtained by carrying out an extensive review of the clinical literature as well as a risk analysis and a number of other tasks, but all these can be carried out within one year. Once a CE mark is obtained it will be simpler to carry out human trials which will be needed to provide the clinical evidence of efficacy as required by clinicians.

This project has now reached an impasse where significant investment is required to take it further towards a commercial reality. It is expected that the patent written during this project will form the start of a family of patents to protect individual applications of this novel method to manufacture synthetic bone. The author is presently in discussions with a number of medical companies who are interested in commercialising this concept.

Chapter 8 Conclusions

This work has demonstrated that calcium phosphate monoliths can be manufactured using an established ceramic extrusion process. These monoliths possess important physical and biological properties considered essential in bone graft substitutes. The research has resulted in a number of key conclusions which are highlighted below:

The bone graft substitute market

In 2008, the global orthobiologics market was worth £1.65 billion and growing at 9 % per annum. Of this total value, BGSs currently have a market share of 20 % although this is increasing rapidly due to greater clinical understanding and therefore confidence in their use. There are approximately 600,000 bone graft procedures carried out annually in the US, 50% of which are in spinal arthrodeses and 35 – 40 % used in general orthopaedic applications.

The global market for spinal devices was worth £3.8 billion per annum in 2008 and is growing at 13 % annually. Thus, it is a highly attractive market segment in which to target a new medical device.

The BGS market is populated with approximately 65 products manufactured by 32 companies mainly offering void filling products with low strength. There is currently an urgent need for a BGS with properties similar to autograft and allograft for use in a wide range of clinical conditions, especially for high strength applications.

Manufacturing process research

A wide range of manufacturing processes have been attempted by researchers worldwide to produce an ‘ideal’ BGS. These are broadly classified into Rapid Prototyping (RP) and conventional methods. Each RP process has specific disadvantages which include long build and post-processing times, poor availability of suitable materials, and undesirable surface finish. In particular, the SLS process is highly sensitive to the precursor powder and its morphology, the components must be cooled after processing and then have the unbonded powder removed from the component leaving a loose powdery surface. SLA suffers from a poor availability of UV curable biopolymers as well as the requirement for support structures in the model and subsequent removal of them.

Conventional manufacturing techniques include solvent casting and particulate leaching, injection moulding and machining. Solvent casting has been investigated extensively and has well documented disadvantages which include poor repeatability, trapped solvent or porogen, poor mechanical strength and unconnected pores. Machining, extrusion, and injection moulding are well understood, low cost mass production techniques that are likely to prove useful for the manufacture of low cost and off the shelf BGSs.

Injection moulded and laser drilled PLA cubes were manufactured as a part of this research work with a compressive strength of 67 – 80 MPa and compressive modulus of 1.5 – 2.2 GPa. Laser drilling of ceramics proved more challenging but opened up a new research direction in the extrusion of ceramic monoliths.

Material properties research

The genesis of a novel BGS is a huge challenge requiring a thorough understanding of the interaction between biomaterial and cells. Early research identified that 20 % more cells would grow on the surface of a ceramic (HA) filled polymer (PCL) compared with PCL alone. Hence the inclusion of a bioactive calcium phosphate ceramic in a BGS is highly beneficial in terms of cell proliferation.

There is no existing single material that is considered ideal for a BGS. Each has their own positive and negative merits. The material should be selected or developed according to its

specific application. It is important to state here that this work was not focused to develop novel synthetic biomaterials but to utilise off the shelf materials. This was so designed as to ease the path to innovation and eventual device approval.

The essential specifications for a BGS have been identified during this work. These include mechanical properties, porosity, form or shape of the product, BGS market, clinical requirements including the ability to be sculpted by the surgeon in theatre and possess 'eye appeal' to aid with product sales. The specification for a BGS will alter dependent upon the indication for which it is intended. Hence the design of a specific device can only proceed following determination of a detailed specification for a particular indication.

Hydroxyapatite monoliths

HA monoliths have been successfully manufactured with compressive strength ranging from 142 – 265 MPa and compressive modulus ranging from 3.2 – 4.4 GPa. These values are comparable with *cortical* bone whose compressive strength ranges from 90 – 215 MPa and compressive modulus 5 – 25 GPa. Such high strength has been achieved whilst retaining a level of porosity of 54.4 – 63.1 %. This compares favourably with *cancellous* bone whose porosity varies from 30 – 90 %. This high porosity in the form of channels ranging from 1.08 - 2.53 mm will aid the supply of nutrients and removal of metabolites, thus making it possible to successfully heal large defects. These values were achieved after only two process iterations. There is, however room for improvement and optimisation in the future.

The nature and value of the monolith porosity achieved is suitable as a delivery vehicle for demineralised bone matrix (DBM). This can be packed into the channels forming a highly osteoinductive matrix. Also, the channels allow for simple coating with a range of biodegradable biopolymers which may elute drugs. This in turn will enhance both the healing and mechanical properties of the fabricated implant.

HA monoliths have been proved comparable with a market leading bone substitute, Orthovita Vitoss® in terms of cell proliferation as measured by MTT assay, and cell differentiation as measured by expression of ALP and OC. Current work employed 2D cell culture testing, a deeper understanding of the biological performance will be obtained using

3D cell culture or *in vivo* experimentation. A recent leading opinion paper highlighted the wide range of test methodologies and animal models previously attempted and determined that most experimental settings do not represent the actual clinical conditions faced [185]. Therefore, the *in vivo* testing strategy should be carefully considered prior to starting experimentation.

The biological testing results confirm that the material composition of the HA monolith has a significant effect on cell response as compared to the minimal effect of the wall thickness and cell size. The future work should examine the effect of alternative calcium phosphate ceramics on mechanical and biological properties.

This work has highlighted the need for stricter control over the manufacturing process in order to eliminate any sources of contamination in the final product. The future work should employ dedicated furnaces and clean manufacturing facilities to ensure strict quality control.

The extrusion of ceramic monoliths is a process capable of manufacturing highly consistent and economical implants. It is eminently flexible allowing any ceramic or glass ceramic material to be extruded. Hence, it is possible to manufacture a range of monoliths where bioresorption time and bioactivity can be tailored to suit a specific indication.

The sintered HA monoliths have successfully been machined into patient specific forms and they can easily be shaped by surgeons in theatre to conform with bony defects. The monoliths can also be shaped pre-firing into any range of complex geometric forms that will match any bone in the skeleton. Thus it is possible to manufacture and market a range of off the shelf standard products available to surgeons for many indications.

This research has successfully met the challenge of collaborative relationships with clinicians in order to identify suitable indications for this innovative technology. Discussions with various experts and clinicians alike have thus far identified a number of indications where there is an urgent need for high strength bone graft materials. These include lumbar and cervical fusion, revision hip and knee arthroplasties as well as large segmental defects arising

from trauma, infection and disease. To this end, a specification for a posterior lumbar interbody fusion device was established and a theoretical design study carried out to successfully produce the first medical device utilising this technology.

Much effort has also been expended in establishing the critical collaborations for this research. These include our industrial partner who are a leading International manufacturer of ceramics and our academic partners who are Warwick University Medical School and the department of Biological Sciences, without whom this work could not have been completed.

Output

An international patent (WO 2007/125323) filed in the UK with priority date 27th April 2006. The International Preliminary Examination Report (IPER) from the European Patent Office determined that all 45 claims contained novelty and an inventive step. Furthermore 43 of the 45 claims therein contained industrial applicability.

Four funding proposals have been submitted, two of which have been successful and raised nearly £50,000. These have funded the manufacture and biological testing of the HA monolith samples as well as costs related to the patent and expert advice necessary for commercialisation.

Thus far there have been constraints on publication of this work due to filing of the patent. Now the work is in the public domain and hence two publications are in preparation for submission to high impact International journals.

- “Calcium Phosphate Monoliths for High Strength Bone Graft Applications”
- “The Market for Bone Graft Substitute Materials and Future Research Directions”

A poster presentation at the Bioversity conference in December 2008.

Discussions are now ongoing with a number of interested medical companies who wish to collaborate on this project in the future.

Bone tissue engineering is a multi disciplinary challenge that will engage many researchers for the years to come. The background to this topic has been examined in great detail and so the author has become more knowledgeable in human anatomy and pathology, orthopaedic surgery, the biological sciences, material science and engineering. Overall, this work has proved that it is possible to manufacture porous calcium phosphate monoliths with compressive strength comparable with cortical bone and compressive modulus just below cortical bone whilst retaining a remarkable level of porosity compared to cancellous bone. Furthermore, the biological properties have been found to match one of the most clinically respected BGSs on the market. It is expected that this work will result in a new family of high strength, high porosity BGSs for use in some of the more challenging clinical situations that can be introduced to the market within two years.

References

1. Margareta Nordin and Victor H. Frankel (1989) Basic Biomechanics of the Musculoskeletal system, Williams & Wilkins, USA
2. Dale Layman (2004) Physiology demystified, McGraw-Hill, USA
3. Alexander P. Spence (1986) Basic Human Anatomy, Benjamin-Cummings, USA
4. Turner, C. H. Functional determinants of bone structure: Beyond Wolff's law of bone transformation. Bone 13(6), 403-409. 92.
5. Turner, Charles H. On Wolff's law of trabecular architecture. Journal of Biomechanics 25(1), 1-9. 92.
6. Chamay, A. and Tschantz, P. Mechanical influences in bone remodeling. Experimental research on Wolff's law. Journal of Biomechanics 5(2), 173-180. 72.
7. Jeffrey B Kerr (2000) Atlas of Functional Histology, Mosby, USA
8. Karin A. Hing. Bone repair in the twenty-first century: biology, chemistry or engineering? Philosophical Transactions of the Royal Society A: Mathematical, Physical and Engineering Sciences 362, 2821-2850. 2004.
9. Surveillance, Epidemiology and End Results SEER. Structure of bone tissue. 2006.
Notes: http://training.seer.cancer.gov/module_anatomy/unit3_2_bone_tissue.html.
10. University of Michigan. Bone structure. 2006.
Notes: <http://www.engin.umich.edu/class/bme456/bonestructure/bonestructure.htm>.
11. Riminucci, M. and Bianco, P. (2003) Building bone tissue: matrices and scaffolds in physiology and biotechnology. Braz J Med Biol Res 36, 1027-36.
12. Hong, Sun, Hong, Soon, and Kohn, David. Nanostructural analysis of trabecular bone. 20(7), 1419-1426. 2009-.
13. Liebschner, Michael A. K. Biomechanical considerations of animal models used in tissue engineering of bone: Animal Models for Tissue Engineering Applications. Biomaterials 25(9), 1697-1714. 2004.
14. Hamer, A. J., Colwell, A., and Eastell, R. Biomechanical and biochemical changes in cortical allograft bone after gamma irradiation. Bone 19(6), 696. 96.
15. Mroz, Thomas E., Lin, Eric L., Summit, Matthew C., Bianchi, John R., Keesling, Jr. Jim E., Roberts, Michael, Vangsness, Jr. C. Thomas, and Wang, Jeffrey C. Biomechanical analysis of allograft bone treated with a novel tissue sterilization process. The Spine Journal 6(1), 34-39. 2006.
16. Liebschner, Michael A. K. Biomechanical considerations of animal models used in tissue engineering of bone. Biomaterials 25(9), 1697-1714. 2004.
17. Xiaodu Wang and Qingwen Ni. Determination of cortical bone porosity and pore size distribution using a low field pulsed NMR approach. Journal of Orthopaedic Research 21(2), 312-319. 2003.
18. Zhang, Faming, Chang, Jiang, Lu, Jianxi, Lin, Kaili, and Ning, Congqin. Bioinspired structure of bioceramics for bone regeneration in load-bearing sites. Acta Biomaterialia 3(6), 896-904. 2007.

19. Louis Solomon, David Warwick and Selvadurai Nayagam (2005) Apley's Concise System of Orthopaedics and Fractures, Hodder Headline Group, UK
20. T. Duckworth (1995) Orthopaedics and Fractures, Blackwell Science Ltd, UK
21. Gary Delforge (2002) Musculoskeletal Trauma: Implications for Sports Injury Management, Human Kinetics, USA
22. Novicoff, Wendy M., Manaswi, Abhijit, Hogan, MaCalus V., Brubaker, Shawn M., Mihalko, William M., and Saleh, Khaled J. Critical Analysis of the Evidence for Current Technologies in Bone-Healing and Repair. *J Bone Joint Surg Am* 90(Supplement_1), 85-91. 2008.
Notes: 10.2106/JBJS.G.01521.
23. B. D. Porter, J. B. Oldham, S.-L. He, and M. E. Zobitz. Mechanical Properties of a Biodegradable Bone Regeneration Scaffold. *Journal of Biomechanical Engineering* 122(3), 286-288. 2000. American Society of Mechanical Engineers.
24. Kai-Uwe Lewandrowski, Donald L. Wise, Debra J. Trantolo, Joseph D. Gresser, Michael J. Yazemski, and David E. Altoobelli. *Tissue Engineering and Biodegradable Equivalents - Scientific and Clinical Applications*. 2002. USA, Marcel Dekker Inc. 2002.
25. Finkemeier, Christopher G. Bone-Grafting and Bone-Graft Substitutes. *J Bone Joint Surg Am* 84(3), 454-464. 2002.
26. Greenwald, A. Seth, Boden, Scott D., Goldberg, Victor M., Khan, Yusuf, Laurencin, Cato T., and Rosier, Randy N. Bone-Graft Substitutes: Facts, Fictions, and Applications. *J Bone Joint Surg Am* 83(2_suppl_2), S98-103. 2001.
27. Oxford University Press (2003) Concise colour medical dictionary, Oxford University Press, UK
28. Hench, L. L. (ii) The challenge of orthopaedic materials. *Current Orthopaedics* 14(1), 7-15. 2000.
29. M. J. W. Hubble. Bone transplantation. *Current Orthopaedics Volume 15*(Issue 3), Pages 199-205. 2001.
30. Guelinckx P J and Sinsel N K. The "Eve" procedure: the transfer of vascularized seventh rib, fascia, cartilage, and serratus muscle to reconstruct difficult defects. *Plast Reconstr Surg* 97(3), 527-35. 96.
31. Mikos, A.G., McIntire, L.V., Anderson, J.M. and Babensee, J.E. (1998) Host response to tissue engineered devices. *Adv Drug Deliv Rev* **33**, 111-139.
32. Erbe, E. M., Marx, J. G., Clineff, T. D., and Bellincampi, L. D. Potential of an ultraporous beta-tricalcium phosphate synthetic cancellous bone void filler and bone marrow aspirate composite graft. *Eur Spine J* 10 Suppl 2, S141-6. 2001.
33. Giannoudis, Peter V., Dinopoulos, Haralambos, and Tsiridis, Eleftherios. Bone substitutes: An update: Proceedings from the 1st European Clinical Symposium on Bone and Tissue Regeneration 27-28 November 2004. *Injury* 36(3, Supplement 1), S20-S27. 2005.
34. Botez, P., Sirbu, P., Simion, L., Munteanu, Fl., and Antoniac, I. Application of a biphasic macroporous synthetic bone substitutes CERAFORM: clinical and histological results. *European journal of orthopaedic surgery and traumatology* 19(6), 387-395. 2009.
35. Livingston, T., Ducheyne, P., and Garino, J. In vivo evaluation of a bioactive scaffold for bone tissue engineering. *J Biomed Mater Res* 62(1), 1-13. 2002.
36. Barriga, A., Diaz-de-Rada, P., Barroso, J. L., Alfonso, M., Lamata, M., Hernaez, S., Beguiristain, J. L.,

- San-Julian, M., and Villas, C. Frozen cancellous bone allografts: positive cultures of implanted grafts in posterior fusions of the spine. *European Spine Journal* 13(2), 152-156. 2004.
37. Lerner, Thomas, Bullmann, Viola, Schulte, Tobias, Schneider, Marc, and Liljenqvist, Ulf. A level-1 pilot study to evaluate of ultraporous α -tricalcium phosphate as a graft extender in the posterior correction of adolescent idiopathic scoliosis. 18(2), 170-179. 2009-.
 38. BBC. Alistair Cooke's bones 'stolen'. 2005.
Notes: <http://news.bbc.co.uk/1/hi/world/americas/4552742.stm>.
 39. Sarazin, Pierre, Roy, Xavier, and Favis, Basil D. Controlled preparation and properties of porous poly(lactide) obtained from a co-continuous blend of two biodegradable polymers. *Biomaterials* 25(28), 5965-5978. 2004.
 40. Gogolewski, S. Bioresorbable polymers in trauma and bone surgery: Bioresorbierbare Polymere in der Trauma- und Knochenchirurgie: Polymeres bioresorbables en traumatologie et chirurgie orthopedique: Los polimeros biorreabsorbibles en la cirugia osea y traumatologica. *Injury* 31(Supplement 4), D28-D32. 2000.
 41. Buddy D. Ratner, Allan S. Hoffman, Frederick J. Schoen and Jack E. Lemons (2004) *Biomaterials Science: An Introduction to Materials in Medicine*, Elsevier Inc.,
 42. Todo, Mitsugu, Park, Sang Dae, Arakawa, Kazuo, and Takenoshita, Yasuharu. Relationship between microstructure and fracture behavior of bioabsorbable HA/PLLA composites: The 11th US-Japan Conference on Composite Materials. *Composites Part A: Applied Science and Manufacturing* 37(12), 2221-2225. 2006.
 43. C. Mauli Agrawal and Kyriacos A. Athanasiou. Technique to control pH in vicinity of biodegrading PLA-PGA implants. *Journal of Biomedical Materials Research* 38(2), 105-114. 97.
 44. Pamela Habibovic and Klaas de Groot. Osteoinductive biomaterials-properties and relevance in bone repair. *Journal of Tissue Engineering and Regenerative Medicine* 1(1), 25-32. 2007.
 45. Habibovic, Pamela, Gbureck, Uwe, Doillon, Charles J., Bassett, David C., van Blitterswijk, Clemens A., and Barralet, Jake E. Osteoconduction and osteoinduction of low-temperature 3D printed bioceramic implants. *Biomaterials* 29(7), 944-953. 2008.
 46. Larry L. Hench and June Wilson (1999) *An Introduction to Bioceramics*, World Scientific Publishing Co., UK
 47. Rezwan, K., Chen, Q. Z., Blaker, J. J., and Boccaccini, Aldo Roberto. Biodegradable and bioactive porous polymer/inorganic composite scaffolds for bone tissue engineering. *Biomaterials* 27(18), 3413-3431. 2006.
 48. Hench, Larry L. Genetic design of bioactive glass. *Journal of the European Ceramic Society* 29(7), 1257-1265. 2009.
 49. Bucholz, Robert W. MD. Nonallograft Osteoconductive Bone Graft Substitutes. *Clinical Orthopaedics & Related Research* February 395, 44-52. 2002.
 50. AAP Implantate AG. Bone replacement. 2009.
Notes: http://www.aap.de/en/Produkte/Orthobiologie/Knochenersatz/index_html.
 51. Apatech Ltd. Actifuse. 2009.
Notes: <http://www.apatech.com/>.

52. Food and Drug Administration. GenerOs 510(k) Summary. 2005.
Notes: <http://www.fda.gov/cdrh/pdf5/K051914.pdf>.
53. Biocomposites. Biocomposites biologics. 2009.
Notes: http://www.biocomposites.com/ortho/biocomposites_biologics.asp.
54. Food and Drug Administration. GeneX 510(k) Summary. 2004.
Notes: <http://www.fda.gov/cdrh/pdf4/k040600.pdf>.
55. Biomet Europe. Bone substitutes. 2007.
Notes: http://www.biomet.co.uk/index.php?id=55&no_cache=1&PHPSESSID=c4a02219c.
56. Cambioceramics. Bone substitutes. 2009.
Notes: http://www.cambioceramics.com/nl/1617-Bone_substitutes.html.
57. Ceramisisys. Bone Graft Substitutes (Orthopaedics). 2009.
Notes: http://www.ceramisisys.com/products_bone_graft.html.
58. Johnson & Johnson. Bone Substitute Material. 2007.
Notes:
http://www.jnjgateway.com/home.jhtml?loc=USENG&page=viewContent&contentId=09008b988017c0ac&nodekey=/Prod_Info/Type/Orthobiologics/Bone_Grafting&parentId=09008b988017fc43.
59. DePuy Spine. Healos Bone Graft Replacement. 2007.
Notes: <http://www.depuysspine.com/products/biologicssolutions/healos.asp>.
60. Food and Drug Administration. Healos 510(k) Summary. 2006.
Notes: <http://www.fda.gov/cdrh/pdf6/K062495.pdf>.
61. Dot GmbH. BONITmatrix. 2007.
Notes: http://www.dot-coating.de/index.php?strg=9_11_31&baseID=85.
62. Food and Drug Administration. Inion BioRestore 510(k) Summary. 2007.
Notes: <http://www.fda.gov/cdrh/pdf7/K070998.pdf>.
63. IsoTis. OsSatura. 2007.
Notes: http://www.isotis.com/prod_ossatura.php.
64. Food and Drug Administration. OsSatura Dental 510(k) Summary. 2004.
Notes: <http://www.fda.gov/cdrh/pdf4/k042706.pdf>.
65. Kasios. Bone products. 2009.
Notes: <http://www.kasios.com>.
66. JMM/Kyocera. Orthopaedic field. 2009.
Notes: <http://www.jmmc.jp/en/ourfields/orthopaedic.html>.
67. NovaBone. New Generation of Regeneration. 2009.
Notes: <http://www.novabone.com/prod.php>.
68. Food and Drug Administration. OSferion 510(k) Summary. 2007.
Notes: <http://www.fda.gov/cdrh/pdf6/K061499.pdf>.
69. Osteobiologics. Polygraft technology. 2006.
Notes: <http://www.obl.com/docs/Tech%20detail%20sheet.pdf>.

70. Takiron. Osteotrans system. 2007.
Notes: http://www.takiron.co.jp/english/product/10/product/osteotrans_ot/contents01a.html.
71. Wright Medical Technology. Osteoset. 2006.
Notes: <http://www.wmt.com/Physicians/Products/Biologics/OSTEOSETBoneGraftSubstitute.asp>.
72. Food and Drug Administration. CopiOs 510(k) Summary. 2004.
Notes: <http://www.fda.gov/cdrh/pdf3/k033679.pdf>.
73. Therics. Shaping bone growth. 2009.
Notes: <http://www.therics.com/therics-prodgallery/>.
74. Margareth Gagliardi. BCC Research: Bioactive glasses, ceramics, composites, other advanced materials. 2006.
75. Berkeley Advanced Biomaterials Inc. Products. 2009. 2009.
Notes: <http://www.hydroxyapatite.com/>.
76. Ceraver. Calcium Phosphates. 2009.
Notes: http://www.ceraver.fr/?p_id=308.
77. Curasan. Cerasorb. 2009.
Notes: http://www.curasan.de/com/professionals/cerasorb/brief_description.php.
78. Dot GmbH. Bonitmatrix. 2009.
Notes: http://www.metradel.com/pdf/BONIT_General%20PresentationBONITmatrix.pdf.
79. Exactech. OpteMX. 2009.
Notes: <http://www.exac.com/products/biologics/optemx>.
80. Integra. Orthobiologics. 2009.
Notes: http://www.integra-ls.com/orthobiologics/prod_ossatura.aspx.
81. Olympus Terumo biomaterials. Products. 2009.
Notes: <http://www.biomaterial.co.jp/en/products/osferion.html>.
82. Olympus spine. Tripore. 2009.
Notes: <http://www.olympusspine.com/product-orthogem.aspx>.
83. Orthovita. Cortoss. 2009.
Notes: <http://www.orthovita.com/cortoss/technicalspecs.aspx>.
84. Ossacur AG. Colloss E. 2009.
Notes: http://www.ossacur.com/sites/colloss%20eng/colloss_europa_e.htm.
85. Ossacur AG. Targobone E. 2009.
Notes: http://www.ossacur.com/sites/targobone%20eng/targobone_europa_eng.htm.
86. Pentax. Apaceram. 2009.
Notes: <http://www.pentax.jp/english/lifecare/newceramics/apaceram/index.html>.
87. Smith and Nephew. Jax bone void filler. 2009.
Notes: <http://ortho.smith-nephew.com/uk/Standard.asp?NodeId=3287>.
88. Stryker. Orthobiologics. 2009.
Notes: <http://www.stryker.com/en-us/products/Orthobiologics/index.htm>.

89. Synthes. Products - bone void fillers. 2009.
Notes: <http://us.synthes.com/Products/Biomaterials/Bone+Void+Fillers/>.
90. Wright medical. Orthobiologics. 2009.
Notes: <http://www.wmt.com/Physicians/Products/Biologics/default.asp>.
91. Zimmer. CopiOs. 2009.
Notes: <http://www.zimmer.com/z/ctl/op/global/action/1/id/9399/template/IN/navid/2021>.
92. William R. Moore, Stephen E. Graves, and Gregory I. Bain. Synthetic bone graft substitutes. *ANZ Journal of Surgery* 71(6), 354-361. 2001. Blackwell Publishing Ltd.
93. Vacanti, Joseph P and Langer, Robert. Tissue engineering: the design and fabrication of living replacement devices for surgical reconstruction and transplantation. *The Lancet* 354(Supplement 1), S32-S34. 99.
94. Malafaya, P. B., Silva, G. A., Baran, E. T., and Reis, R. L. Drug delivery therapies II.: Strategies for delivering bone regenerating factors. *Current Opinion in Solid State and Materials Science* 6(4), 297-312. 2002.
95. Murphy, W. L., Peters, M. C., Kohn, D. H., and Mooney, D. J. Sustained release of vascular endothelial growth factor from mineralized poly(lactide-co-glycolide) scaffolds for tissue engineering. *Biomaterials* 21(24), 2521-7. 2000.
96. Urist, Marshall R. Bone: Formation by Autoinduction. *Science* 150(3698), 893-899. 65.
Notes: 10.1126/science.150.3698.893.
97. Rihn, Jeffrey A., Gates, Charley, Glassman, Steven D., Phillips, Frank M., Schwender, James D., and Albert, Todd J. The Use of Bone Morphogenetic Protein in Lumbar Spine Surgery. *J Bone Joint Surg Am* 90(9), 2014-2025. 2008.
98. Tseng, Susan S., Lee, Mark A., and Reddi, A. Hari. Nonunions and the Potential of Stem Cells in Fracture-Healing. *J Bone Joint Surg Am* 90(Supplement_1), 92-98. 2008.
Notes: 10.2106/JBJS.G.01192.
99. E. Sachlos and J.T. Czernuska. Making Tissue Engineering Scaffolds Work. Review on the Application of Solid Freeform Fabrication Technology to the Production of Tissue Engineering Scaffolds. *European Cells and Materials* 5, 29-40. 2003.
100. Wendt, D., Marsano, A., Jakob, M., Heberer, M., and Martin, I. Oscillating perfusion of cell suspensions through three-dimensional scaffolds enhances cell seeding efficiency and uniformity. *Biotechnol Bioeng* 84(2), 205-14. 2003.
101. Stevens, Molly M. Biomaterials for bone tissue engineering. *Materials Today* 11(5), 18-25. 2008.
102. Stevens, Molly M., Marini, Robert P., Schaefer, Dirk, Aronson, Joshua, Langer, Robert, and Shastri, V. Prasad. In vivo engineering of organs: The bone bioreactor. *PNAS* , 0504705102. 2005.
103. Carofino, Bradley C. and Lieberman, Jay R. Gene Therapy Applications for Fracture-Healing. *J Bone Joint Surg Am* 90(Supplement_1), 99-110. 2008.
Notes: 10.2106/JBJS.G.01546.
104. Patterson, Thomas E., Kumagai, Ken, Griffith, Linda, and Muschler, George F. Cellular Strategies for Enhancement of Fracture Repair. *J Bone Joint Surg Am* 90(Supplement_1), 111-119. 2008.
Notes: 10.2106/JBJS.G.01572.

105. Rice, J. M., Hunt, J. A., Gallagher, J. A., Hanarp, P., Sutherland, D. S., and Gold, J. Quantitative assessment of the response of primary derived human osteoblasts and macrophages to a range of nanotopography surfaces in a single culture model in vitro. *Biomaterials* 24(26), 4799-4818. 2003.
106. Stendahl, John C., Li, Leiming, Claussen, Randal C., and Stupp, Samuel I. Modification of fibrous poly(lactic acid) scaffolds with self-assembling triblock molecules. *Biomaterials* 25(27), 5847-5856. 2004.
107. Antonio J. Salgado, Olga P. Coutinho, and Rui L. Reis. Bone Tissue Engineering: State of the Art and Future Trends. *Macromolecular Bioscience* 4(8), 743-765. 2004. WILEY-VCH Verlag GmbH.
108. Leong, K. F., Cheah, C. M., and Chua, C. K. Solid freeform fabrication of three-dimensional scaffolds for engineering replacement tissues and organs. *Biomaterials* 24(13), 2363-2378. 2003.
109. Burg, Karen J. L., Porter, Scott, and Kellam, James F. Biomaterial developments for bone tissue engineering. *Biomaterials* 21(23), 2347-2359. 2000.
110. Barrere, F., Mahmood, T. A., de Groot, K., and van Blitterswijk, C. A. Advanced biomaterials for skeletal tissue regeneration: Instructive and smart functions. *Materials Science and Engineering: R: Reports* 59(1-6), 38-71. 2008.
111. von Doernberg, Marie-Cecile, von Rechenberg, Brigitte, Böhner, Marc, Grunfelder, Sonja, van Lenthe, G Harry, Müller, Ralph, Gasser, Beat, Mathys, Robert, Baroud, Gamal, and Auer, Jorg. In vivo behavior of calcium phosphate scaffolds with four different pore sizes. *Biomaterials* 27(30), 5186-5198. 2006.
112. Babis, George C. and Soucacos, Panayotis N. Bone scaffolds: The role of mechanical stability and instrumentation: Proceedings from the 2nd European Symposium on Bone and Tissue Regeneration 25-27 November 2005. *Injury* 36(4, Supplement 1), S38-S44. 2005.
113. Li, JiaPing, Habibovic, Pamela, Yuan, Huipin, van den Doel, Mirella, Wilson, Clayton E., de Wijn, Joost R., van Blitterswijk, Clemens A., and de Groot, Klass. Biological performance in goats of a porous titanium alloy-biphasic calcium phosphate composite. *Biomaterials* 28(29), 4209-4218. 2007.
114. Habibovic, Pamela, Yuan, Huipin, van der Valk, Chantal M., Meijer, Gert, van Blitterswijk, Clemens A., and de Groot, Klaas. 3D microenvironment as essential element for osteoinduction by biomaterials. *Biomaterials* 26(17), 3565-3575. 2005.
115. Chu, T. M. Gabriel, Orton, David G., Hollister, Scott J., Feinberg, Stephen E., and Halloran, John W. Mechanical and in vivo performance of hydroxyapatite implants with controlled architectures. *Biomaterials* 23(5), 1283-1293. 2002.
116. Jones, Anthony C., Milthorpe, Bruce, Averdunk, Holger, Limaye, Ajay, Senden, Tim J., Sakellariou, Arthur, Sheppard, Adrian P., Sok, Rob M., Knackstedt, Mark A., and Brandwood, Arthur. Analysis of 3D bone ingrowth into polymer scaffolds via micro-computed tomography imaging. *Biomaterials* 25(20), 4947-4954. 2004.
117. Erich Krestel (1990) Imaging Systems for Medical Diagnostics, Siemens-Aktienges, Germany
118. Holdsworth, David W. and Thornton, Michael M. Micro-CT in small animal and specimen imaging. *Trends in Biotechnology* 20(8), S34-S39. 2002.
119. Ho, SaeY Tuan and Hutmacher, Dietmar W. A comparison of micro CT with other techniques used in the characterization of scaffolds. *Biomaterials* 27(8), 1362-1376. 2006.
120. Mintel International Group Ltd. Medical Equipment (Industrial Report) - UK. 2004.

121. Stryker. 2006 - 2007 Fact book. 2007. USA.
122. Stryker. Fact book 2008 - 2009. 2009. USA.
123. Taboas, J. M., Maddox, R. D., Krebsbach, P. H., and Hollister, S. J. Indirect solid free form fabrication of local and global porous, biomimetic and composite 3D polymer-ceramic scaffolds. *Biomaterials* 24(1), 181-194. 2003.
124. Ang, T. H., Sultana, F. S. A., Hutmacher, D. W., Wong, Y. S., Fuh, J. Y. H., Mo, X. M., Loh, H. T., Burdet, E., and Teoh, S. H. Fabrication of 3D chitosan-hydroxyapatite scaffolds using a robotic dispensing system. *Materials Science and Engineering: C* 20(1-2), 35-42. 2002.
125. Lin, A. S., Barrows, T. H., Cartmell, S. H., and Guldberg, R. E. Microarchitectural and mechanical characterization of oriented porous polymer scaffolds. *Biomaterials* 24(3), 481-9. 2003.
126. Schiller, Carsten, Rasche, Christian, Wehmoller, Michael, Beckmann, Felix, Eufinger, Harald, Epple, Matthias, and Weihe, Stephan. Geometrically structured implants for cranial reconstruction made of biodegradable polyesters and calcium phosphate/calcium carbonate. *Biomaterials* 25(7-8), 1239-1247. 2004.
127. Wei, Guobao and Ma, Peter X. Structure and properties of nano-hydroxyapatite/polymer composite scaffolds for bone tissue engineering. *Biomaterials* 25(19), 4749-4757. 2004.
128. Kim, Hae-Won, Lee, Seung-Yong, Bae, Chang-Jun, Noh, Yoon-Jung, Kim, Hyoun-Ee, Kim, Hyun-Man, and Ko, Jea Seung. Porous ZrO₂ bone scaffold coated with hydroxyapatite with fluorapatite intermediate layer. *Biomaterials* 24(19), 3277-3284. 2003.
129. Jones, Anthony C., Milthorpe, Bruce, Averdunk, Holger, Limaye, Ajay, Senden, Tim J., Sakellariou, Arthur, Sheppard, Adrian P., Sok, Rob M., Knackstedt, Mark A., and Brandwood, Arthur. Analysis of 3D bone ingrowth into polymer scaffolds via micro-computed tomography imaging. *Biomaterials* 25(20), 4947-4954. 2004.
130. Muller, R., Van Campenhout, H., Van Damme, B., Van der Perre, G., Dequeker, J., Hildebrand, T., and Ruegsegger, P. Morphometric Analysis of Human Bone Biopsies: A Quantitative Structural Comparison of Histological Sections and Micro-Computed Tomography. *Bone* 23(1), 59-66. 98.
131. T. Uchiyama, T. Tanizawa, H. Muramatsu, N. Endo, H. E. Takahashi, and T. Hara. A Morphometric Comparison of Trabecular Structure of Human Ilium Between Microcomputed Tomography and Conventional Histomorphometry. *Calcified Tissue International* 61(6), 493-498. 97-.
132. Warwick School of Engineering. 3D Microstructures. 2007.
Notes: <http://www2.warwick.ac.uk/fac/sci/eng/research/microtec/3dmicrostructures/>.
133. Burdick, J. A., Frankel, D., Dernell, W. S., and Anseth, K. S. An initial investigation of photocurable three-dimensional lactic acid based scaffolds in a critical-sized cranial defect. *Biomaterials* 24(9), 1613-20. 2003.
134. Fisher, J. P., Holland, T. A., Dean, D., Engel, P. S., and Mikos, A. G. Synthesis and properties of photocross-linked poly(propylene fumarate) scaffolds. *J Biomater Sci Polym Ed* 12(6), 673-87. 2001.
135. Gu, Xuenan, Zheng, Yufeng, Cheng, Yan, Zhong, Shengping, and Xi, Tingfei. In vitro corrosion and biocompatibility of binary magnesium alloys. *Biomaterials* 30(4), 484-498. 2009.
136. Williams, Jessica M., Adewunmi, Adebisi, Schek, Rachel M., Flanagan, Colleen L., Krebsbach, Paul H., Feinberg, Stephen E., Hollister, Scott J., and Das, Suman. Bone tissue engineering using polycaprolactone scaffolds fabricated via selective laser sintering. *Biomaterials* 26(23). 2005.

137. Ciapetti, G., Ambrosio, L., Savarino, L., Granchi, D., Cenni, E., Baldini, N., Pagani, S., Guizzardi, S., Causa, F., and Giunti, A. Osteoblast growth and function in porous poly [epsiv]-caprolactone matrices for bone repair: a preliminary study. *Biomaterials* 24(21), 3815-3824. 2003.
138. Tamimi, Faleh, Torres, Jesus, Gbureck, Uwe, Lopez-Cabarcos, Enrique, Bassett, David C., Alkhraisat, Mohammad H., and Barralet, Jake E. Craniofacial vertical bone augmentation: A comparison between 3D printed monolithic monetite blocks and autologous onlay grafts in the rabbit. *Biomaterials* 30(31), 6318-6326. 2009.
139. Schantz, Jan-Thorsten, Ng, Mary Mah-Lee, Netto, Patricia, Chong Lai Ming, June, Wong, Kit Mui, Hutmacher, Dietmar Werner, and Teoh, Swee Hin. Application of an X-ray microscopy technique to evaluate tissue-engineered bone-scaffold constructs. *Materials Science and Engineering: C* 20(1-2), 9-17. 2002.
140. Dutta Roy, T., Simon, J. L., Ricci, J. L., Rekow, E. D., Thompson, V. P., and Parsons, J. R. Performance of hydroxyapatite bone repair scaffolds created via three-dimensional fabrication techniques. *J Biomed Mater Res* 67A(4), 1228-37. 2003.
141. Kim Groshong. Unbreakable: the tough secrets of natures glue. *New Scientist* (2607), 43-45. 2007. UK. 2007.
142. Salonitis, Konstantinos, Stournaras, Aristidis, Tsoukantas, George, Stavropoulos, Panagiotis, and Chrysosouris, George. A theoretical and experimental investigation on limitations of pulsed laser drilling. *Journal of Materials Processing Technology* 183(1), 96-103. 2007.
143. William M. Steen (1998) *Laser Material Processing*, Springer-Verlag London Ltd, UK
144. Michael Scheffler and Paolo Colombo (2005) *Cellular Ceramics: Structure, Manufacturing, Properties and Applications*, Wiley-VCH Verlag GmbH & Co., Germany
145. Ma, J., Wang, C., and Peng, K. W. Electrophoretic deposition of porous hydroxyapatite scaffold. *Biomaterials* 24(20), 3505-3510. 2003.
146. Ciapetti, G., Ambrosio, L., Savarino, L., Granchi, D., Cenni, E., Baldini, N., Pagani, S., Guizzardi, S., Causa, F., and Giunti, A. Osteoblast growth and function in porous poly [epsiv]-caprolactone matrices for bone repair: a preliminary study. *Biomaterials* 24(21), 3815-3824. 2003.
147. Lu, H. H., El-Amin, S. F., Scott, K. D., and Laurencin, C. T. Three-dimensional, bioactive, biodegradable, polymer-bioactive glass composite scaffolds with improved mechanical properties support collagen synthesis and mineralization of human osteoblast-like cells in vitro. *J Biomed Mater Res* 64A(3), 465-74. 2003.
148. Botchwey, E. A., Pollack, S. R., Levine, E. M., and Laurencin, C. T. Bone tissue engineering in a rotating bioreactor using a microcarrier matrix system. *J Biomed Mater Res* 55(2), 242-53. 2001.
149. Tan, Jian and Saltzman, W. Mark. Biomaterials with hierarchically defined micro- and nanoscale structure. *Biomaterials* 25(17), 3593-3601. 2004.
150. Verrier, Sophie, Blaker, Jonny J., Maquet, Veronique, Hench, Larry L., and Boccaccini, Aldo R. PDLA/Bioglass(R) composites for soft-tissue and hard-tissue engineering: an in vitro cell biology assessment. *Biomaterials* 25(15), 3013-3021. 2004.
151. Bitar, Malak, Salih, Vehid, Mudera, Vivek, Knowles, Jonathan C., and Lewis, Mark P. Soluble phosphate glasses: in vitro studies using human cells of hard and soft tissue origin. *Biomaterials* 25(12), 2283-2292. 2004.

152. Zhao, Feng, Yin, Yuji, Lu, William W., Leong, J. Chiyan, Zhang, Wenyi, Zhang, Jingyu, Zhang, Mingfang, and Yao, Kangde. Preparation and histological evaluation of biomimetic three-dimensional hydroxyapatite/chitosan-gelatin network composite scaffolds. *Biomaterials* 23(15), 3227-3234. 2002.
153. Lee, Jue-Yeon, Nam, Sung-Heon, Im, Su-Yeon, Park, Yoon-Jeong, Lee, Yong-Moo, Seol, Yang-Jo, Chung, Chong-Pyoung, and Lee, Seung-Jin. Enhanced bone formation by controlled growth factor delivery from chitosan-based biomaterials. *Journal of Controlled Release* 78(1-3), 187-197. 2002.
154. Marques, A. P., Reis, R. L., and Hunt, J. A. The biocompatibility of novel starch-based polymers and composites: in vitro studies. *Biomaterials* 23(6), 1471-1478. 2002.
155. Gomes, M. E., Reis, R. L., Cunha, A. M., Blitterswijk, C. A., and de Bruijn, J. D. Cytocompatibility and response of osteoblastic-like cells to starch-based polymers: effect of several additives and processing conditions. *Biomaterials* 22(13), 1911-1917. 2001.
156. Yoshimoto, H., Shin, Y. M., Terai, H., and Vacanti, J. P. A biodegradable nanofiber scaffold by electrospinning and its potential for bone tissue engineering. *Biomaterials* 24(12), 2077-82. 2003.
157. Petite, H., Viateau, V., Bensaid, W., Meunier, A., de Pollak, C., Bourguignon, M., Oudina, K., Sedel, L., and Guillemain, G. Tissue-engineered bone regeneration. *Nat Biotechnol* 18(9), 959-63. 2000.
158. Lisignoli, G., Zini, N., Remiddi, G., Piacentini, A., Puggioli, A., Trimarchi, C., Fini, M., Maraldi, N. M., and Facchini, A. Basic fibroblast growth factor enhances in vitro mineralization of rat bone marrow stromal cells grown on non-woven hyaluronic acid based polymer scaffold. *Biomaterials* 22(15), 2095-105. 2001.
159. Marra, K. G., Szem, J. W., Kumta, P. N., DiMilla, P. A., and Weiss, L. E. In vitro analysis of biodegradable polymer blend/hydroxyapatite composites for bone tissue engineering. *J Biomed Mater Res* 47(3), 324-35. 99.
160. Vozzi, G., Flaim, C., Ahluwalia, A., and Bhatia, S. Fabrication of PLGA scaffolds using soft lithography and microsyringe deposition. *Biomaterials* 24(14), 2533-40. 2003.
161. Clover, J. and Gowen, M. Are MG-63 and HOS TE85 human osteosarcoma cell lines representative models of the osteoblastic phenotype? *Bone* 15(6), 585-591. 94.
162. Gitimoy Kar, Kenneth Hrdina, John Wight, and Charles Yu. Titanium coating silica glass honeycomb structure from silica soot extraction. Corning Inc. 2002. US6479129.
163. YANG, Yun-fa, ZHANG, Guang-ming, XU, Zhong-he, WANG, Jian-wei, HOU, Zhi-qi, and WEN, Shi-feng. Structural bone allografts with intramedullary vascularized fibular autografts for the treatment of massive bone defects in extremities. *Journal of Medical Colleges of PLA* 22(5), 298-302. 2007.
164. Donati, Davide, Di Bella, Claudia, Col angeli, Marco, Bianchi, Giuseppe, and Mercuri, Mario. The use of massive bone allografts in bone tumour surgery of the limb. *Current Orthopaedics* 19(5), 393-399. 2005.
165. Muscolo, D. Luis, Ayerza, Miguel A., and Aponte-Tinao, Luis A. Massive Allograft Use in Orthopedic Oncology: Oncology. *Orthopedic Clinics of North America* 37(1), 65-74. 2006.
166. Yasuaki Tokuhashi, Yasumitsu Ajiro, and Natsuki Umezawa. Subsidence of Metal Interbody Cage After Posterior Lumbar Interbody Fusion With Pedicle Screw Fixation. *Orthopedics* 32(259). 2009.
167. Schiffman, Michael, Brau, Salvador A., Henderson, Robin, and Gimmestad, Gwen. Bilateral implantation of low-profile interbody fusion cages: subsidence, lordosis, and fusion analysis. *The Spine Journal* 3(5), 377-387. 2003.

168. Katz, Jeffrey N. Lumbar Disc Disorders and Low-Back Pain: Socioeconomic Factors and Consequences. *J Bone Joint Surg Am* 88(suppl_2), 21-24. 2006.
Notes: 10.2106/JBJS.E.01273.
169. Backpain-guide.com. The complete spine. 2004.
Notes: http://www.backpain-guide.com/Chapter_Fig_folders/Ch05_Anatomy_Folder/4OverallSpine.html.
170. Thomas A. Zdeblick. Spine cages help to restore correct spinal alignment. 2008. 2008.
Notes: <http://www.spineuniverse.com/displayarticle.php/article1523.html>.
171. Okuda, Shinya, Oda, Takenori, Miyauchi, Akira, Haku, Takamitsu, Yamamoto, Tomio, and Iwasaki, Motoki. Surgical Outcomes of Posterior Lumbar Interbody Fusion in Elderly Patients. *Surgical Technique. J Bone Joint Surg Am* 89(2_suppl_2), 310-320. 2007.
Notes: 10.2106/JBJS.G.00307.
172. Stryker. Interbody devices. 2008.
Notes: http://www.europe.stryker.com/index/st_pag_medic-home/st_pag_detailed-product-info/st_pag_spinal-implants/eu_pag_spine-interbody.htm.
173. Medtronic Sofamor Danek. Spinal technologies. 2006.
Notes: <http://www.sofamordanek.com/patient-spinal-ltcage.html>.
174. Synthes. Spinal products. 2007.
Notes: <http://www.sofamordanek.com/patient-spinal-ltcage.html>.
175. M. Janssen, C. Lam, and R. Beckham. Outcomes of allogenic cages in anterior and posterior lumbar interbody fusion. *European Spine Journal* 10(0), S158-S168. 2001-.
176. Rohlmann, Antonius, Graichen, Friedmar, Bender, Alwina, Kayser, Ralph, and Bergmann, Georg. Loads on a telemeterized vertebral body replacement measured in three patients within the first postoperative month. *Clinical Biomechanics* 23(2), 147-158. 2008.
177. Smith & Nephew. Summary Financial Statement. 2004. Smith & Nephew.
Notes: www.smithandnephew.com.
178. Yamaguchi, Kazuhiro, Hirano, Tom, Yoshida, Goich, and Iwasaki, Katsuro. Degradation-resistant character of synthetic hydroxyapatite blocks filled in bone defects. *Biomaterials* 16(13), 983-985. 95.
179. Webster, Thomas J., Massa-Schlueter, Elizabeth A., Smith, Jennifer L., and Slamovich, Elliot B. Osteoblast response to hydroxyapatite doped with divalent and trivalent cations. *Biomaterials* 25(11), 2111-2121. 2004.
180. Porter, Alexandra E., Patel, Nelesh, Skepper, Jeremy N., Best, Serena M., and Bonfield, William. Effect of sintered silicate-substituted hydroxyapatite on remodelling processes at the bone-implant interface. *Biomaterials* 25(16), 3303-3314. 2004.
181. Hing, Karin A., Revell, Peter A., Smith, Nigel, and Buckland, Thomas. Effect of silicon level on rate, quality and progression of bone healing within silicate-substituted porous hydroxyapatite scaffolds. *Biomaterials* 27(29), 5014-5026. 2006.
182. Patel, N., Best, S. M., Bonfield, W., Gibson, I. R., Hing, K. A., Damien, E., and Revell, P. A. A comparative study on the in vivo behavior of hydroxyapatite and silicon substituted hydroxyapatite granules. *Journal of Materials Science: Materials in Medicine* 13(12), 1199-1206. 2002-.
183. Wang, Wei, Itoh, Soichiro, Tanaka, Yumi, Nagai, Akiko, and Yamashita, Kimihiro. Comparison of

enhancement of bone ingrowth into hydroxyapatite ceramics with highly and poorly interconnected pores by electrical polarization. *Acta Biomaterialia* . 2009.

184. Sobrinho L.C., Glover R.H., Knowles J.C., and Cattell M.J. Comparison of the wet and dry fatigue properties of all ceramic crowns. *Journal of Materials Science: Materials in Medicine* 9(5), 517-521. 98.
185. Schutte, Robert J., Xie, Lola, Klitzman, Bruce, and Reichert, William M. In vivo cytokine-associated responses to biomaterials. *Biomaterials* 30(2), 160-168. 2009.